Neurální a buněčné procesy smyslové transdukce – jak smyslové podněty vstupují do nervového systému.

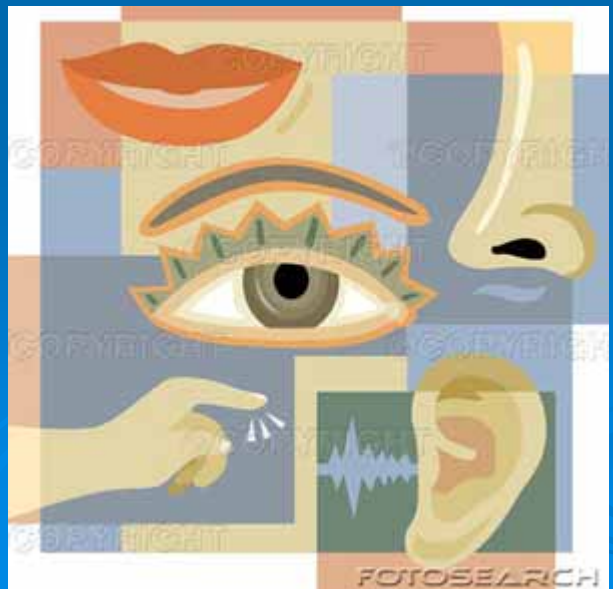

Všech 5 pohromadě

Hranice smyslového a ne-smyslového signálu

- Schopnosti receptorů na hranici možného.
- Co se děje na membránách smyslových buněk, jak mohou smyslové podněty zasáhnou do metabolismu buněk?
- Paralely se známými signálními drahami diferenciace, imunity, apoptózy
- Společně využívané „vyzkoušené“ funkce

Kanály – prostředek pasivního transportu
udržování integrity buňky a komunikace

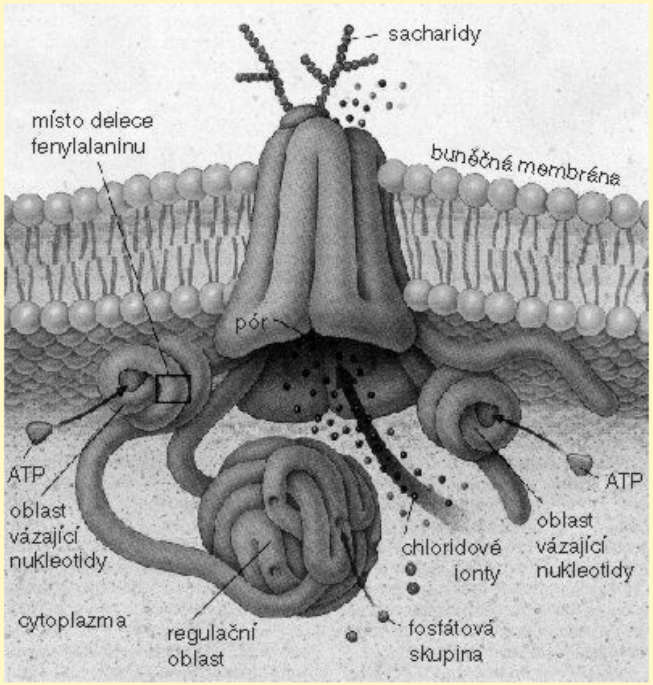

Po ukotvení v membráně se protein CFTR složitě přizpůsobuje – vytváří kanálky, kterými mohou přes membránu proudit chloridové ionty. V cytoplazmatické části proteinu jsou tři regulační oblasti, které se podílejí na uzavírání a otevírání póru. Kanálek se otevře jedině tehdy, když se na CFTR navážou dvě molekuly ATP a zároveň je fosforylována třetí regulační oblast. U mutovaného proteinu je jedna z oblastí vázajících ATP intaktní a membránový kanálek se neotevírá.

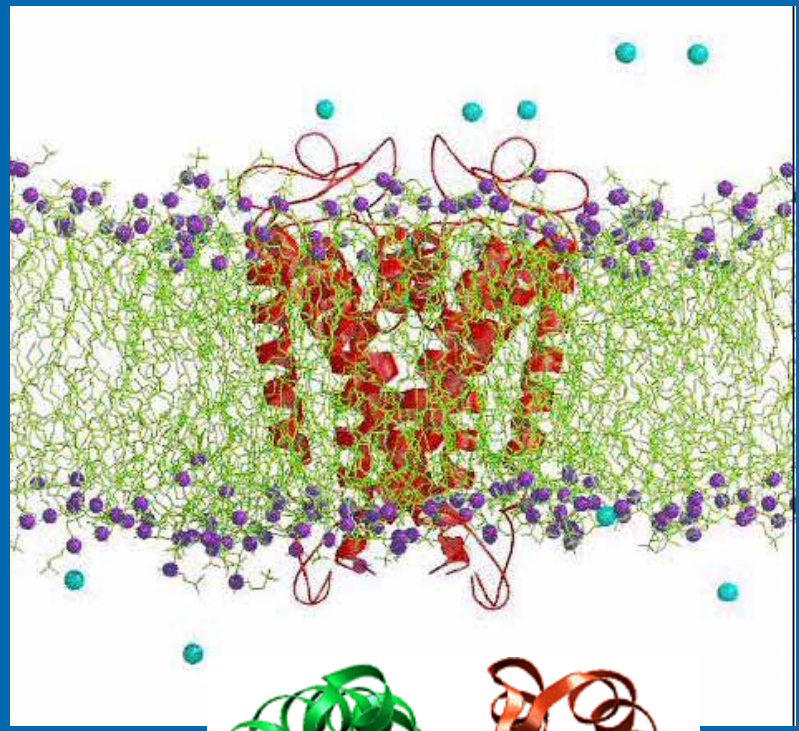

Ionotropní
transdukce – receptor přímo na kanálu

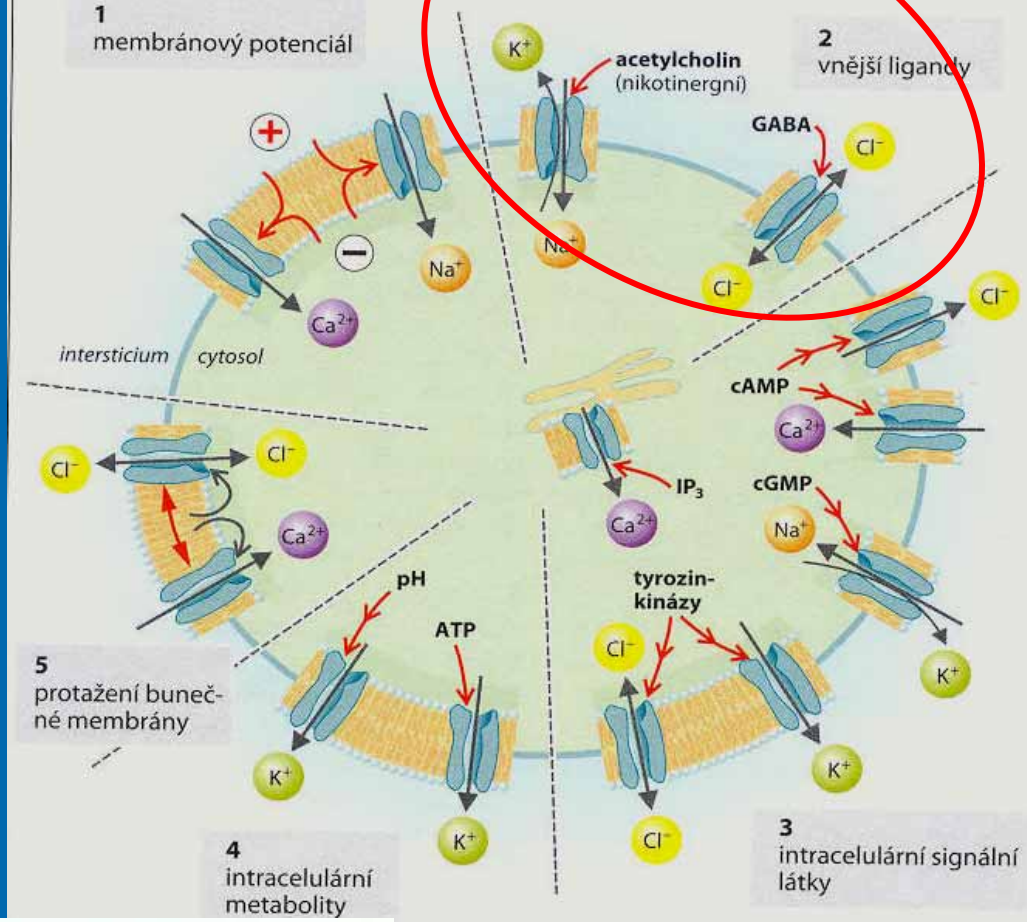

TABLE 12.3 Ionotropic and metabotropic receptors: Structural, functional, and mechanistic differences

Characteristic	Ionotropic receptors	Metabotropic receptors
Receptor molecule	Ligand-gated channel receptor	G protein–coupled receptor
Molecular structure	Five subunits around an ion channel	Protein with seven transmembrane segments; no channel
Molecular action	Open ion channel	Activate G protein; metabolic cascade
Second messenger	No	Yes (usually)
Gating of ion channels	Direct	Indirect (or none)
Type of synaptic effect	Fast EPSP or IPSP	Slow PSPs; modulatory changes (in channel properties, cell metabolism, or gene expression)

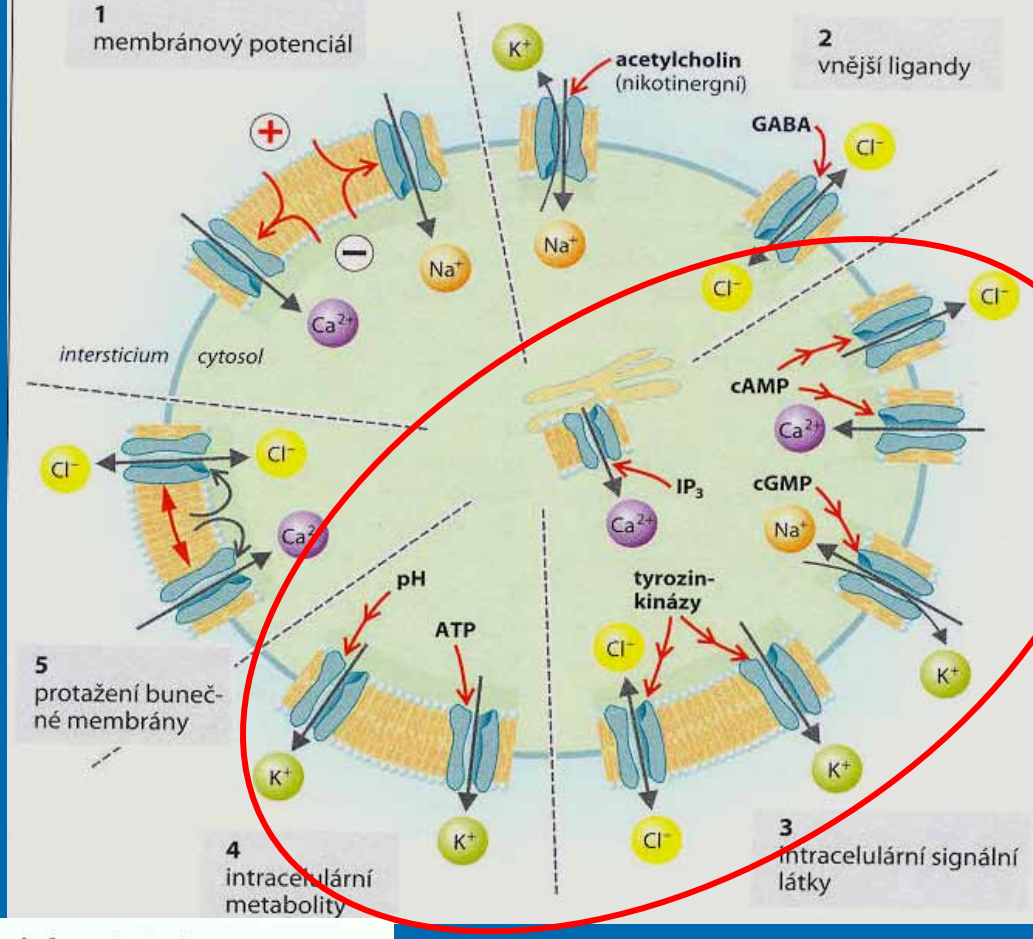

TABLE 12.3 Ionotropic and metabotropic receptors: Structural, functional, and mechanistic differences

Characteristic	Ionotropic receptors	Metabotropic receptors
Receptor molecule	Ligand-gated channel receptor	G protein–coupled receptor
Molecular structure	Five subunits around an ion channel	Protein with seven transmembrane segments; no channel
Molecular action	Open ion channel	Activate G protein; metabolic cascade
Second messenger	No	Yes (usually)
Gating of ion channels	Direct	Indirect (or none)
Type of synaptic effect	Fast EPSP or IPSP	Slow PSPs; modulatory changes (in channel properties, cell metabolism, or gene expression)

Metabotropní transdukce

Už jste se potkali s kanály?

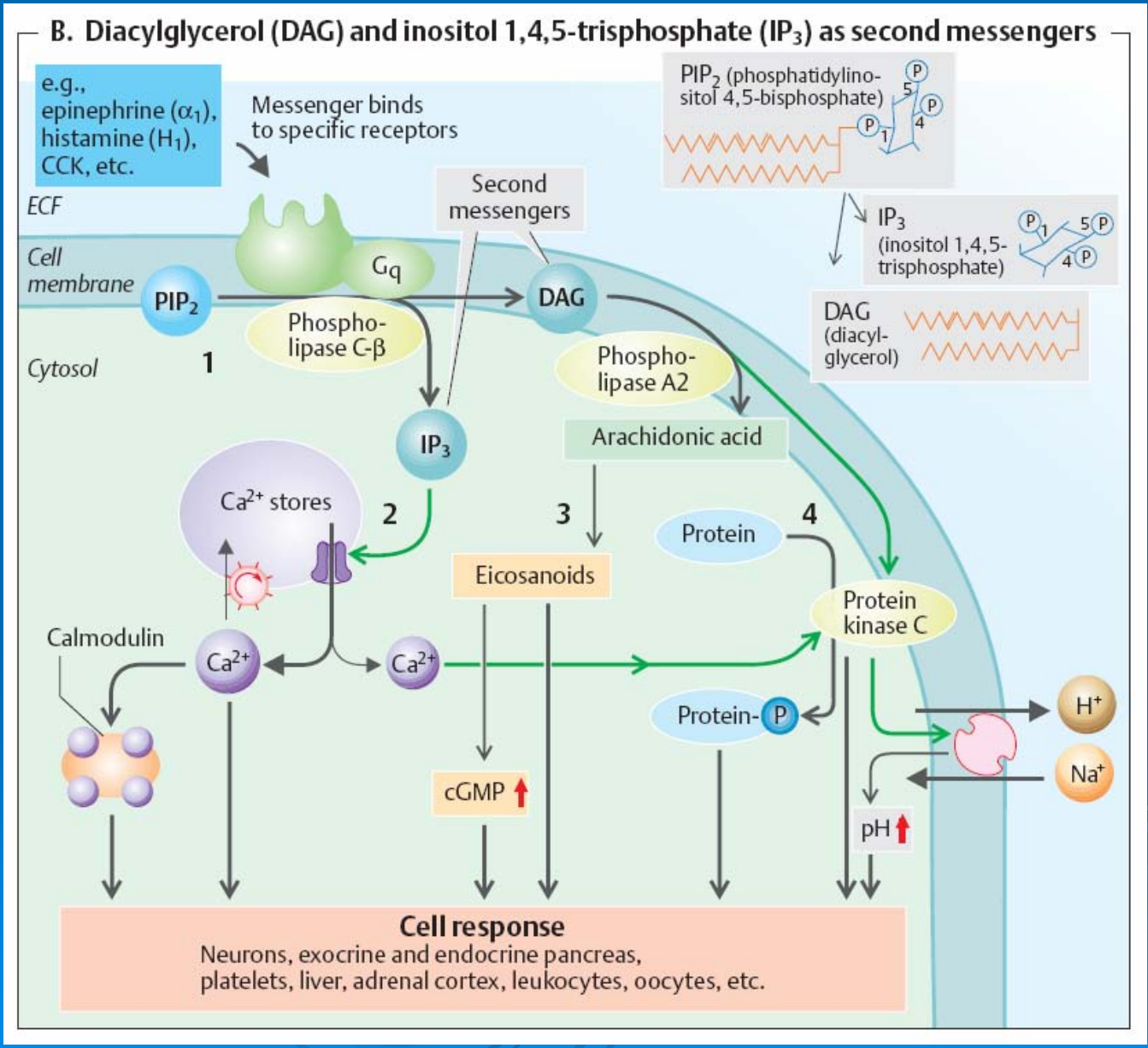

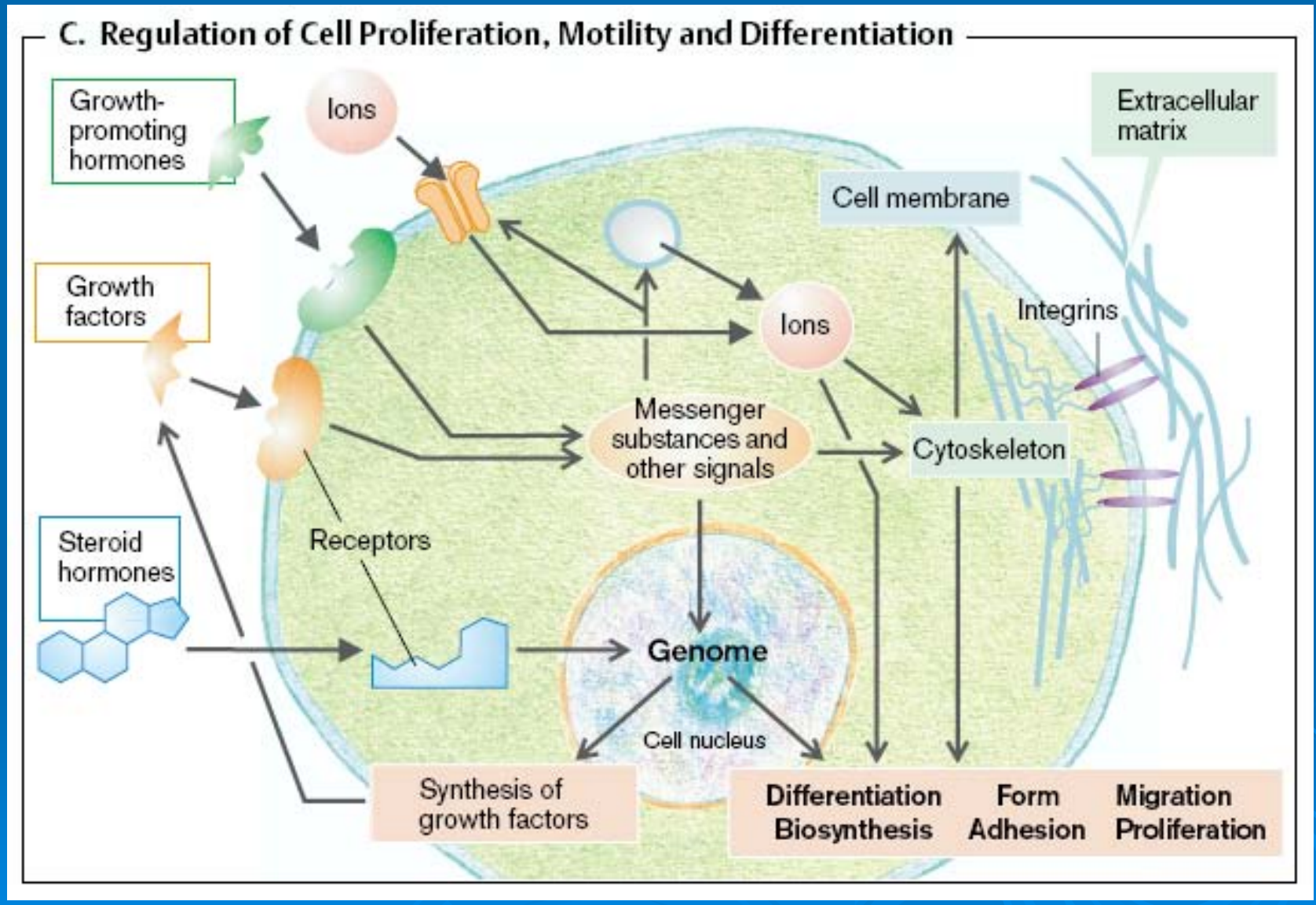
C. Regulation of Cell Proliferation, Motility and Differentiation
Growth-promoting hormones
Ions
Extracellular matrix
Cell membrane
Growth factors
Integrins
Ions
Messenger substances and other signals
Cytoskeleton
Steroid hormones
Receptors
Genome
Cell nucleus
Synthesis of growth factors
Differentiation
Biosynthesis
Form
Adhesion
Migration
Proliferation

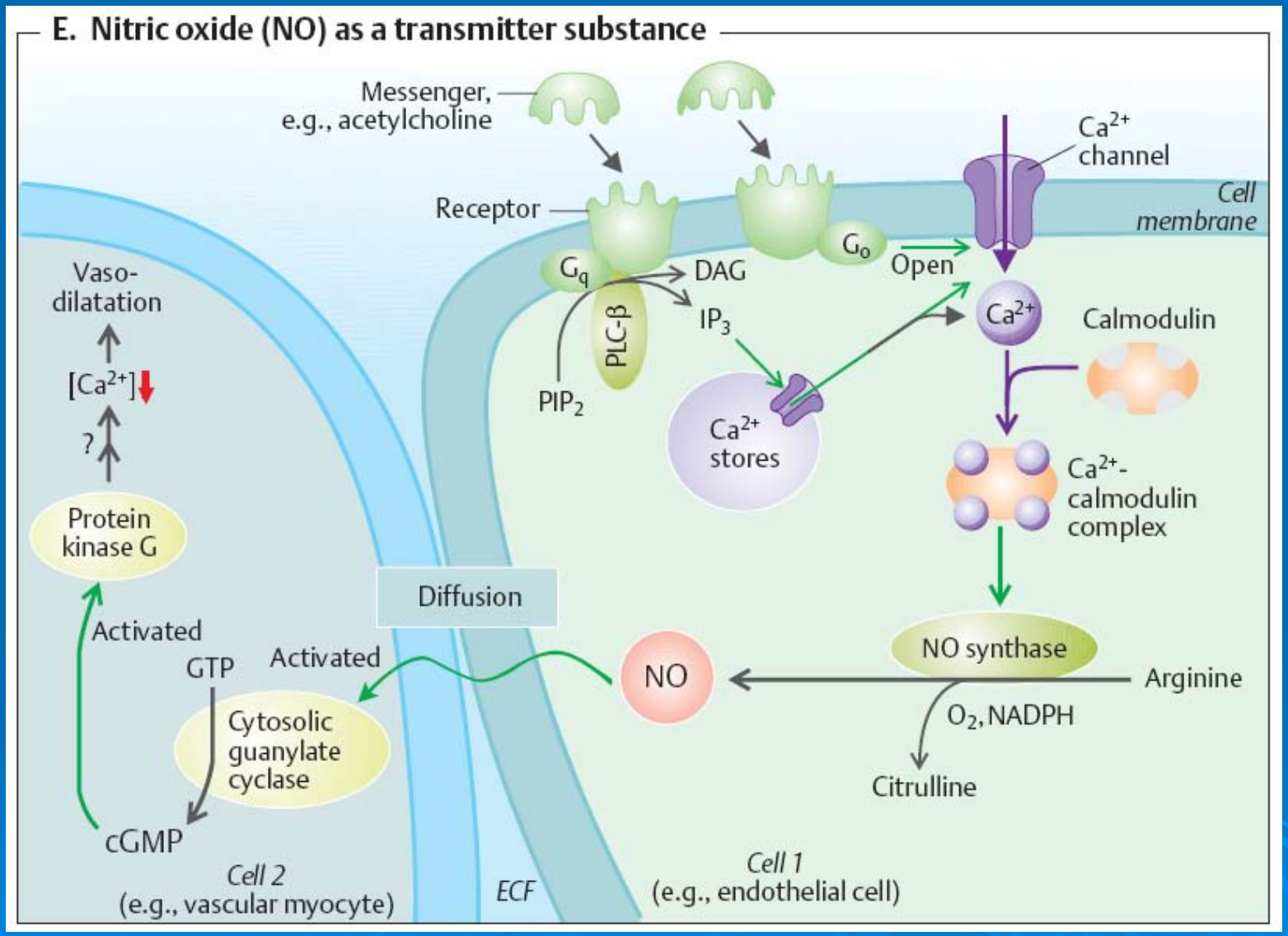
E. Nitric oxide (NO) as a transmitter substance
Messenger, e.g., acetylcholine
Receptor
Ca^{2+} channel
Cell membrane
G_o
G_q
DAG
PLC-β
IP_3
PIP_2
Open
Ca^{2+}
Calmodulin
Ca^{2+} stores
Ca^{2+}-calmodulin complex
Vaso-dilatation
$[Ca^{2+}]$
?
Protein kinase G
Diffusion
Activated
GTP
Activated
Cytosolic guanylate cyclase
cGMP
NO
NO synthase
Arginine
O_2, NADPH
Citrulline
Cell 2 (e.g., vascular myocyte)
ECF
Cell 1 (e.g., endothelial cell)

Vodní hospodářství je otázkou řízené propustnosti membrán.

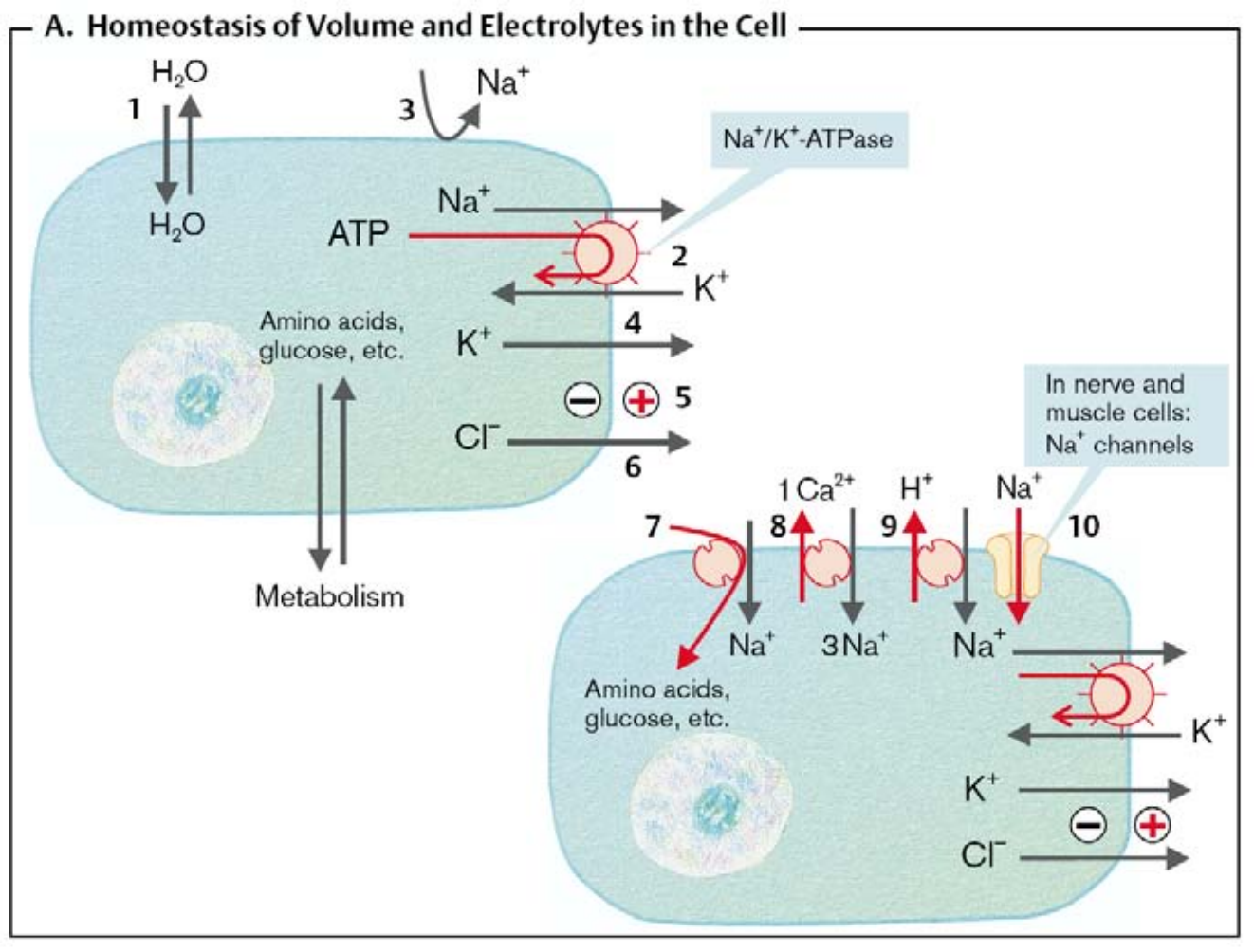

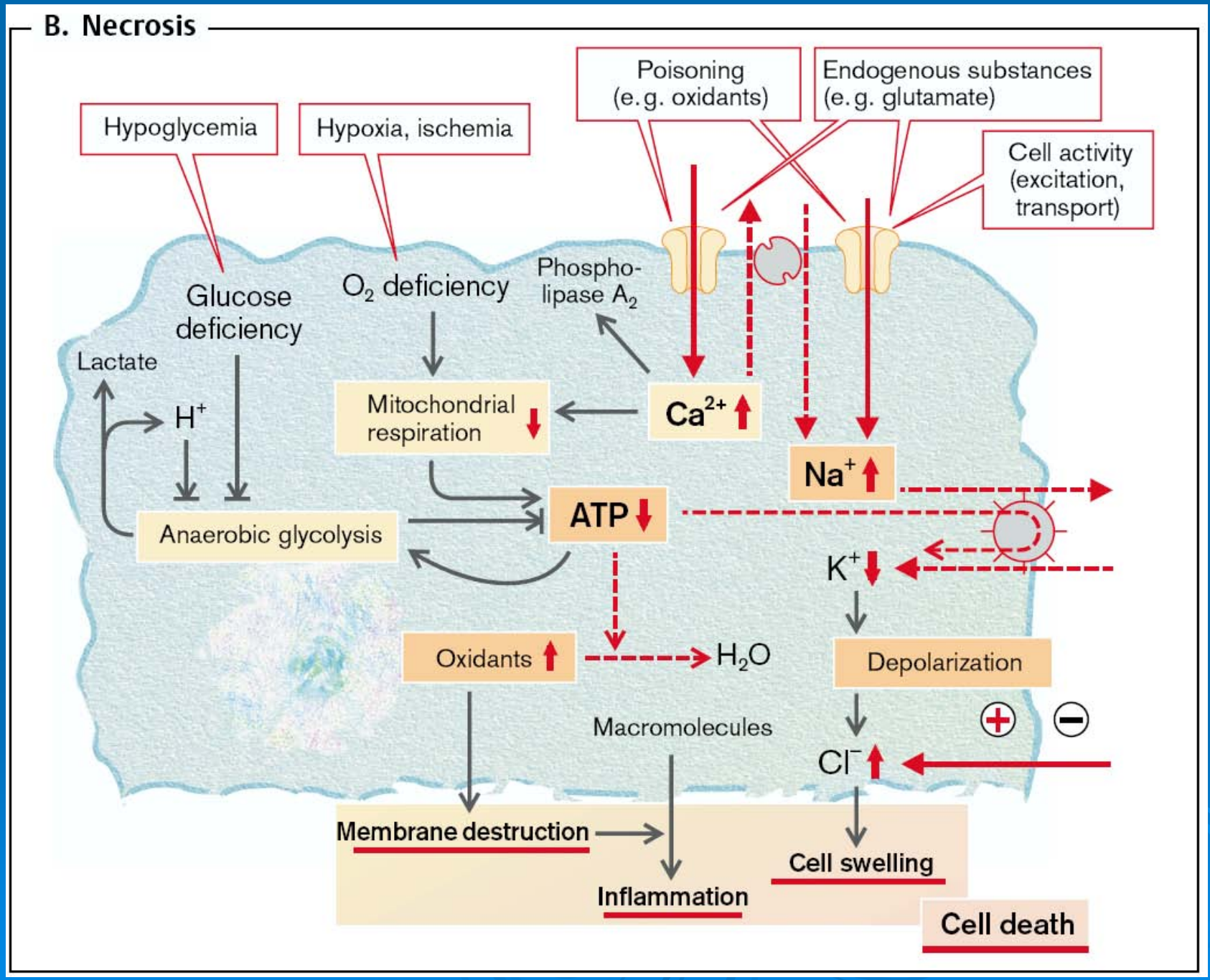
B. Necrosis
Poisoning (e.g. oxidants)
Endogenous substances (e.g. glutamate)
Hypoglycemia
Hypoxia, ischemia
Cell activity (excitation, transport)
Glucose deficiency
O_2 deficiency
Phospho-lipase A_2
Lactate
H^+
Mitochondrial respiration
Ca^{2+}
Na^+
ATP
Anaerobic glycolysis
K^+
Oxidants
H_2O
Depolarization
Macromolecules
Cl^-
Membrane destruction
Cell swelling
Inflammation
Cell death

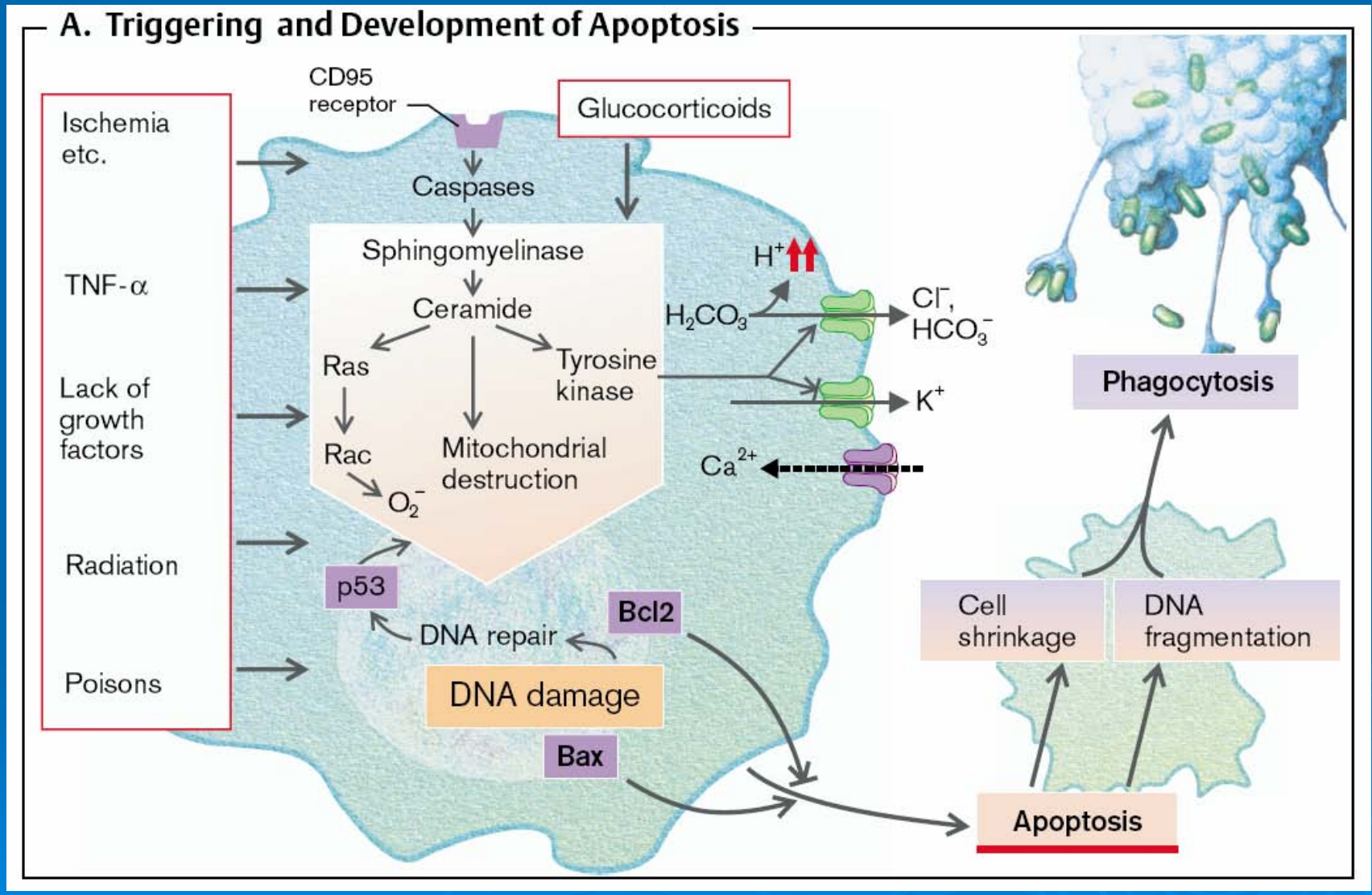
A. Triggering and Development of Apoptosis
CD95 receptor
Glucocorticoids
Ischemia etc.
TNF-α
Lack of growth factors
Radiation
Poisons
Caspases
Sphingomyelinase
Ceramide
Ras
Rac
O_2^-
Tyrosine kinase
Mitochondrial destruction
H^+
H_2CO_3
Cl^-, HCO_3^-
K^+
Ca^{2+}
p53
DNA repair
Bcl2
DNA damage
Bax
Apoptosis
Phagocytosis
Cell shrinkage
DNA fragmentation

Terčíkový zámek – vidíme, jak kanál pracuje

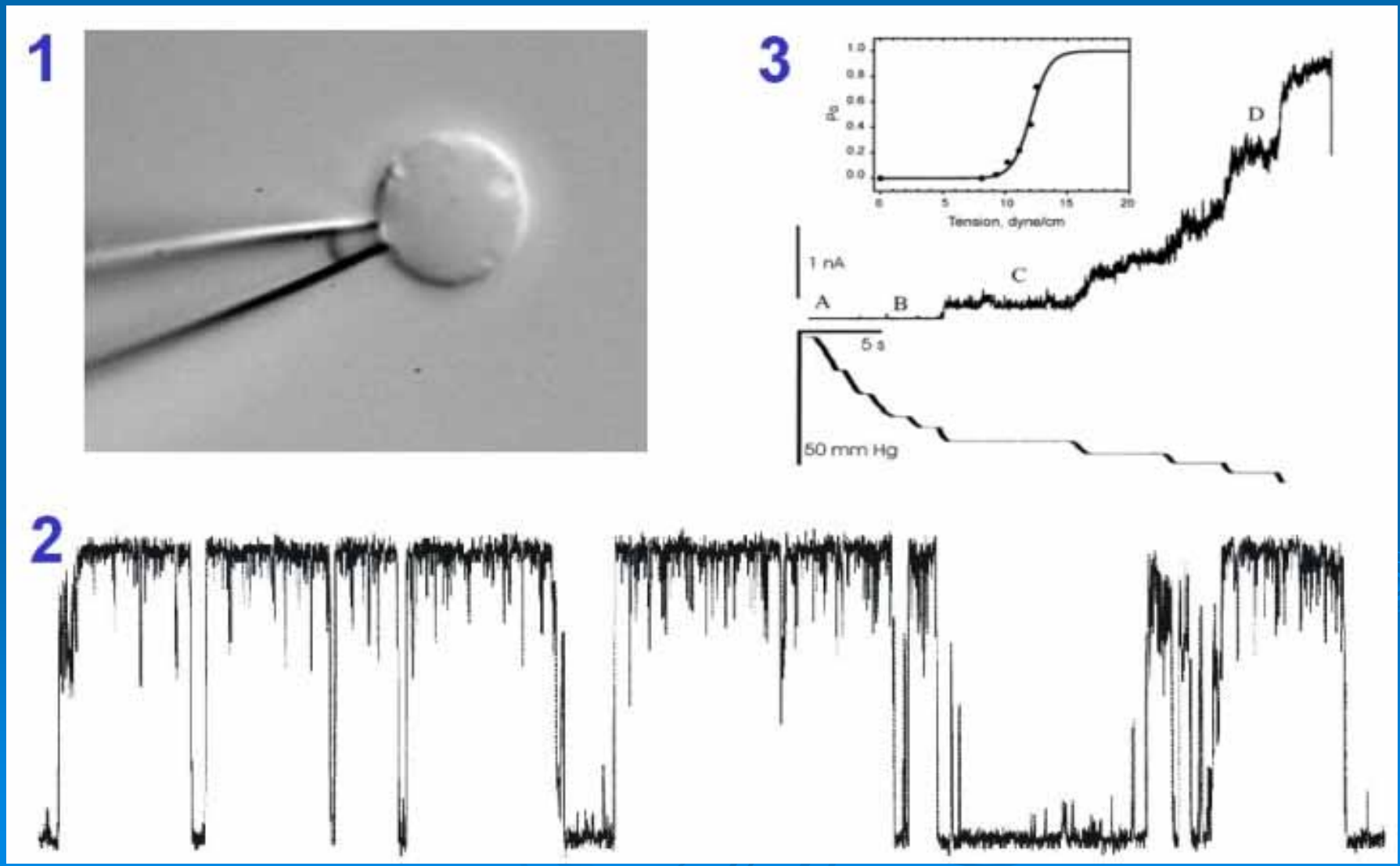

X ray krystalografie
analýza sekvence AK –

Jak kanál vypadá

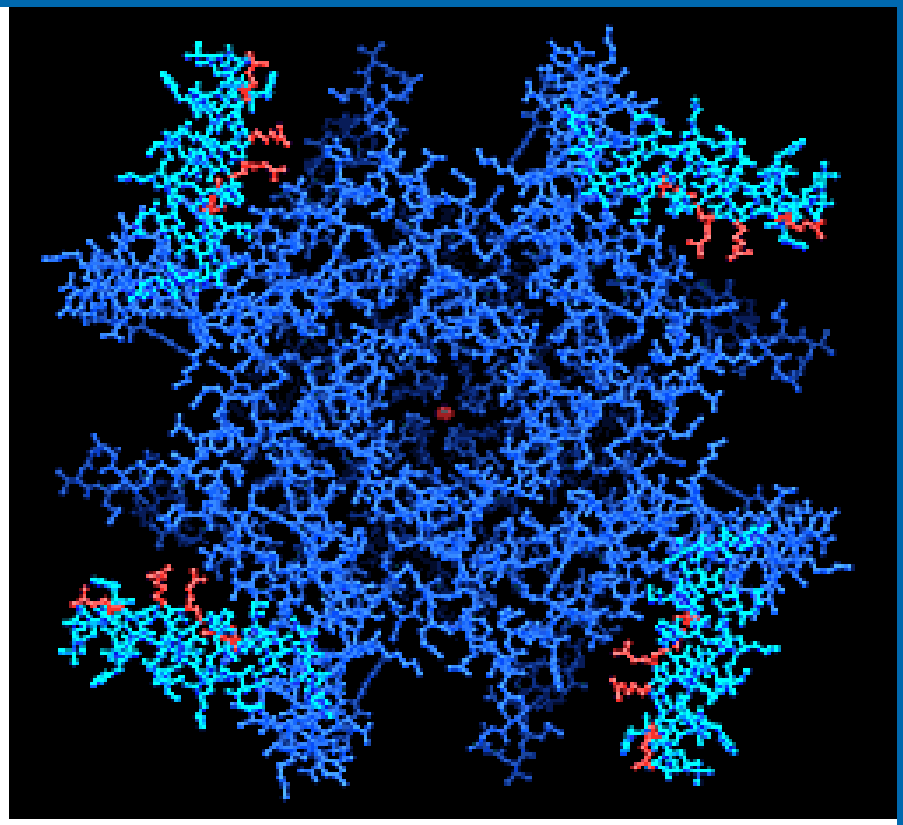

An overhead view of a voltage-dependent potassium ion channel shows four red-tipped "paddles" that open and close in response to positive and negative charges. This structure, discovered by Rockefeller scientists, shows for the first time the molecular mechanism by which potassium ions are allowed in and out of living cells during a nerve or muscle impulse.

Kanály v molekulární fyziologii smyslů

Kanály jsou odpovědné za regulaci membránového napětí a tedy klíčové pro přenášení nervových signálů.

Nervový systém „vidí“ jen to, změní kanálovou propustnost.

Co se děje mezi receptory a kanály

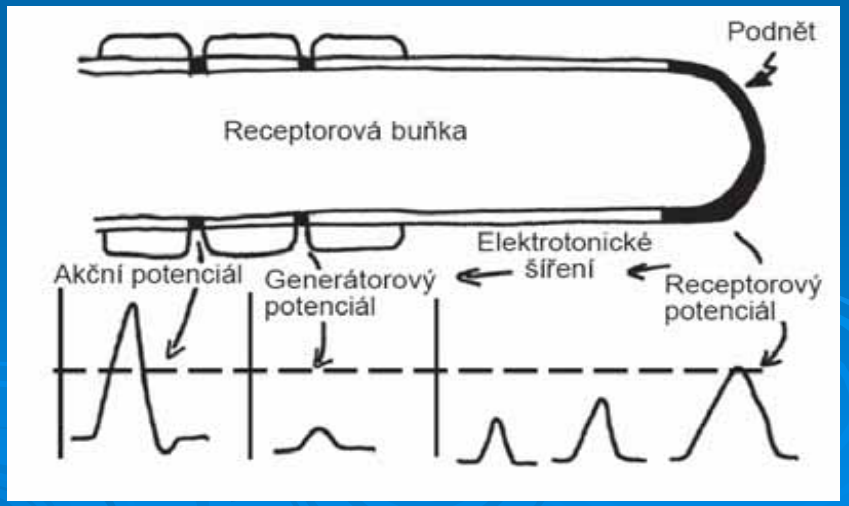

Fotorecepce - Zrak

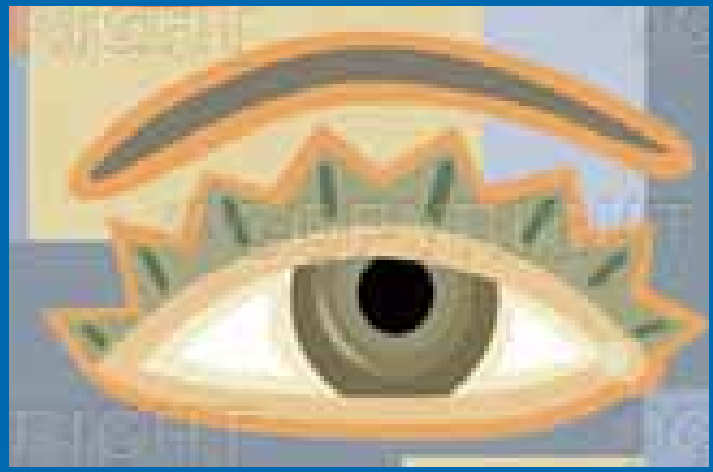

Rhodopsin

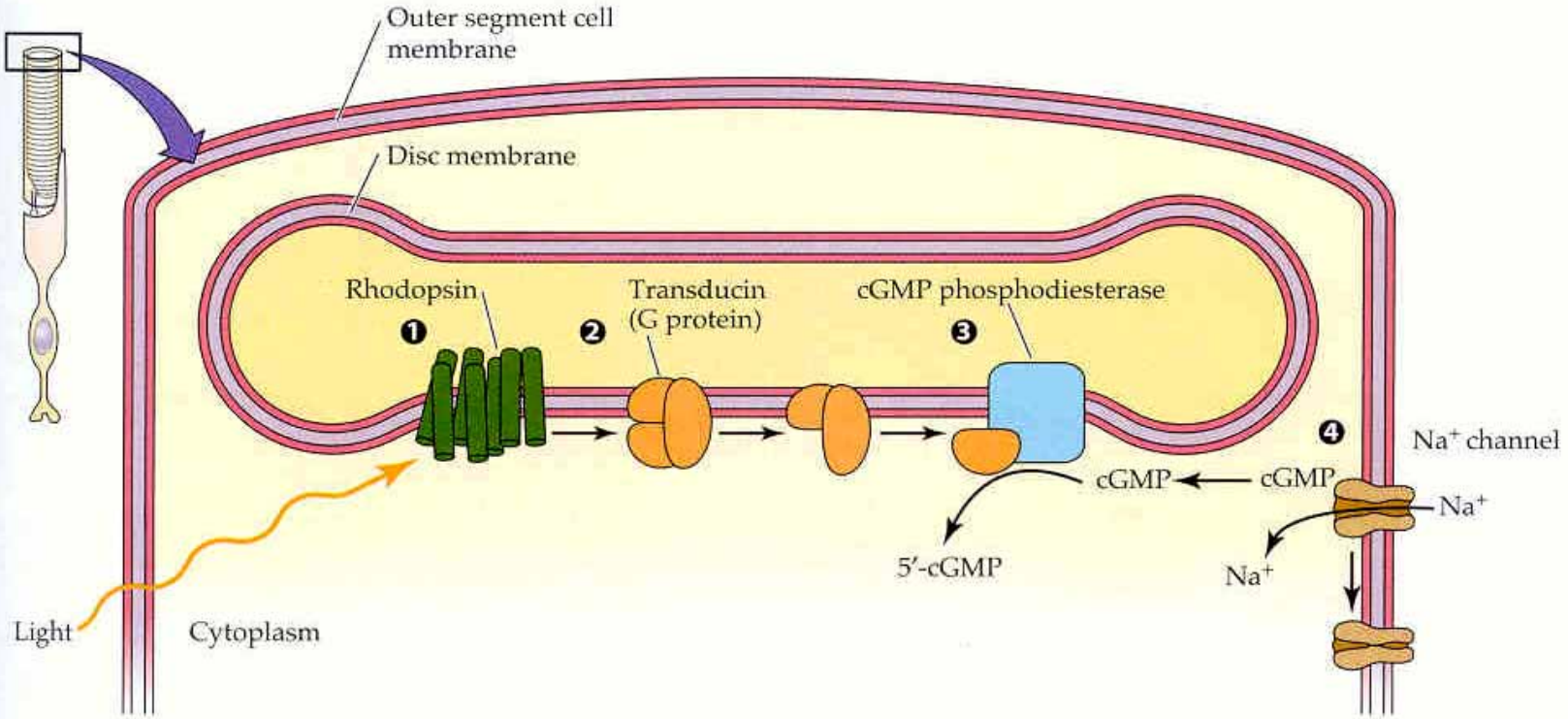

Figure 13.14 Phototransduction closes cation channels in the outer segment of the photoreceptor membrane In the dark, the cation channels are kept open by intracellular cGMP and conduct an inward current, carried largely by Na^+. When light strikes the photoreceptor, these channels are closed by a G protein–coupled mechanism. ❶ Rhodopsin molecules in the disc membrane absorb light and are activated. ❷ The activated rhodopsin stimulates a G protein (transducin in rods), which in turn activates cGMP phosphodiesterase. ❸ The phosphodiesterase catalyzes the breakdown of cGMP to 5′-GMP. ❹ As the cGMP concentration decreases, cGMP detaches from the cation channels, which close.

Od 70. let obecné schéma G-proteinové signalizace

(a) Retinal and vitamin A

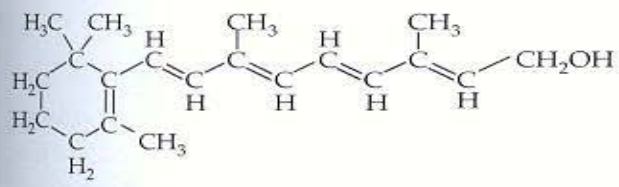

Complete structure of vitamin A (all-*trans*)

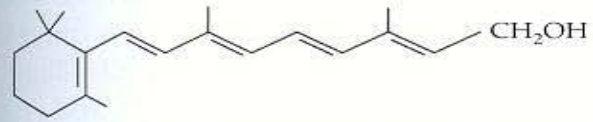

Condensed structure of vitamin A (all-*trans*)

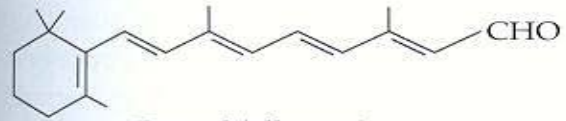

Retinal (all-*trans*)

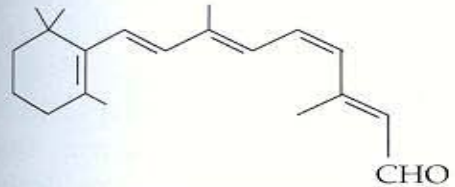

Retinal (11-*cis*)

(b) Opsin

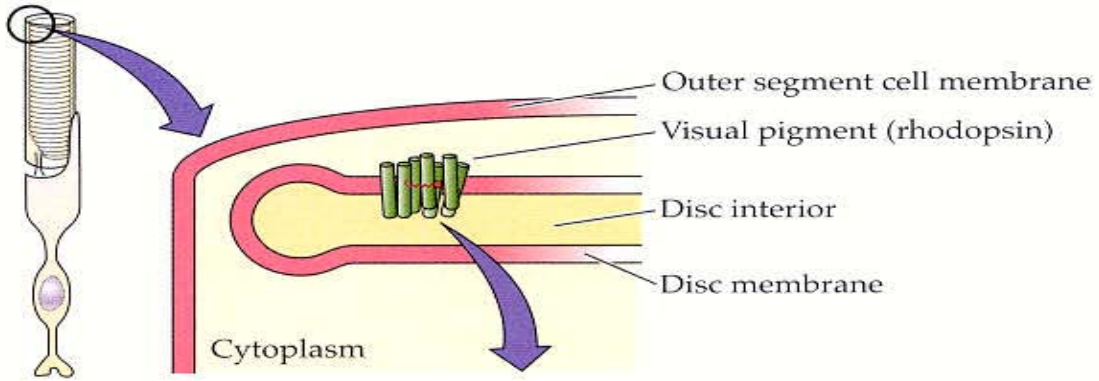

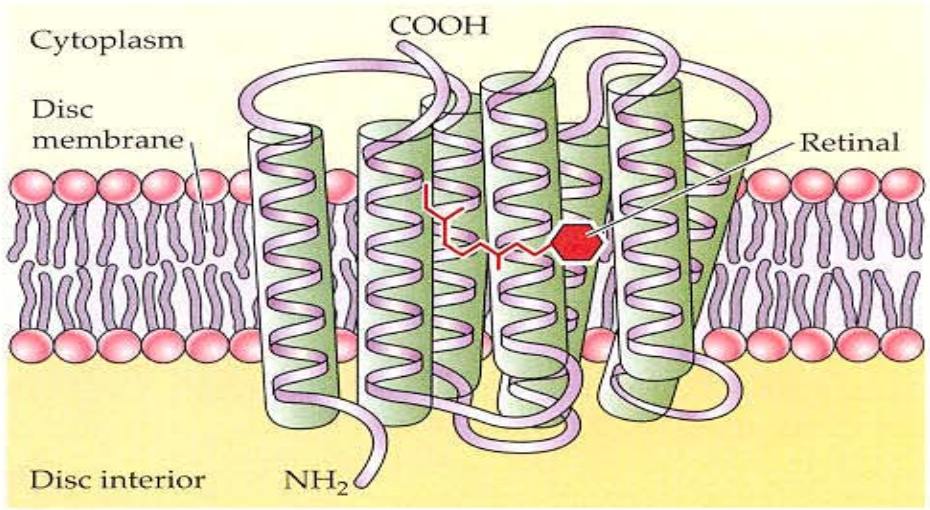

Prostetická skupina – chromofor nezbytná pro absorpci vyšších délek
Chromofor ve funkci ligandu, světlo iniciuje

Drosophila jako model zrakové transdukce:
Zesílení – jediný foton
Nízký šum ve tmě (spontánní termální izomerizace)
Adaptace - 10^6
Terminace odpovědi
Nejrychlejší známá G signální dráha

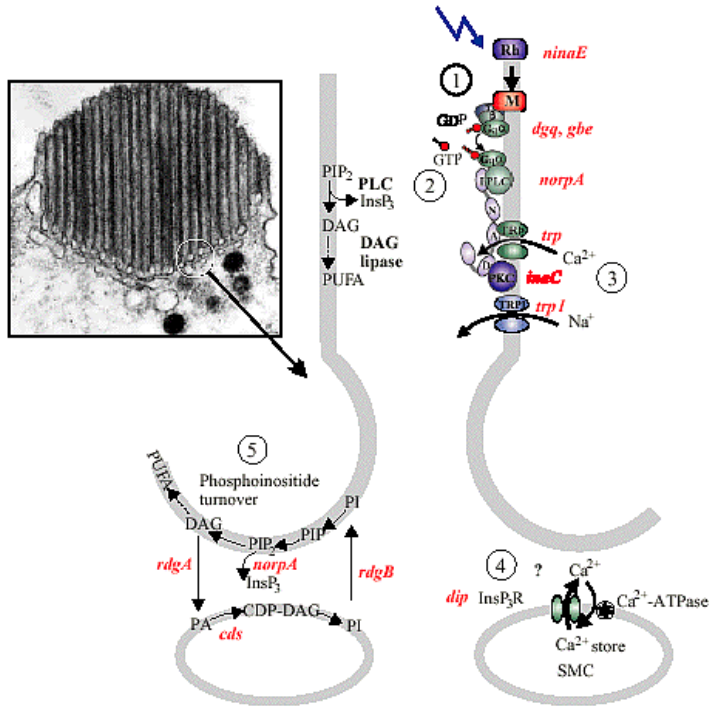

Fig. 1. *Drosophila melanogaster* phototransduction cascade. Inset: cross-section of a *Drosophila melanogaster* rhabdomere (electron micrograph courtesy of Dr A Polyanovsky), which is composed of some 30 000 microvilli, each approximately 1–2 µm in length and 60 nm in diameter. Each microvillus contains approximately 1000 molecules of rhodopsin and most elements of the phototransduction machinery. An enlargement of the circled area in the inset, showing the base of one microvillus with associated phototransduction machinery, is shown schematically in the main figure. Activation: (1) photoisomerization of rhodopsin to metarhodopsin (Rh→M, encoded by the *ninaE* gene) activates heterotrimeric G_q protein *via* GTP–GDP exchange, releasing the $G_q\alpha$ subunit. Genes and mutants for both α (*dgq*) and β (*gbe*) subunits have been identified. (2) $G_q\alpha$ activates phospholipase C (PLC; *norpA* gene), generating inositol 1,4,5-trisphosphate ($InsP_3$) and diacyl glycerol (DAG) from phosphatidyl inositol 4,5-bisphosphate (PIP_2). DAG is also a potential precursor for polyunsaturated fatty acids (PUFAs) *via* DAG lipase (gene yet to be identified in any eukaryote). (3) Two classes of light-sensitive channel (TRP and TRPL; *trp* and *trpl* genes) are activated by an unknown mechanism. Several components of the cascade, including the ion channel TRP, protein kinase C (PKC, *inaC* gene) and PLC are coordinated into a signalling complex by the scaffolding protein, INAD, which contains five PDZ domains. (4) At the base of the microvilli, a system of submicrovillar cisternae (SMC) has traditionally been presumed to represent Ca^{2+} stores endowed with $InsP_3$ receptors ($InsP_3R$; *dip* gene) and smooth endoplasmic reticulum Ca^{2+}-ATPase; however, the SMC may play a more important role in phosphoinositide turnover (5): DAG is converted to phosphatidic acid (PA) *via* DAG kinase (*rdgA* gene) and to CDP-DAG *via* CD synthase (*cds* gene) in the SMC. After conversion to phosphatidyl inositol (PI) by PI synthase, PI is transported back to the microvillar membrane by a PI transfer protein (*rdgB* gene). PI is converted to PIP_2 *via* sequential phosphorylation (PI kinase and PIP kinase).

Taková rychlost? PDE jeden z nejvýkonnějších známých enzymů
Výkonnost transdukce omezena difuzním pohybem v membráně.

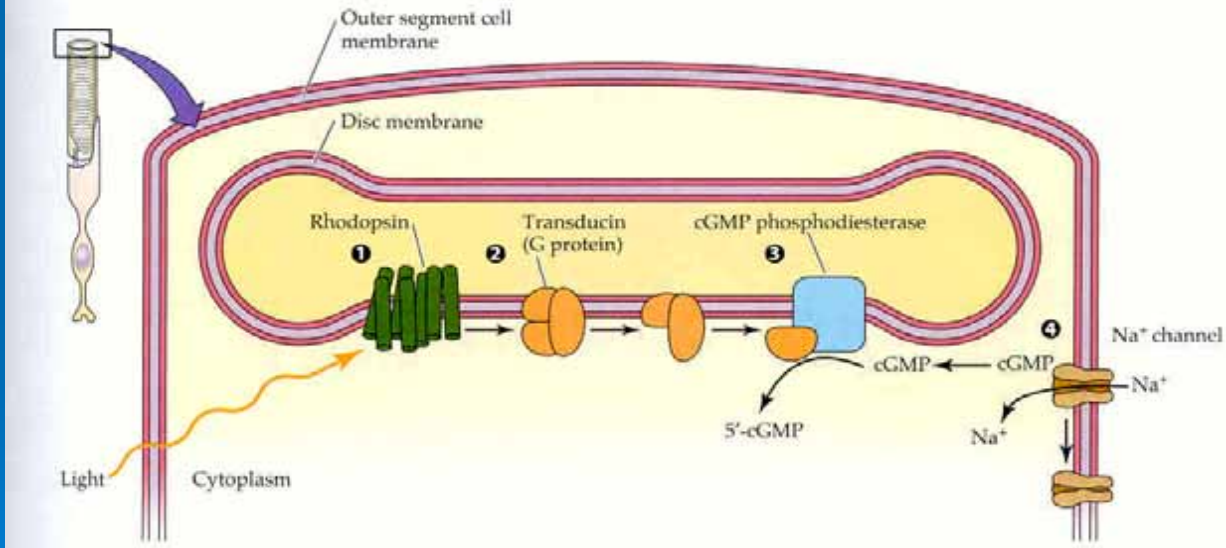

Figure 13.14 Phototransduction closes cation channels in the outer segment of the photoreceptor membrane In the dark, the cation channels are kept open by intracellular cGMP and conduct an inward current, carried largely by Na^+. When light strikes the photoreceptor, these channels are closed by a G protein–coupled mechanism. ❶ Rhodopsin molecules in the disc membrane absorb light and are activated. ❷ The activated rhodopsin stimulates a G protein (transducin in rods), which in turn activates cGMP phosphodiesterase. ❸ The phosphodiesterase catalyzes the breakdown of cGMP to 5′-GMP. ❹ As the cGMP concentration decreases, cGMP detaches from the cation channels, which close.

Difuzní model signálového přenosu x Signalplex, scaffolding proteins
Multimolekulární signalizační komplex

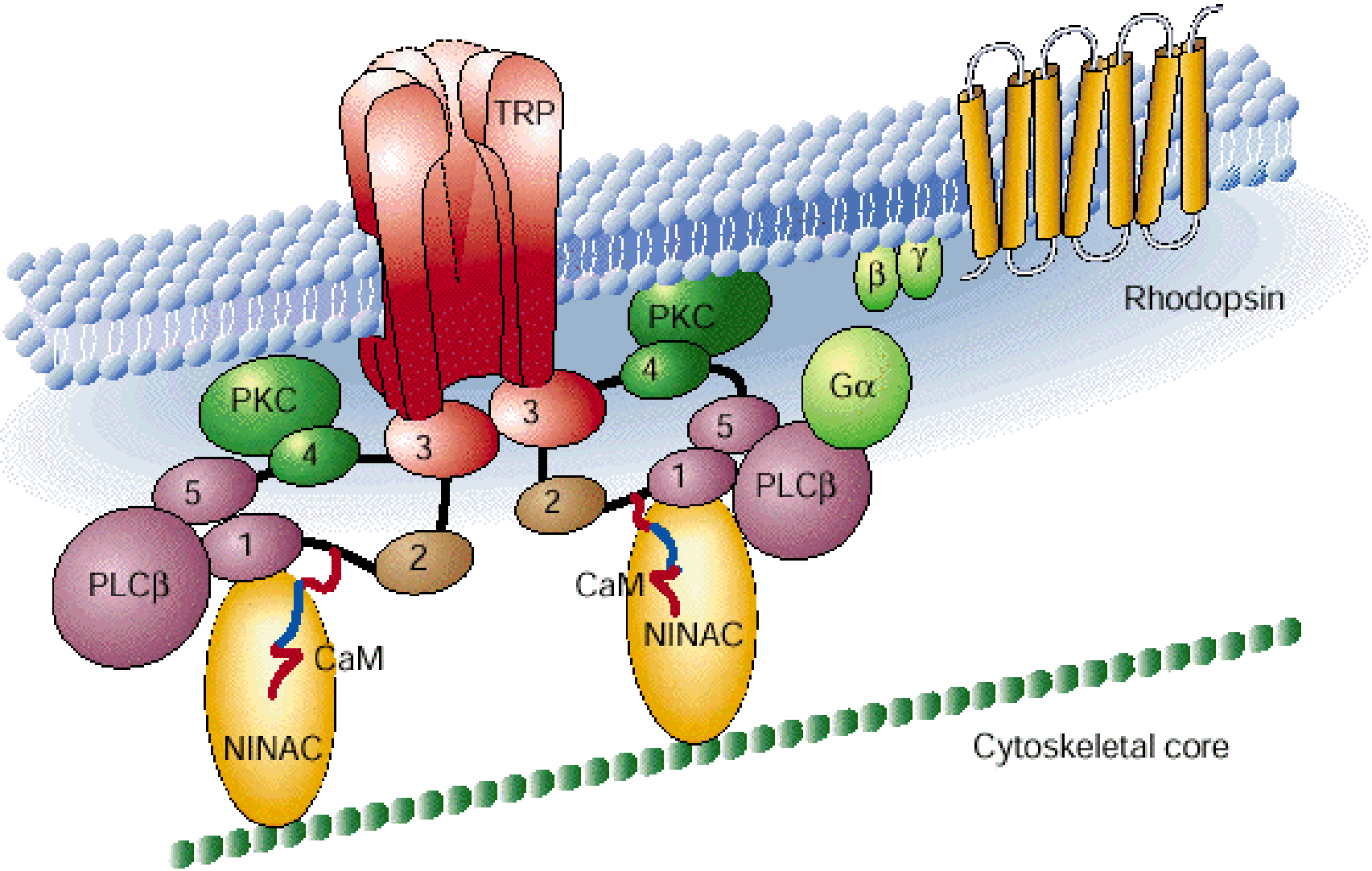

Organizace signálních proteinů
v čase a prostoru – oddělení, zhášení
V odpověď na světlo

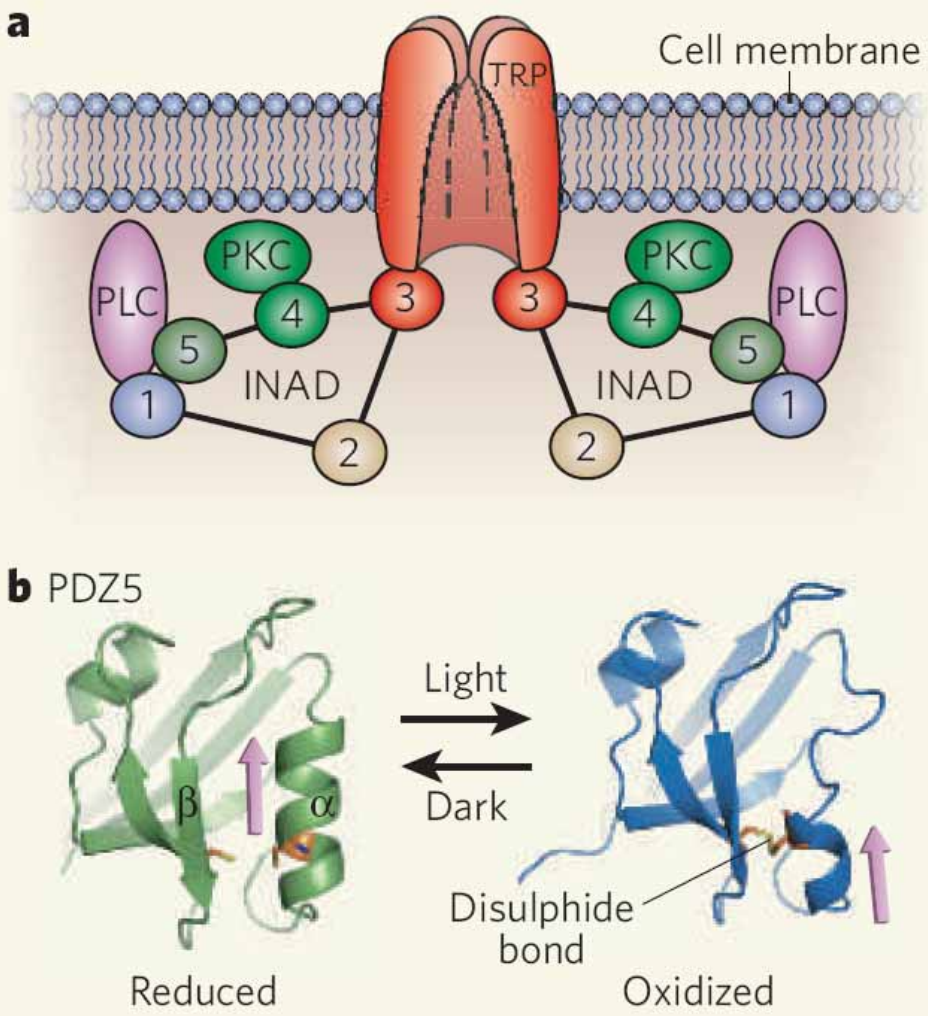

Figure 1 | Phototransduction in *Drosophila* and the INAD complex. **a**, The five PDZ domains of INAD (1–5) assemble components of the phototransduction cascade, including PLC, the TRP channel and PKC, into a signalling complex at the cell membrane. **b**, Mishra *et al.*[2] report that, in response to light, the PDZ5 domain of INAD undergoes a conformational change. In the dark, PDZ5 is in its canonical, reduced form, in which a groove between an α-helix and a β-sheet serves as a ligand-binding site. After stimulation with light, the PDZ5 domain undergoes a conformational change to an oxidized state, whereby the formation of a disulphide bond between two cysteine residues results in the unravelling of the α-helix and the distortion of the ligand-binding groove. Following this conformational switch, the ligand (arrowed) — putatively part of the PLC enzyme — can no longer bind. (Adapted from ref. 2.)

Taková adaptace?
Translokace TRP –
Mechanismus adaptace
na tmu a světlo

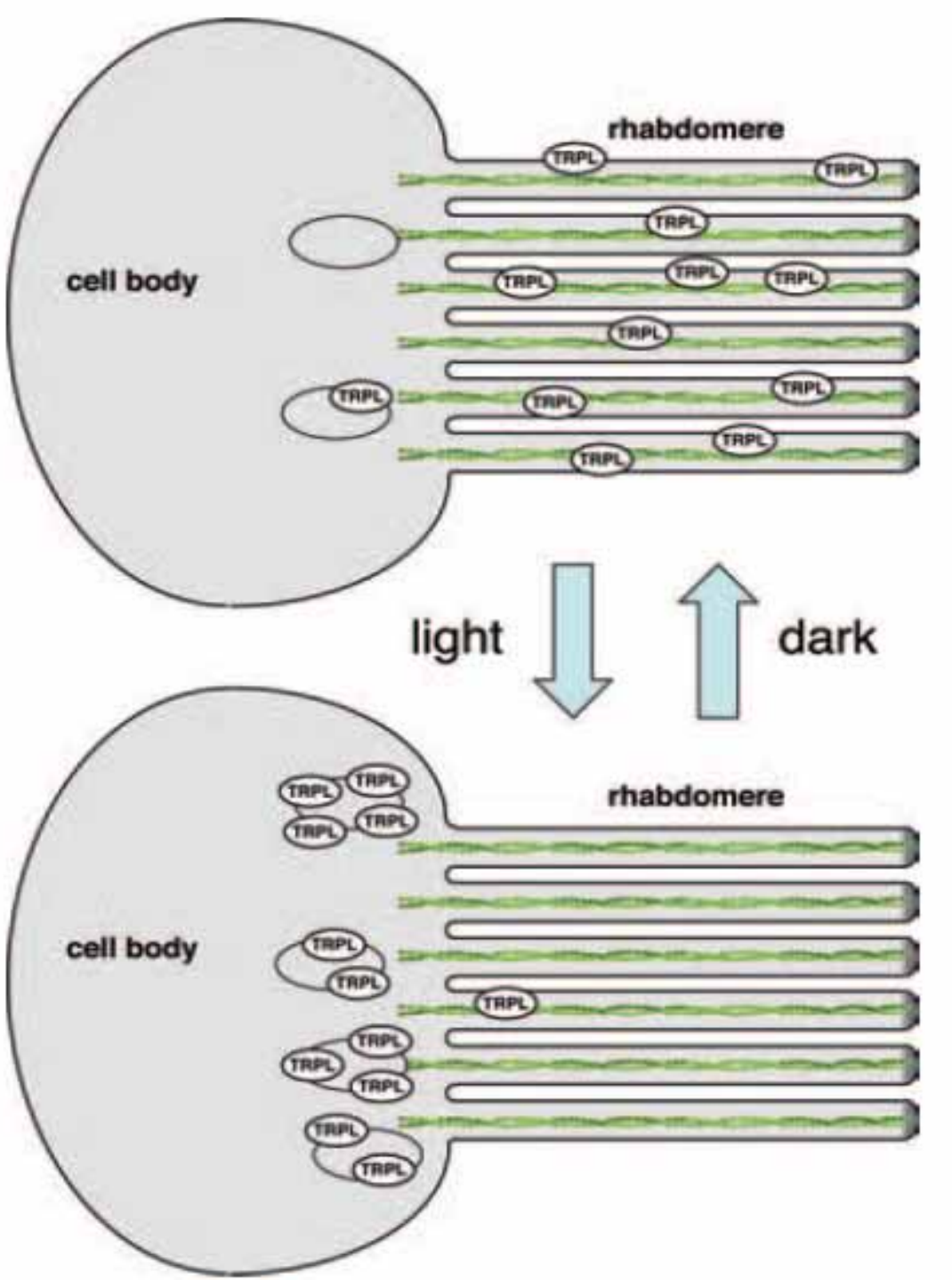

Chemorecepce - čich

Konzervativní organizace
Podobnost s rhodopsinem

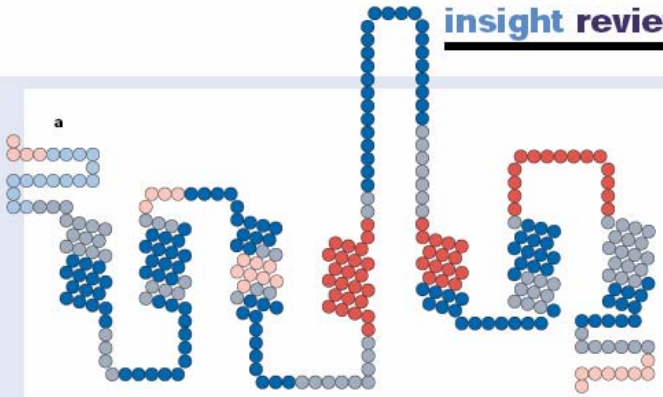

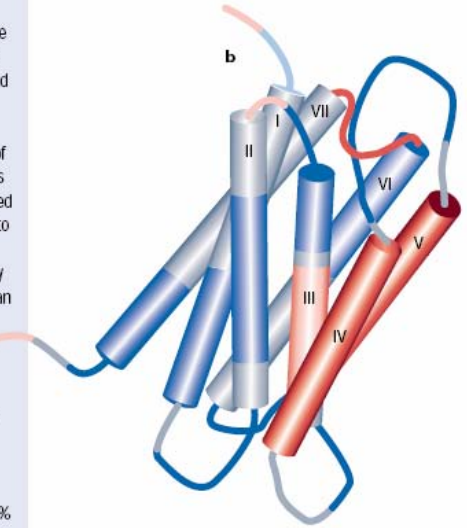

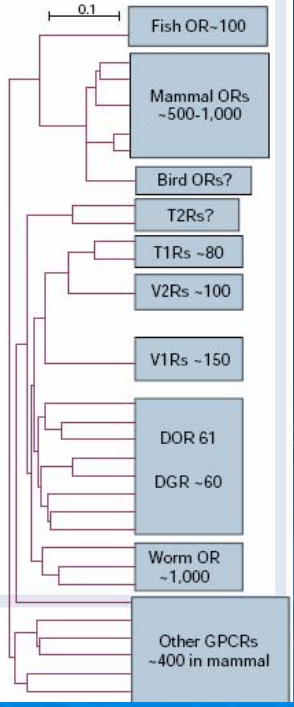

Figure 2 Odorant receptors are the jewel of olfactory research in the past 10 years. The odorant receptors comprise the largest family of GPCRs. In mammals, odour receptors are represented by as many as 1,000 genes and may account for as much as 2% of the genome. Sequence comparison across the receptors has revealed many regions of conservation and variability that may be related to function. **a**, In a 'snake' diagram showing the amino acids for a particular receptor (M71), those residues that are most highly conserved are shown in shades of blue and those that are most variable are shown in shades of red. The seven α-helical regions (boxed) are connected by intracellular and extracellular loops. **b**, A schematic view of the proposed three-dimensional structure of the receptor based on the recently solved structure of rhodopsin. Each of the transmembrane regions is numbered according to that model. The conserved (blue) and variable (red) regions are sketched onto this qualitative view and suggest that a ligand-binding region may be at least partially formed by the variable regions of the receptor. **c**, Mammalian odour receptors are related phylogenetically to other chemosensory receptors. In the tree depicted here the numbers refer to the approximate number of receptors in each family. OR, Odorant receptors; T1R, T2R, taste receptors; V3R, vomeronsal receptors; DOR, DGR, *Drosophila* odour and gustatory receptors; worm refers to *C. elegans*. The scale bar is a graphical distance equal to 10% sequence divergence.

But this ambitious experimental programme has barely progressed, owing to the puzzling difficulty of expressing ORs in heterol-

release that was measured by fura-2 imaging. Finally,

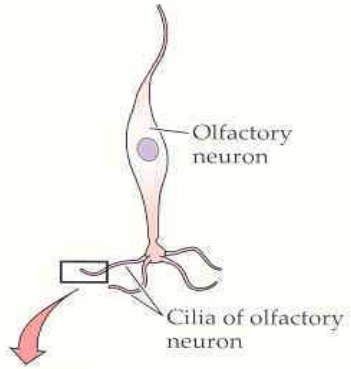

Figure 13.36 Olfactory transduction mechanisms in cilia membranes of olfactory neurons *(a)* Many odorants act to increase cyclic AMP. The odorant binds to an odorant receptor on the ciliary membrane; the receptor activates a G protein to activate adenylyl cyclase, producing cAMP. Cyclic AMP binds to and opens a cation channel, allowing entry of Na^+ and Ca^{2+} ions to depolarize the cell. Ca^{2+} binds to Ca^{2+}-activated Cl^- channels, augmenting the depolarization. *(b)* Some olfactory responses increase IP_3. This mechanism also starts with odorant binding to a G protein–coupled receptor, but in this case the G protein activates phospholipase C, forming IP_3 from PIP_2 (see Figure 12.21). IP_3 binds to and opens a calcium channel, letting Ca^{2+} enter to depolarize the cell. As in *(a)*, Ca^{2+}-activated Cl^- channels augment the depolarization.

(a) Increase in cAMP

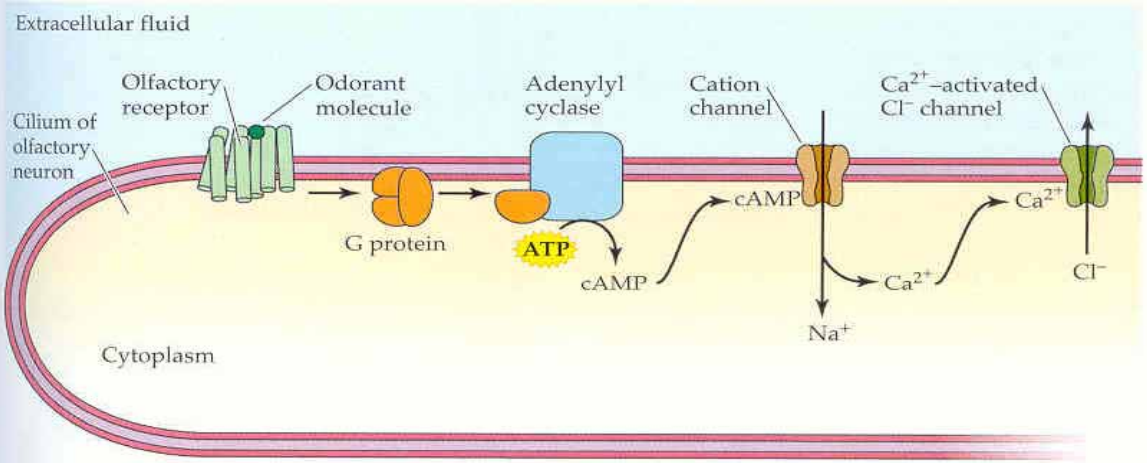

(b) Increase in IP_3

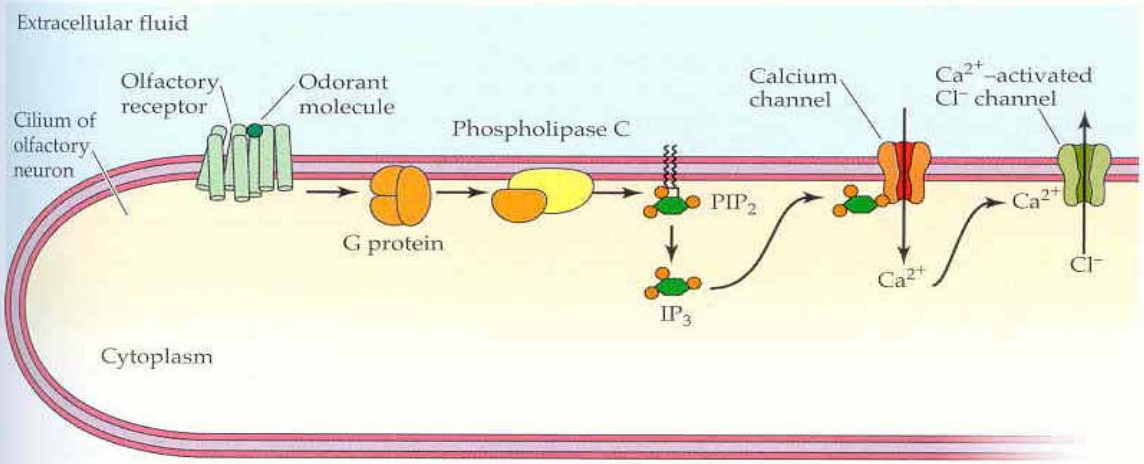

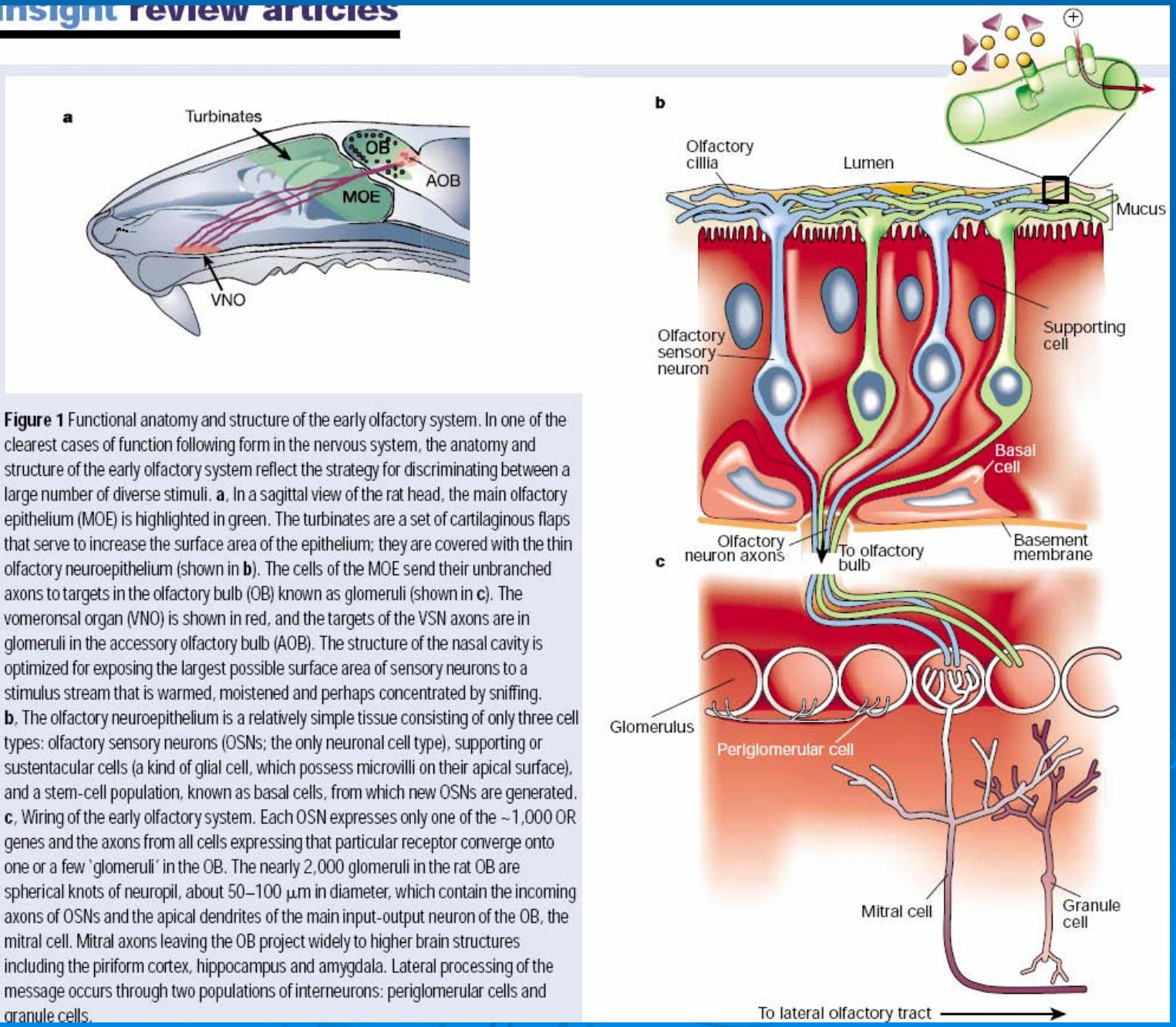

Figure 1 Functional anatomy and structure of the early olfactory system. In one of the clearest cases of function following form in the nervous system, the anatomy and structure of the early olfactory system reflect the strategy for discriminating between a large number of diverse stimuli. **a**, In a sagittal view of the rat head, the main olfactory epithelium (MOE) is highlighted in green. The turbinates are a set of cartilaginous flaps that serve to increase the surface area of the epithelium; they are covered with the thin olfactory neuroepithelium (shown in **b**). The cells of the MOE send their unbranched axons to targets in the olfactory bulb (OB) known as glomeruli (shown in **c**). The vomeronsal organ (VNO) is shown in red, and the targets of the VSN axons are in glomeruli in the accessory olfactory bulb (AOB). The structure of the nasal cavity is optimized for exposing the largest possible surface area of sensory neurons to a stimulus stream that is warmed, moistened and perhaps concentrated by sniffing. **b**, The olfactory neuroepithelium is a relatively simple tissue consisting of only three cell types: olfactory sensory neurons (OSNs; the only neuronal cell type), supporting or sustentacular cells (a kind of glial cell, which possess microvilli on their apical surface), and a stem-cell population, known as basal cells, from which new OSNs are generated. **c**, Wiring of the early olfactory system. Each OSN expresses only one of the ~1,000 OR genes and the axons from all cells expressing that particular receptor converge onto one or a few 'glomeruli' in the OB. The nearly 2,000 glomeruli in the rat OB are spherical knots of neuropil, about 50–100 μm in diameter, which contain the incoming axons of OSNs and the apical dendrites of the main input-output neuron of the OB, the mitral cell. Mitral axons leaving the OB project widely to higher brain structures including the piriform cortex, hippocampus and amygdala. Lateral processing of the message occurs through two populations of interneurons: periglomerular cells and granule cells.

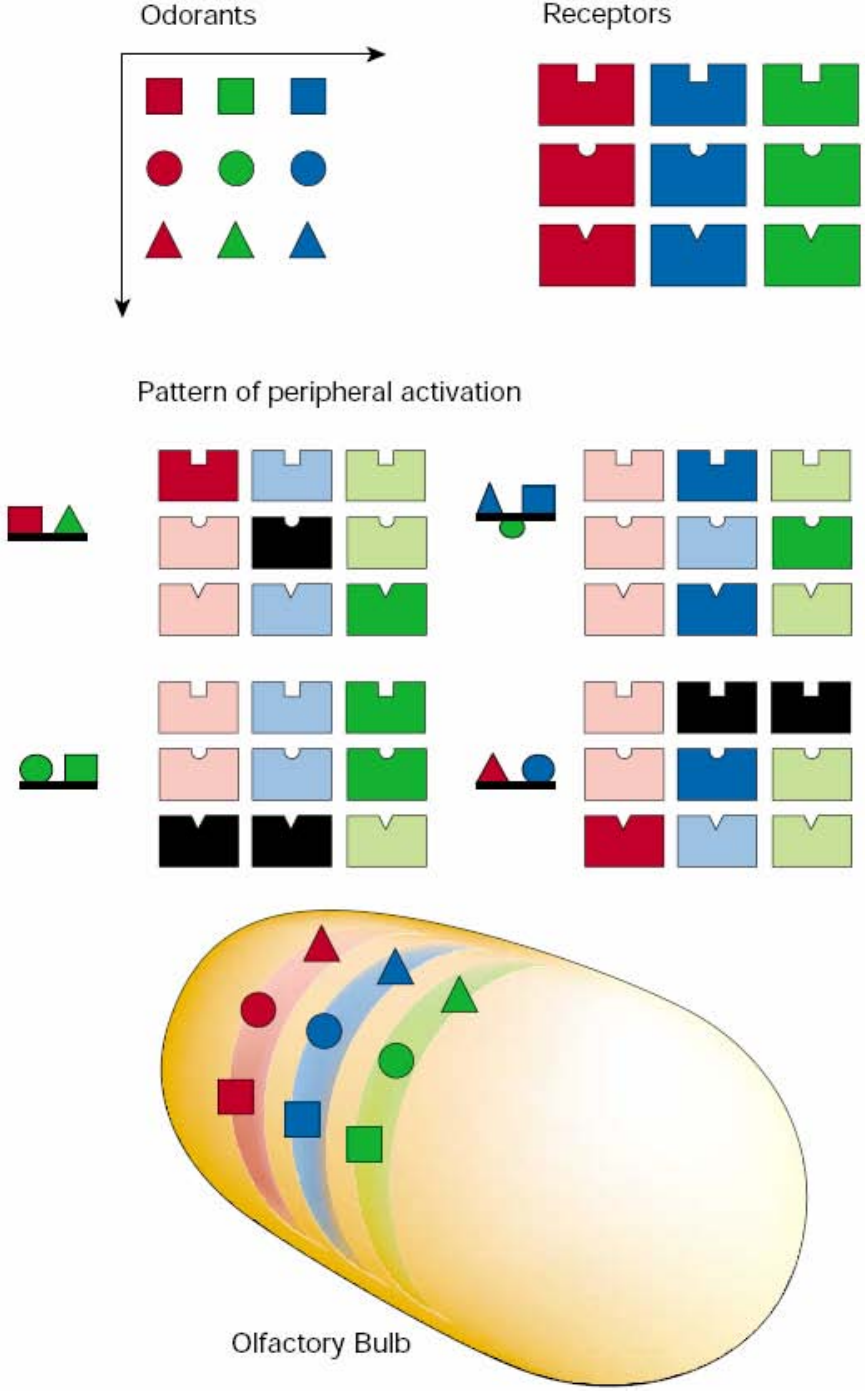

Although there are some 1,000 ORs, detecting the enormous repertoire of odours requires a combinatorial strategy. Most odour molecules are recognized by more than one receptor (perhaps by dozens) and most receptors recognize several odours, probably related by chemical property. The scheme in the figure represents a current consensus model. There are numerous molecular features, two of which are represented here by colour and shape. Receptors are able to recognize different features of molecules, and a particular odour compound may also consist of a number of these 'epitopes' or 'determinants' that possess some of these features. Thus the recognition of an odorant molecule depends on which receptors are activated and to what extent, as shown by the shade of colour (black represents no colour or shape match and thus no activation). Four odour compounds are depicted with the specific array of receptors each would activate. Note that there are best receptors (for example, red square), but also other receptors that are able to recognize some feature of the molecule (for example, any square) and would participate in the discrimination of that compound. In the olfactory bulb there seem to be wide areas of sensitivity to different features (for example, functional group or molecular length). This model is based on current experimental evidence, but is likely to undergo considerable revision as more data become available.

Chemorecepce - chuť

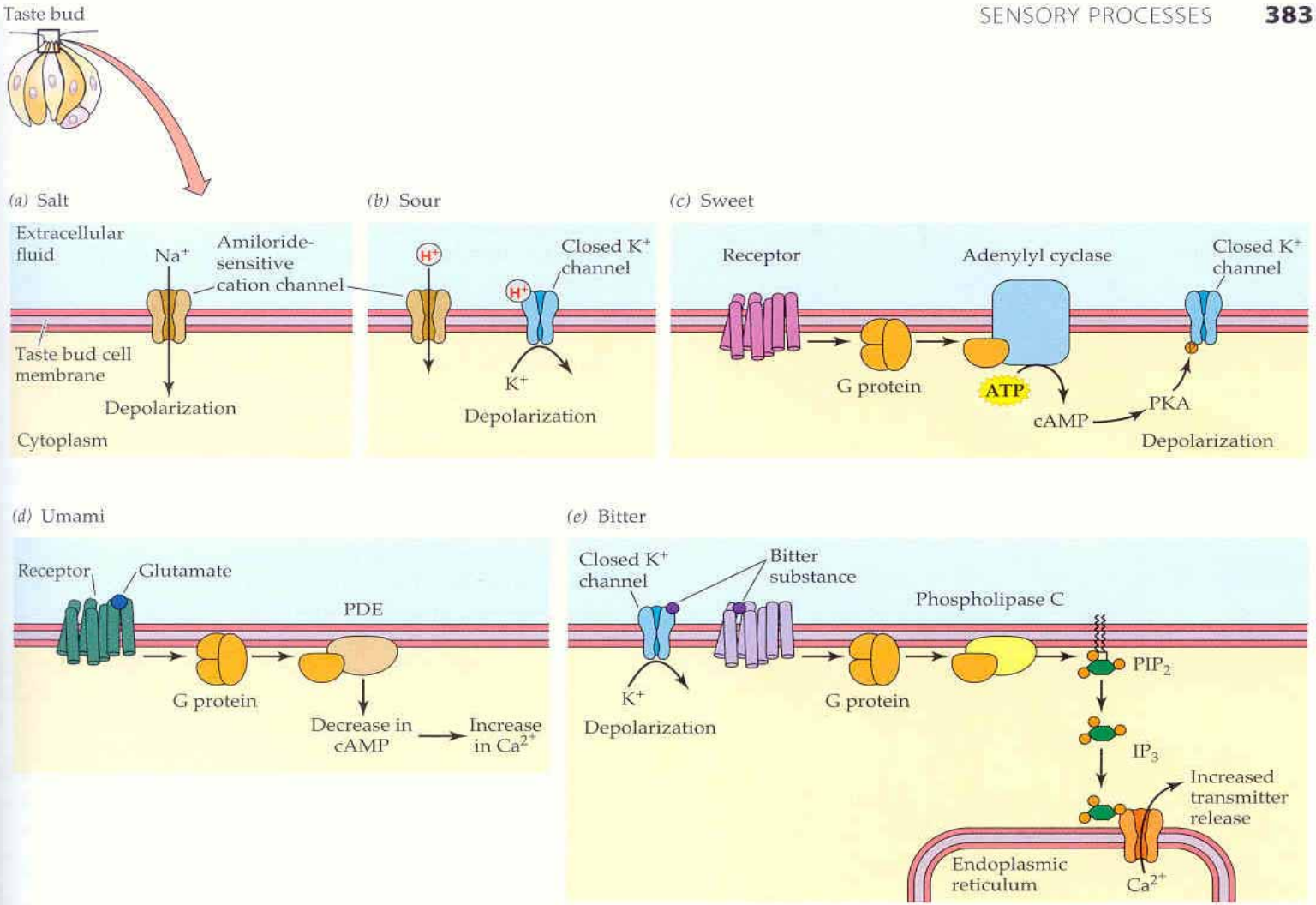

igure 13.34 Taste-transduction mechanisms differ for different aste qualities All transduction mechanisms except the IP_3 action in e) lead to *depolarization*, which spreads to the basal end of the cell nd opens voltage-gated Ca^{2+} channels to allow Ca^{2+} entry and trans-itter release. *(a)* For salt taste, sodium ions enter a taste bud cell hrough amiloride-sensitive cation channels, directly depolarizing the ell. *(b)* In sour taste, either H^+ ions enter the cell through amiloride-ensitive cation channels, or they close K^+ channels to produce depo-arization. *(c)* Sweet taste is most commonly mediated by the binding f sugars to a G protein–coupled receptor, which acts via a G protein to ctivate adenylyl cyclase and produce cyclic AMP. Cyclic AMP then acti-ates protein kinase A (PKA) to close a K^+ channel (by phosphorylating it), producing depolarization. *(d)* The amino acid glutamate (monosodium glutamate, MSG) stimulates the taste quality umami (a savory or meaty quality). Glutamate binds to a G protein–coupled receptor (related to synaptic metabotropic glutamate receptors) to activate a phosphodiesterase (PDE) and decrease the concentration of cAMP. The decrease in cAMP leads to an increase in intracellular Ca^{2+} concentration. *(e)* Bitter taste mechanisms can involve a G protein–coupled receptor for bitter substances that acts via a G protein and phospholipase C to produce IP_3. IP_3 liberates Ca^{2+} ions from intracellular stores, eliciting transmitter release without requiring depolarization. Other bitter substances bind to K^+ channels and close them to depolarize the cell.

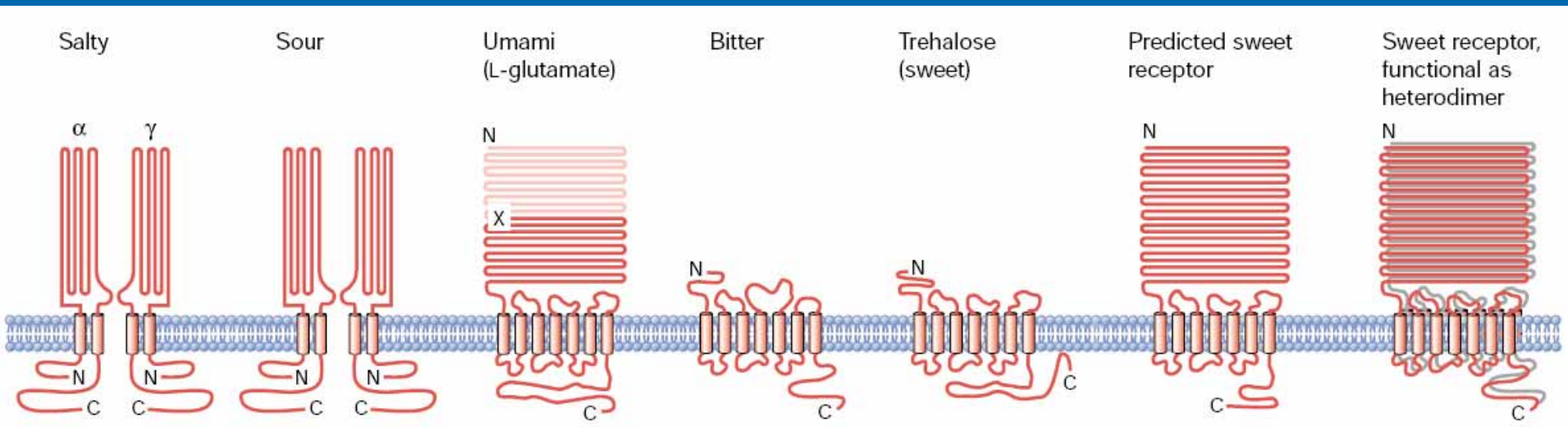

ENaC/Deg, others (refs 34,35)

ENaC, ASIC, HCN, others (refs 40,43)

Taste mGluR4, others (ref. 94)

T2R family, others (refs 47-49)

Predicted receptor of *Drosophila* (ref. 69)

T1R3 (*sac* locus) (refs 72-75)

T1R2/T1R3 (refs 76,77)

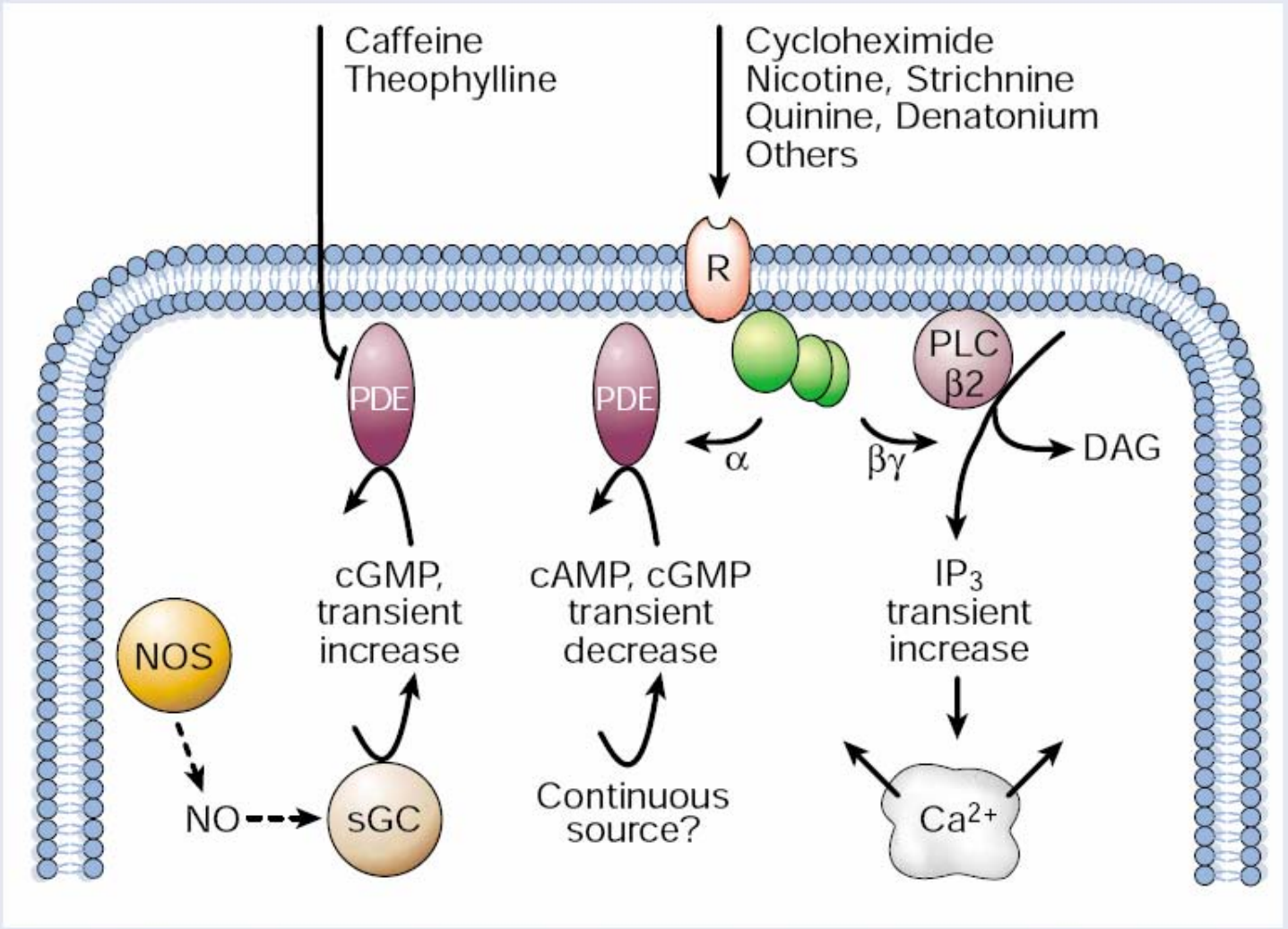

Figure 3 Transduction of bitter taste as elicited by a variety of ligands. Rs, multiple GPCRs of the T2R family, coupled to the G protein gustducin[47–49]; α, α-subunit of gustducin[6,57]; βγ, G-protein subunits β3 and γ13 (refs 60–62); PLCβ2, phospholipase C subtype[61]; Ins(1,4,5)P_3, inositol-1,4,5-trisphosphate[59]; PDE, taste-specific phosphodiesterase[58]; cAMP, cyclic adenosine monophosphate[59]; cGMP, cyclic guanosine monophosphate[59]; sGC, soluble guanylate cyclase[55]; NO, nitric

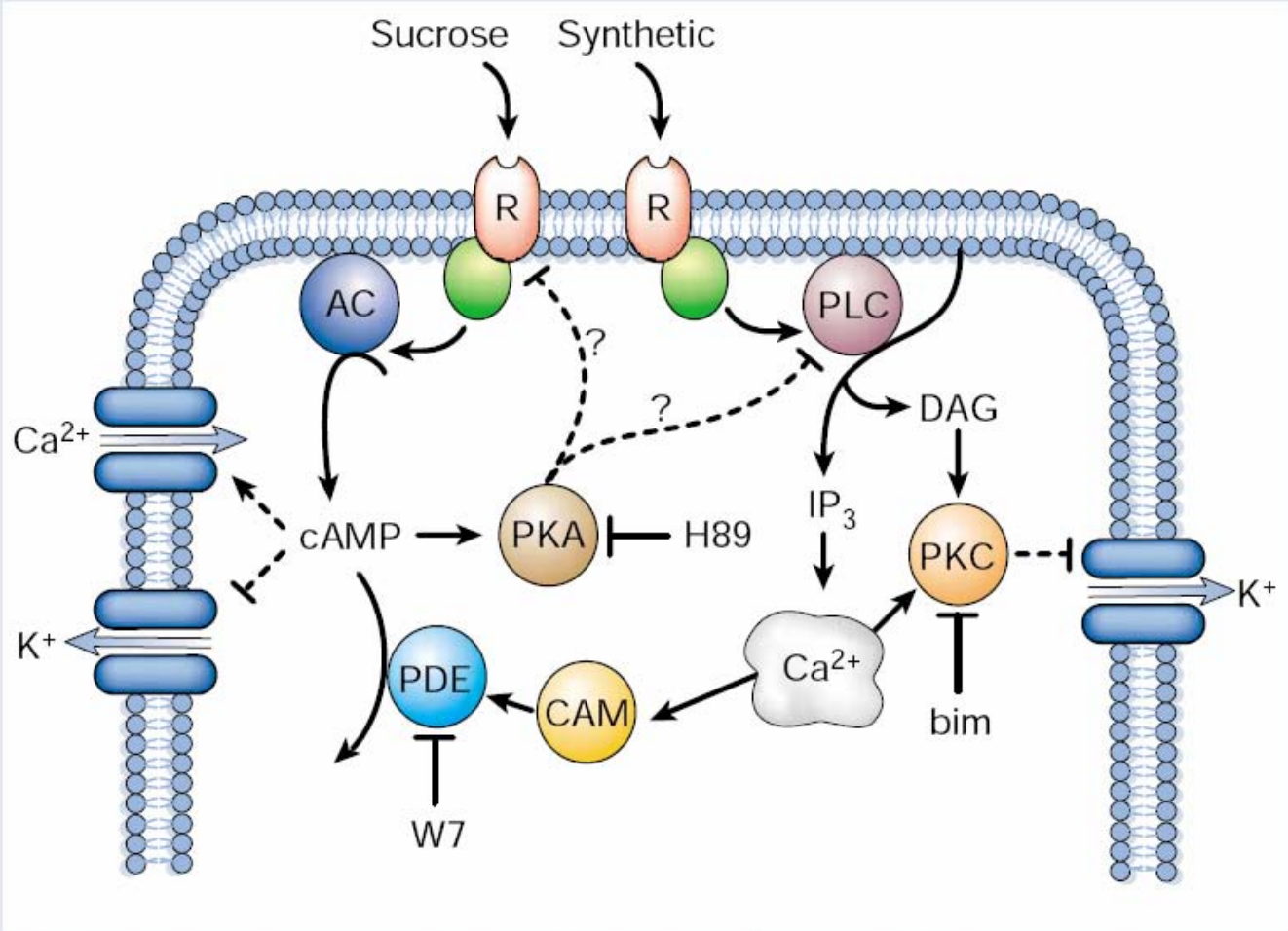

Figure 4 Molecules involved in the transduction of sweet taste. Two separate sweet receptors are shown, but the possibility that one receptor activates both of the transduction pathways[100] is not excluded at this stage. R, candidate receptor(s)[72–75]; AC, adenylate cyclase[81,82,87]; cAMP, cyclic adenosine monophosphate[21]; PDE, phosphodiesterase, inhibitor W7 (ref. 89); CAM, calmodulin[89]; PKA, protein kinase A, inhibitor H89 (ref. 89); PLC, phospholipase C[89]; DAG, diacylglycerol; Ins(1,4,5)P_3, inositol-1,4,5-trisphosphate[21]; PKC, protein kinase C, inhibitor bim (bisindolylmaleimide)[89]. For crosstalk between pathways and effects of inhibitors

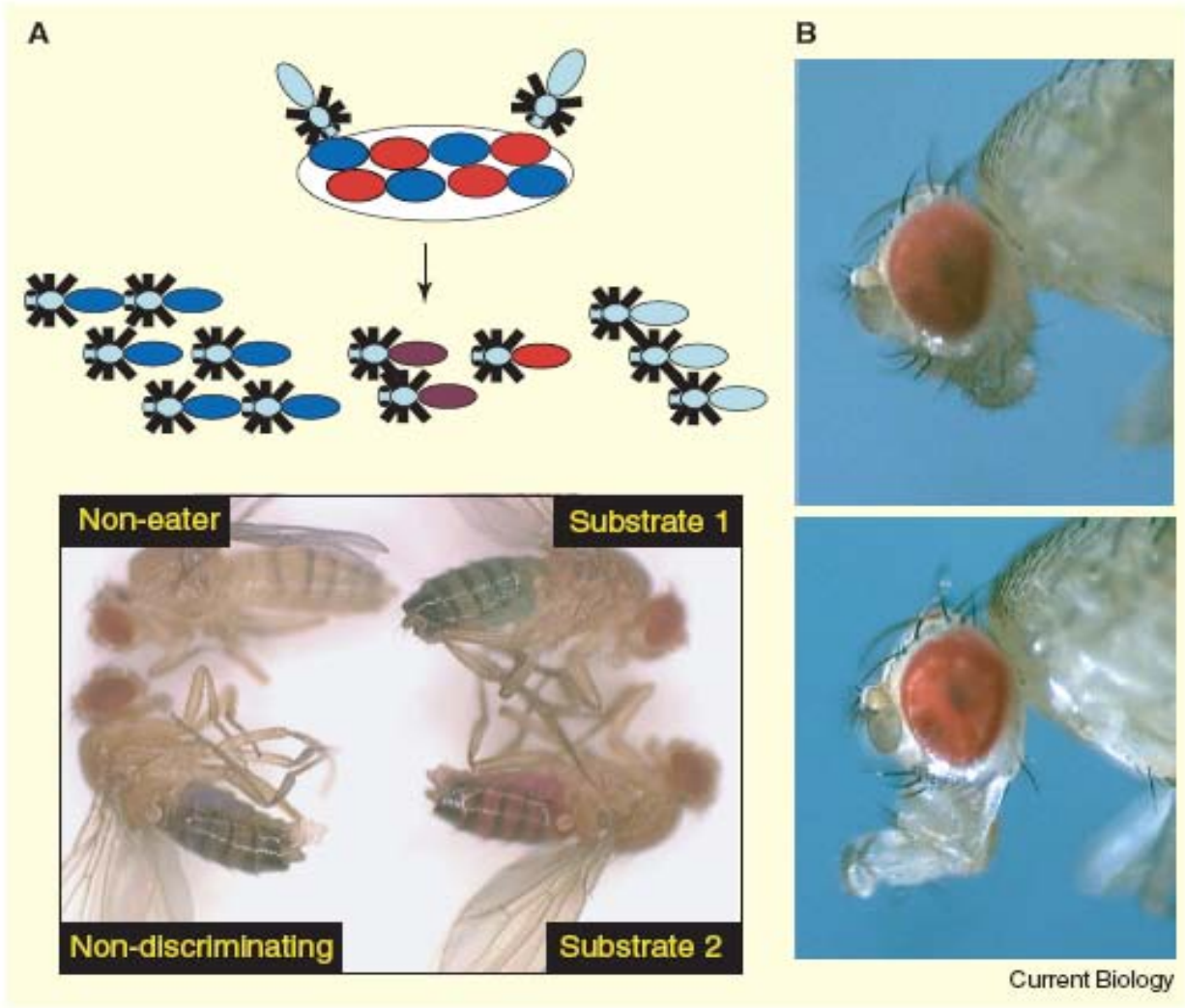

Figure 2. Assays of feeding behavior.

(A) Two-choice preference assay. Flies are first starved for a day and then provided with the choice of two chemicals, presented on a multi-well plate at specific concentrations in an agar medium. The two food substrates also contain different tasteless compounds that have intrinsic colors. For example, sucrose might be added in one half of the wells on a titer plate, along with the sulforhodamine B dye (red) and trehalose, along with an erioglaucine dye (blue) on the other half of the wells. The feeding is carried out in darkness (to exclude any influence of color preference) and the abdomen of the flies is inspected visually. The number of flies feeding on either substrate (red or blue abdomen) and both substrates (purple abdomen) are used to determine the feeding preference index: PI (sucrose) = N(red) + 0.5N(purple) / N(red)+N(blue)+N(purple). (B) Proboscis extension reflex. This does not measure feeding behavior, but rather a reflex behavior associated with feeding. Starved flies are narcotized and immobilized and then let to awaken and recover. Upon satiation with water, the forelegs of the fly — the GRNs — are stimulated with a chemical and the number of proboscis extensions are counted over a short period directly following the stimulation. The proboscis is usually withdrawn (top), but upon stimulation of the foreleg with a feeding stimulus (for example a sugar solution), is frequently extended (bottom). The number of extensions is directly correlated with the attractiveness of the stimulus.

Mechanorecepce – hmat, sluch

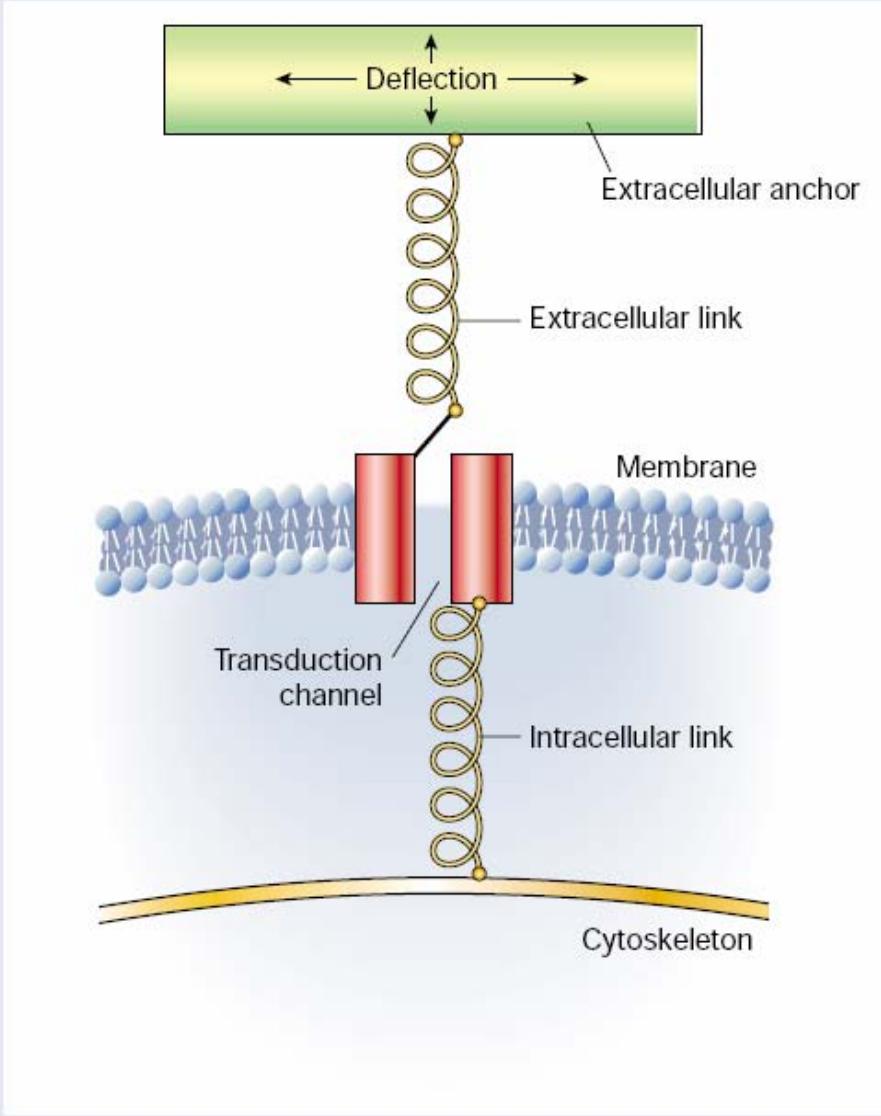

Figure 1 General features of mechanosensory transduction. A transduction channel is anchored by intracellular and extracellular anchors to the cytoskeleton and to an extracellular structure to which forces are applied. The transduction channel responds to tension in the system, which is increased by net displacements between intracellular and extracellular structures.

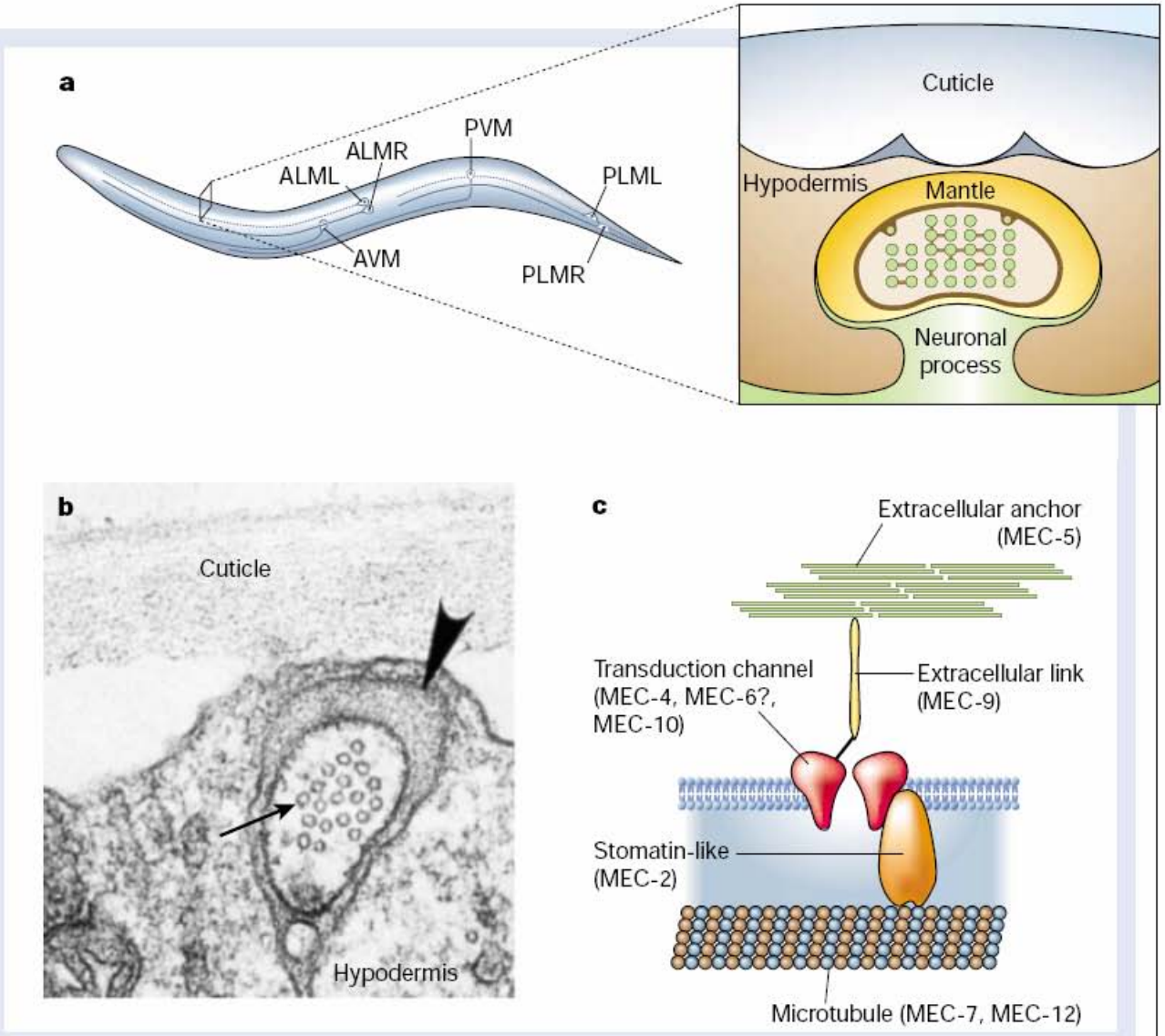

Figure 2 *C. elegans* touch-receptor structure and transduction model. **a**, View of *C. elegans* showing positions of mechanoreceptors. AVM, anterior ventral microtubule cell; ALML/R, anterior lateral microtubule cell left/right; PVM, posterior ventral microtubule cell; PLML/R, posterior lateral microtubule cell left/right. **b**, Electron micrograph of a touch-receptor neuron process. Mechanotransduction may ensue with a net deflection of the microtubule array relative to the mantle, a deflection detected by the transduction channel. Arrow, 15-protofilament microtubules; arrowhead, mantle. Modified from ref. 3. **c**, Proposed molecular model for touch receptor. Hypothetical locations of *mec* proteins are indicated.

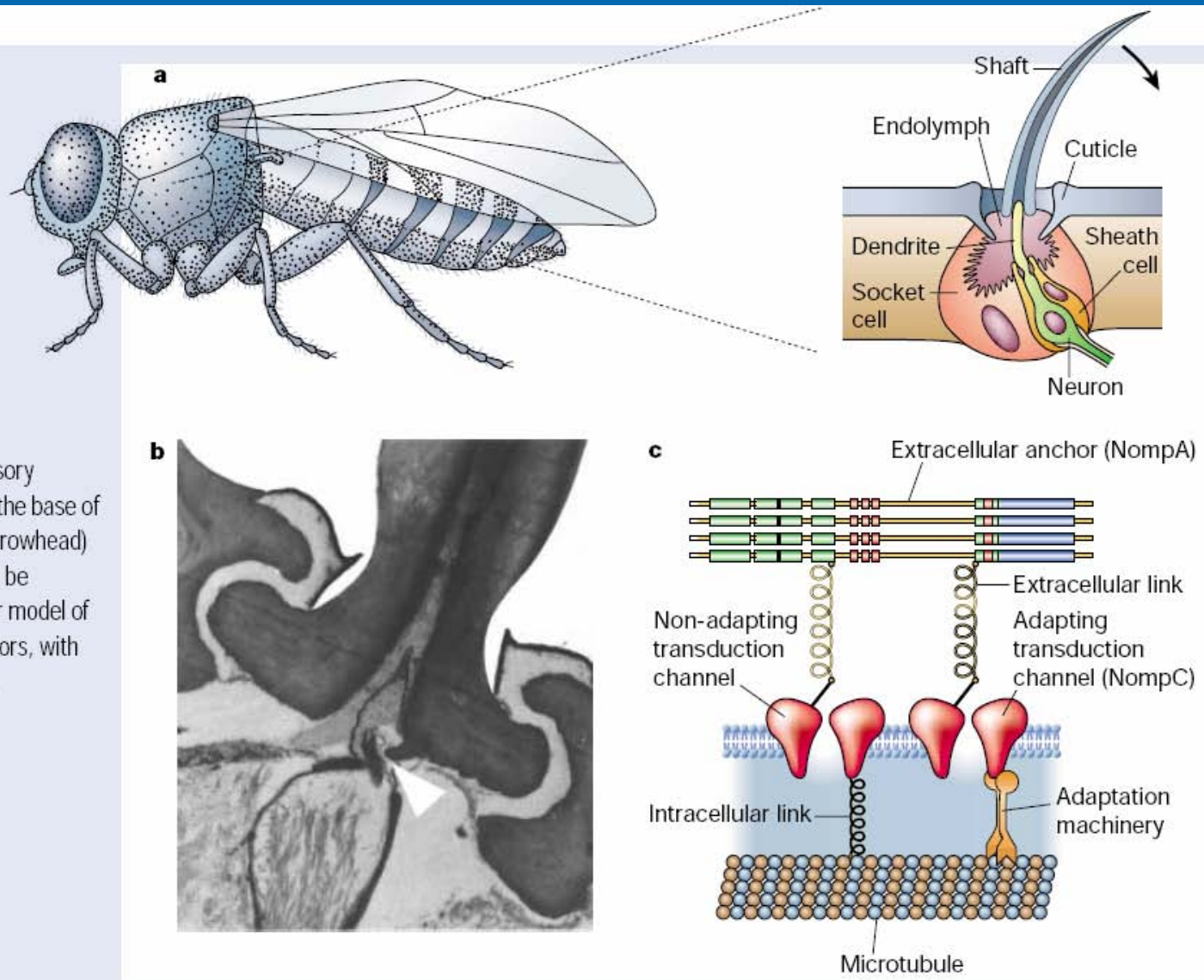

Figure 3 *Drosophila* bristle-receptor model. **a**, Lateral view of *D. melanogaster* showing the hundreds of bristles that cover the fly's cuticle. The expanded view of a single bristle indicates the locations of the stereotypical set of cells and structures associated with each mechanosensory organ. Movement of the bristle towards the cuticle of the fly (arrow) displaces the dendrite and elicits an excitatory response in the mechanosensory neuron. **b**, Transmission electron micrograph of an insect mechanosensory bristle showing the insertion of the dendrite at the base of the bristle. The bristle contacts the dendrite (arrowhead) so that movement of the shaft of the bristle will be detected by the neuron. **c**, Proposed molecular model of transduction for ciliated insect mechanoreceptors, with the locations of NompC and NompA indicated.

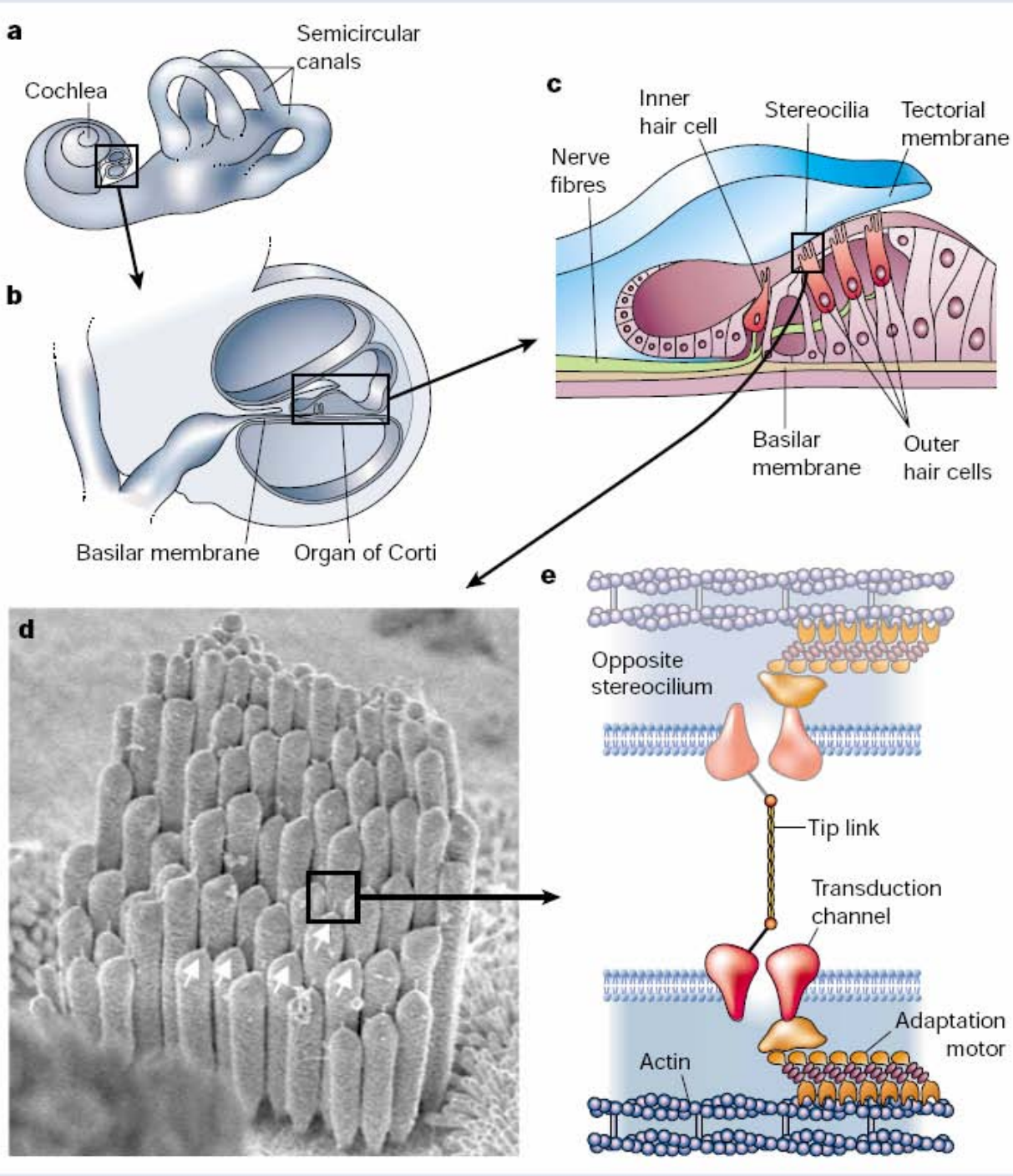

Figure 4 Inner-ear structure and hair-cell transduction model. **a**, Gross view of part of the inner ear. Sound is transmitted through the external ear to the tympanic membrane; the stimulus is transmitted through the middle ear to the fluid-filled inner ear. Sound is transduced by the coiled cochlea. **b**, Cross-section through the cochlear duct. Hair cells are located in the organ of Corti, resting on the basilar membrane. **c**, Sound causes vibrations of the basilar membrane of the organ of Corti; because flexible hair-cell stereocilia are coupled to the overlying tectorial membrane, oscillations of the basilar membrane cause back-and-forth deflection of the hair bundles. **d**, Scanning electron micrograph of hair bundle (from chicken cochlea). Note tip links (arrows). **e**, Proposed molecular model for hair-cell transduction apparatus.

Rychlá

Aktivní pohyb:
Adaptace
Tanec v rytmu

Pomalá

Obě závislé na Ca^{2+}

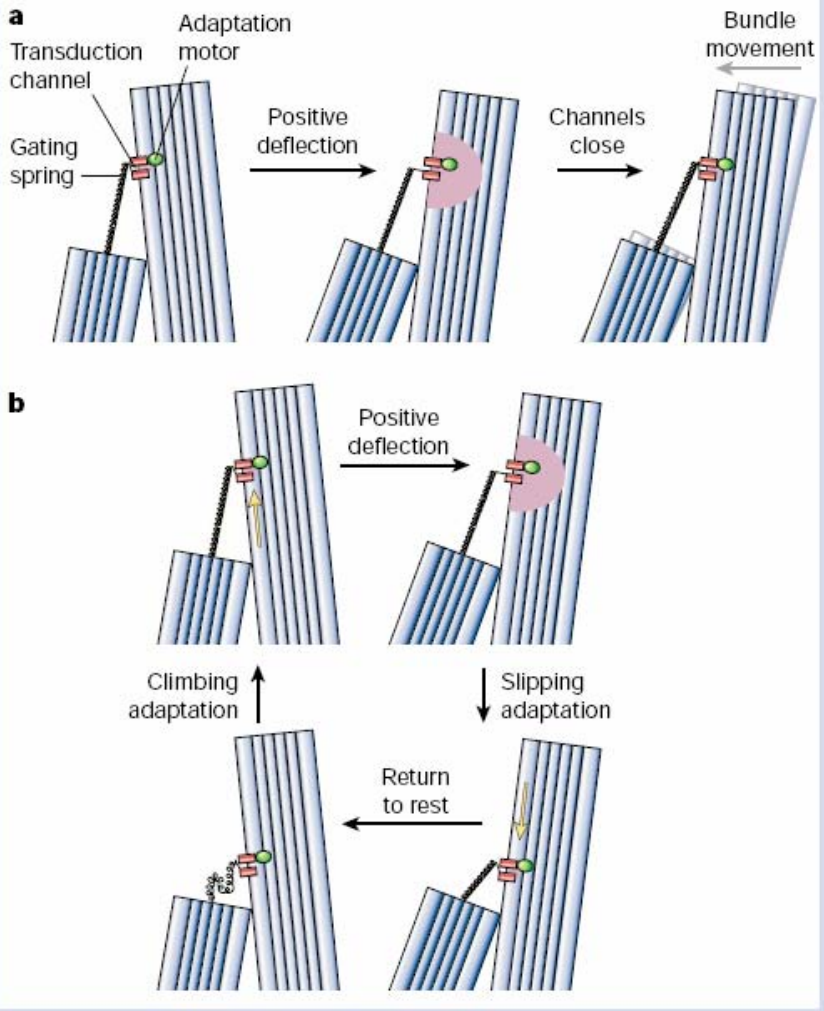

Box 2 Figure Hair-cell transduction and adaptation. **a**, Transduction and fast adaptation. At rest (left panel), transduction channels spend ~5% of the time open, allowing a modest Ca^{2+} entry (pink shading). A positive deflection (middle) stretches the gating spring (drawn here as the tip link); the increased tension propagates to the gate of the transduction channel, and channels open fully. The resulting Ca^{2+} flowing in through the channels shifts the channels' open probability to favour channel closure (right). As the gates close, they increase force in the gating spring, which moves the bundle back in the direction of the original stimulus. **b**, Transduction and slow adaptation. Slow adaptation ensues when the motor (green oval) slides down the stereocilium (lower right), allowing channels to close. After the bundle is returned to rest (lower left), gating-spring tension is very low; adaptation re-establishes tension and returns the channel to the resting state.

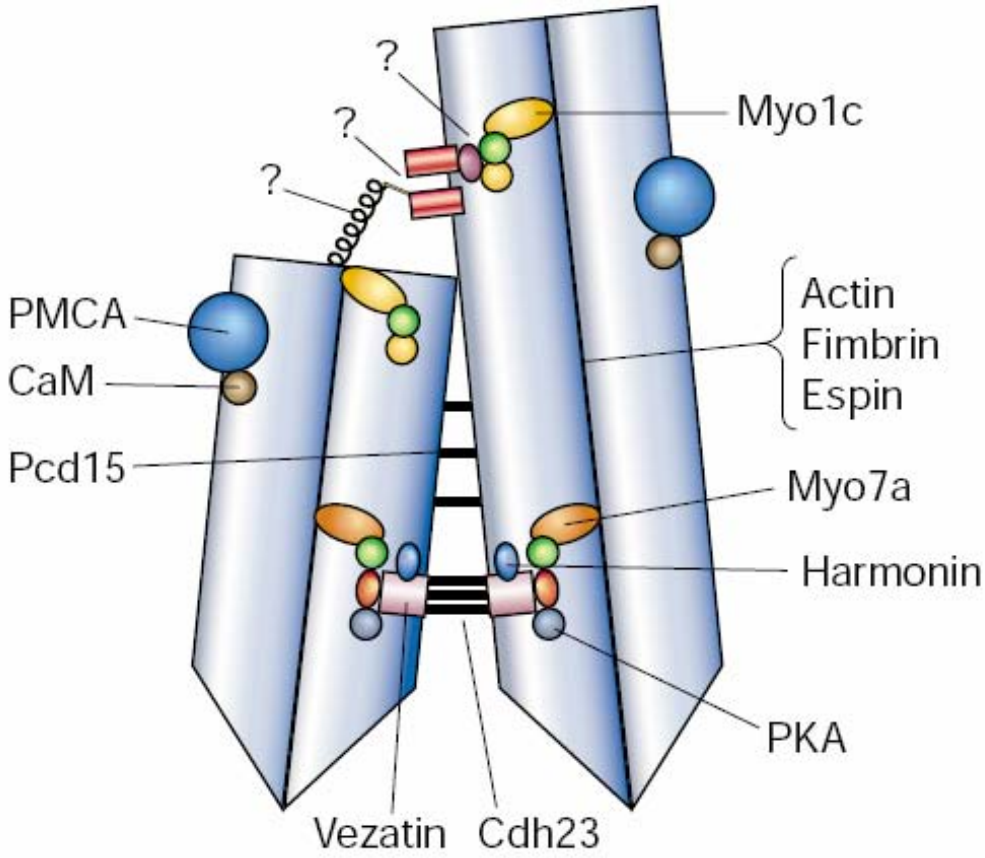

Box 3 Figure Schematic illustration of identified hair-bundle proteins showing hypothetical locations of molecules implicated in stereocilia function. Myo7a, vezatin, Cdh23 and PKA may form the ankle-link complex. Pcd15 presumably also interconnects stereocilia. Myo1c may carry out adaptation, whereas PMCA maintains a low Ca^{2+} concentration. Actin, fimbrin and espin have structural roles; not shown is DFNA1, which may help form the cytoskeleton. Calmodulin regulates several enzymes within the bundle, including PMCA, Myo1c and Myo7a.

Nocicepce – vnímání bolesti

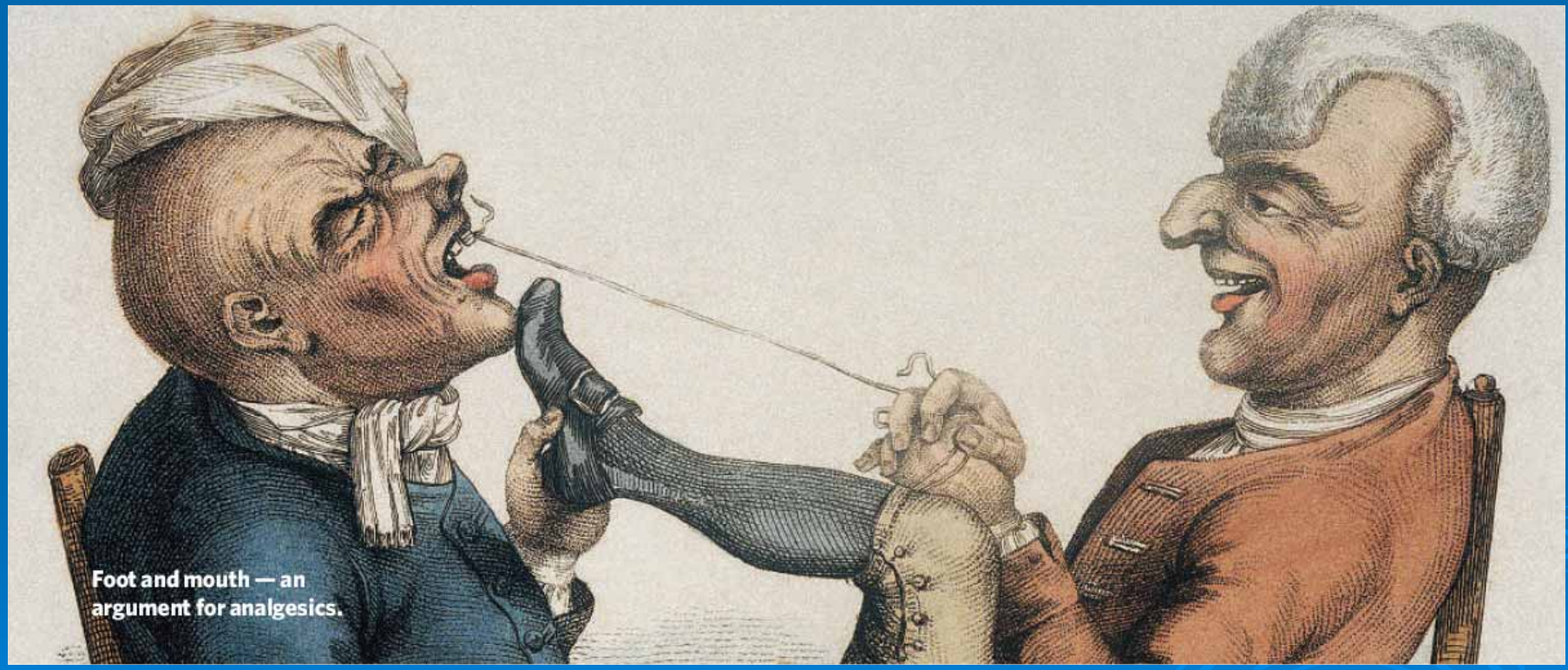

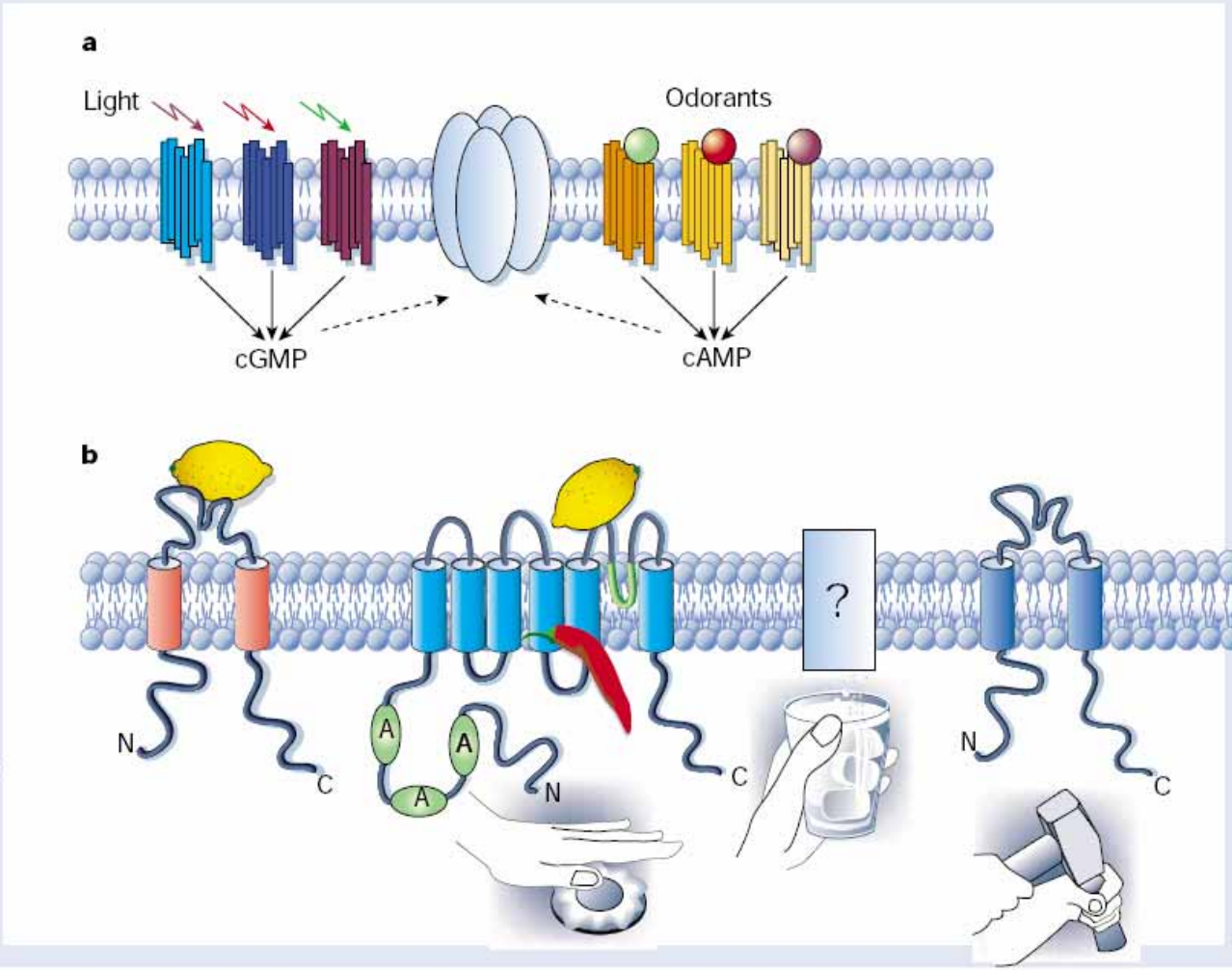

Figure 2 Polymodal nociceptors use a greater diversity of signal-transduction mechanisms to detect physiological stimuli than do primary sensory neurons in other systems. **a**, In mammals, light or odorants are detected by a convergent signalling pathway in which G-protein-coupled receptors modulate the production of cyclic nucleotide second messengers, which then alter sensory neuron excitability by regulating the activity of a single type of cation channel. **b**, In contrast, nociceptors use different signal-transduction mechanisms to detect physical and chemical stimuli. Recent studies suggest that TRP-channel family members (VR1 and VRL-1) detect noxious heat, and that ENaC/DEG-channel family detect mechanical stimuli. Molecular transducers for noxious cold remain enigmatic. Noxious chemicals, such as capsaicin or acid (that is, extracellular protons) may be detected through a common transducer (VR1), illustrating aspects of redundancy in nociception. At the same time, a single type of stimulus can interact with multiple detectors, as shown by the ability of extracellular protons to activate not only VR1, but also ASICs, which are also members of the ENaC/DEG-channel family.

Magnetorecepce

Varianta mechanorecepce-Magnetit?

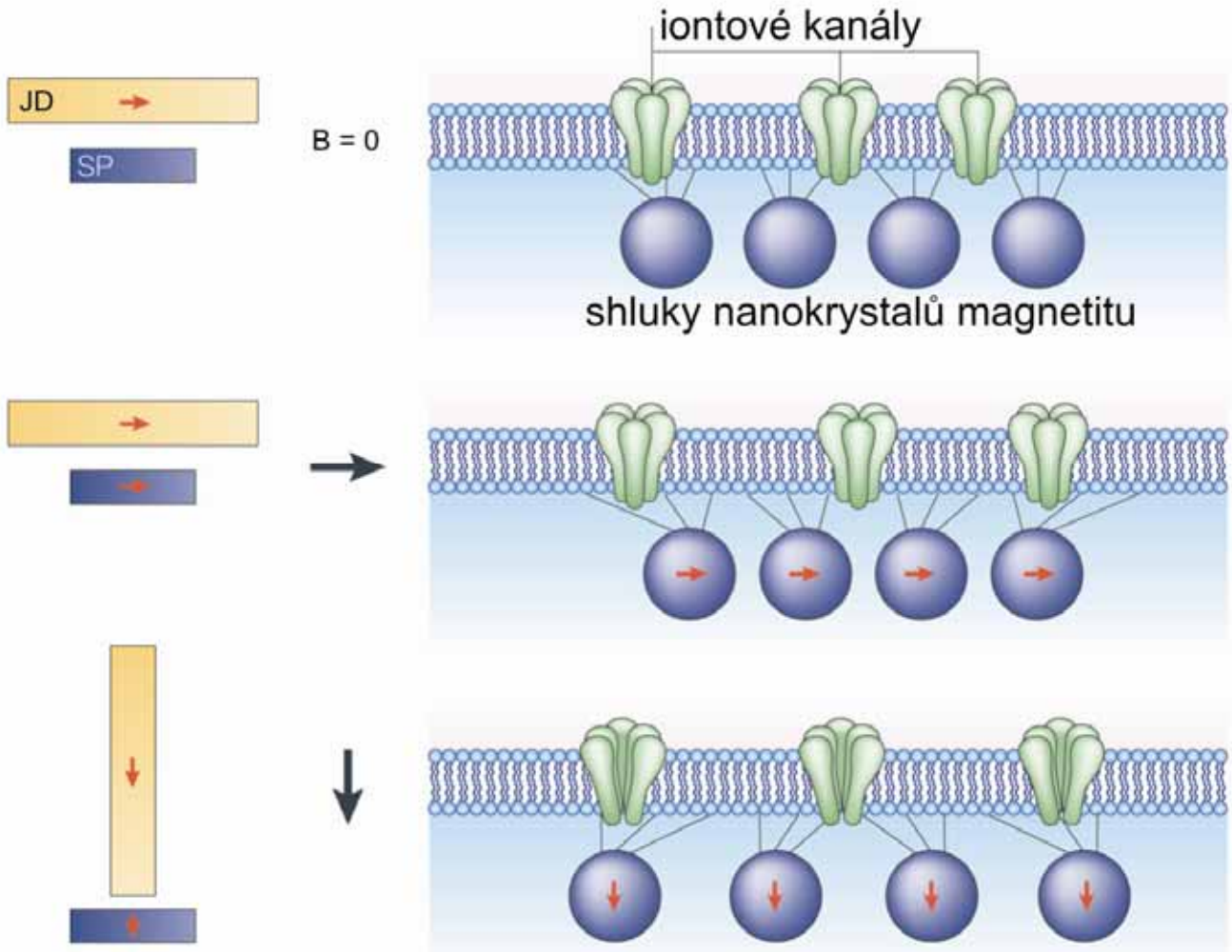

Varianta mechanorecepce-Magnetit?

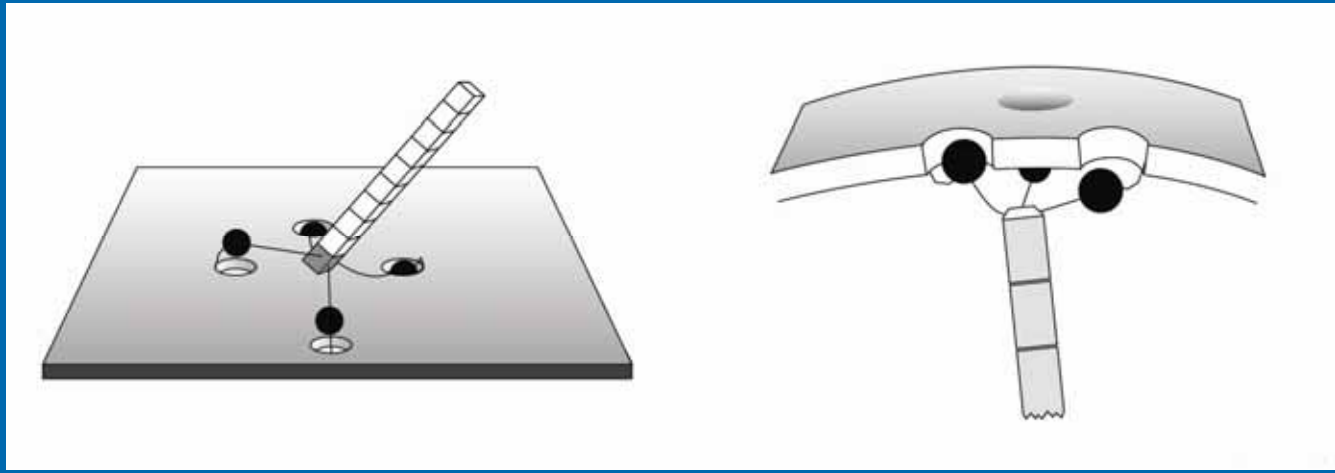

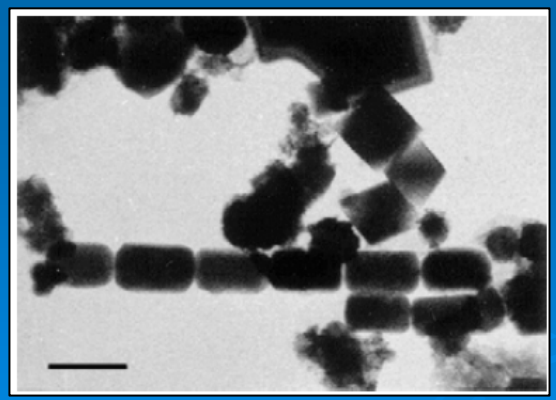

Johnsen, S. and Lohmann, K. J. (2008). Magnetoreception in animals. *Physics Today* March, 29-35.

Varianta mechanorecepce-Magnetit?

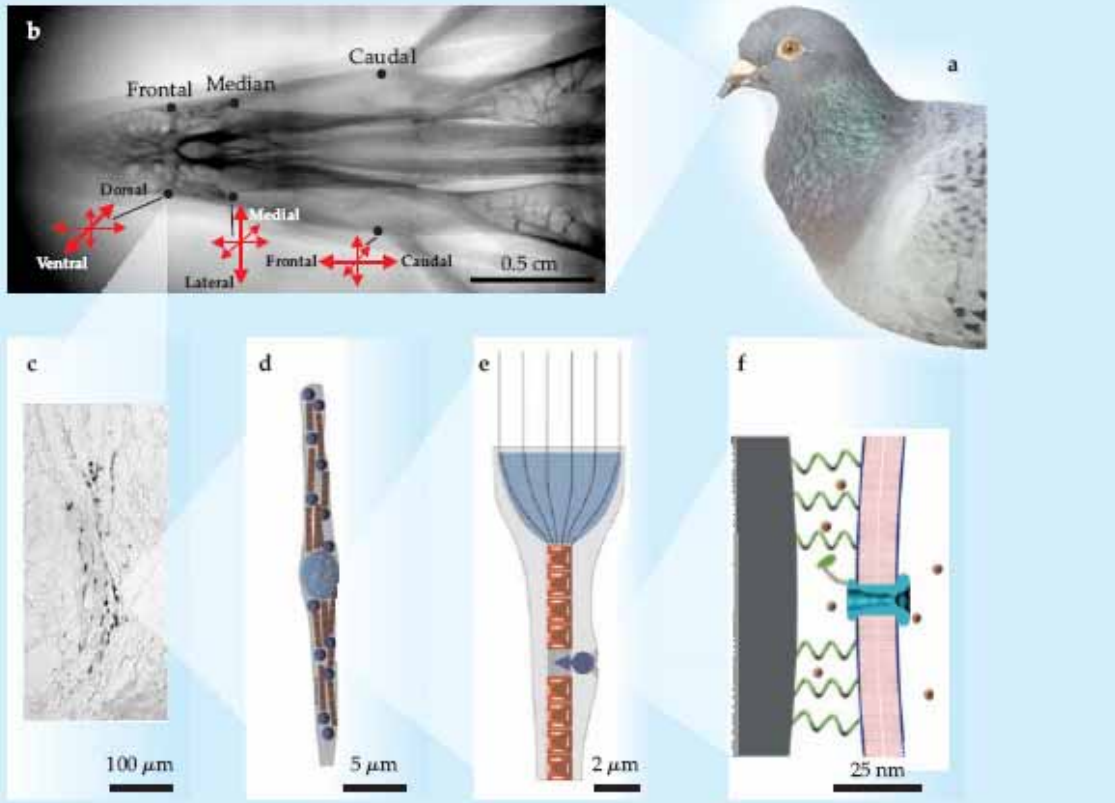

Figure 4. Evidence for magnetite-based magnetoreception. (a) The homing pigeon *Columba livia* provides some of the best evidence. (b) X-ray image of the upper beak of *C. livia*, showing the three pairs of iron-containing areas and the prevailing orientations of their neurons. (c) Stained section of the dendritic region in one of the areas. Dark areas are iron deposits. (d) Schematic of a single neuron, showing the centrally located, iron-coated vesicle (light blue) and the clusters of magnetite crystals (dark blue) alternating with rows of maghemite plates (red). (e) Hypothesized concentration of magnetic flux in a neuron and its effect on the position of one of the magnetite clusters. (f) Magnetite cluster pulling away from a membrane, which bends and opens a mechanically stimulated ion channel. (Panel **a** courtesy of Andreas Trepte; panels **b–c** adapted from G. Fleissner et al., *Naturwissenchaften* **94**, 631, 2007; panels **d–e** adapted from G. Fleissner et al., *J. Ornithol.* **148**, 643, 2007; panel **f** adapted from I. Solov'yov, W. Greiner, *Biophys. J.* **93**, 1493, 2007.)

Varianta fotorecepce?

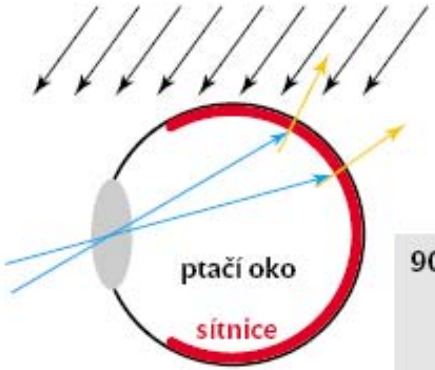

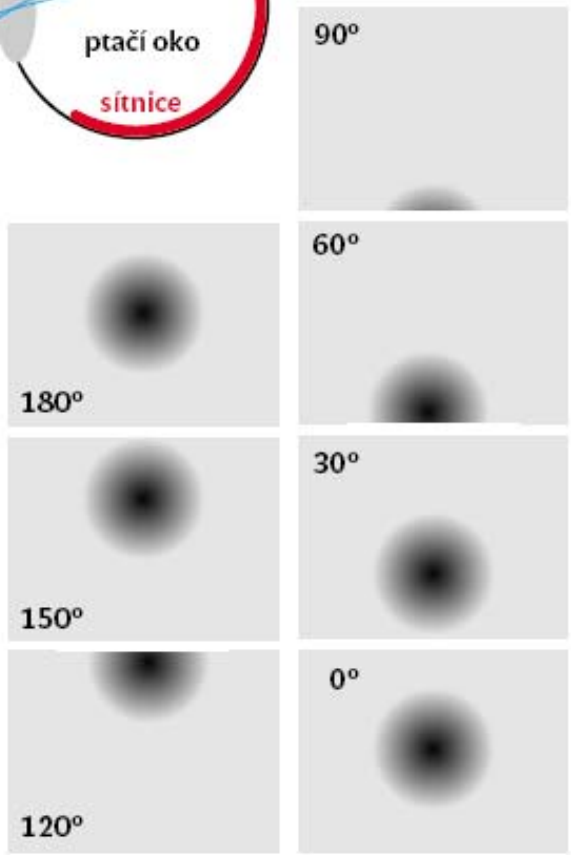

7. Vlevo nahoře je schéma oka obratlovce. Fotoreceptory jsou v různých částech sítnice různě orientovány vůči magnetickému poli (orientace fotoreceptorů znázorněna žlutými, orientace magnetického vektoru černými šipkami). Vlevo dole je počítačová simulace zrakových vjemů modulovaných magnetickým polem. Vnímané vzory se mění v závislosti na orientaci zvířete vzhledem k vektoru magnetického pole. Vpravo je idealizovaná představa – tak nějak může pták vnímat krajinu, nad kterou letí. Podle: Ritz a kol., Biophys. J. 78, 707–718, 2000.
Snímek pobřeží Sardinie © Stanislav Vaněk.

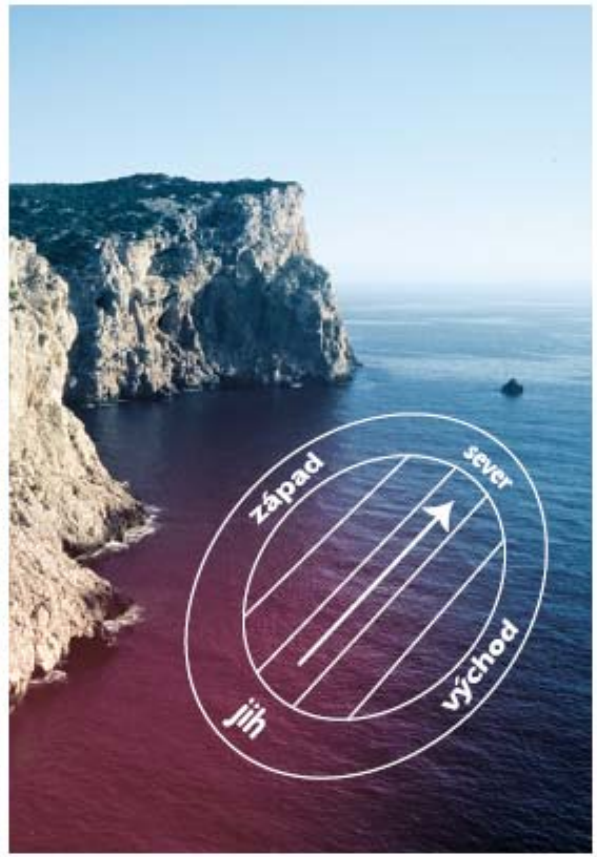

Fotochemický model založený na reakcích radikálových párů.

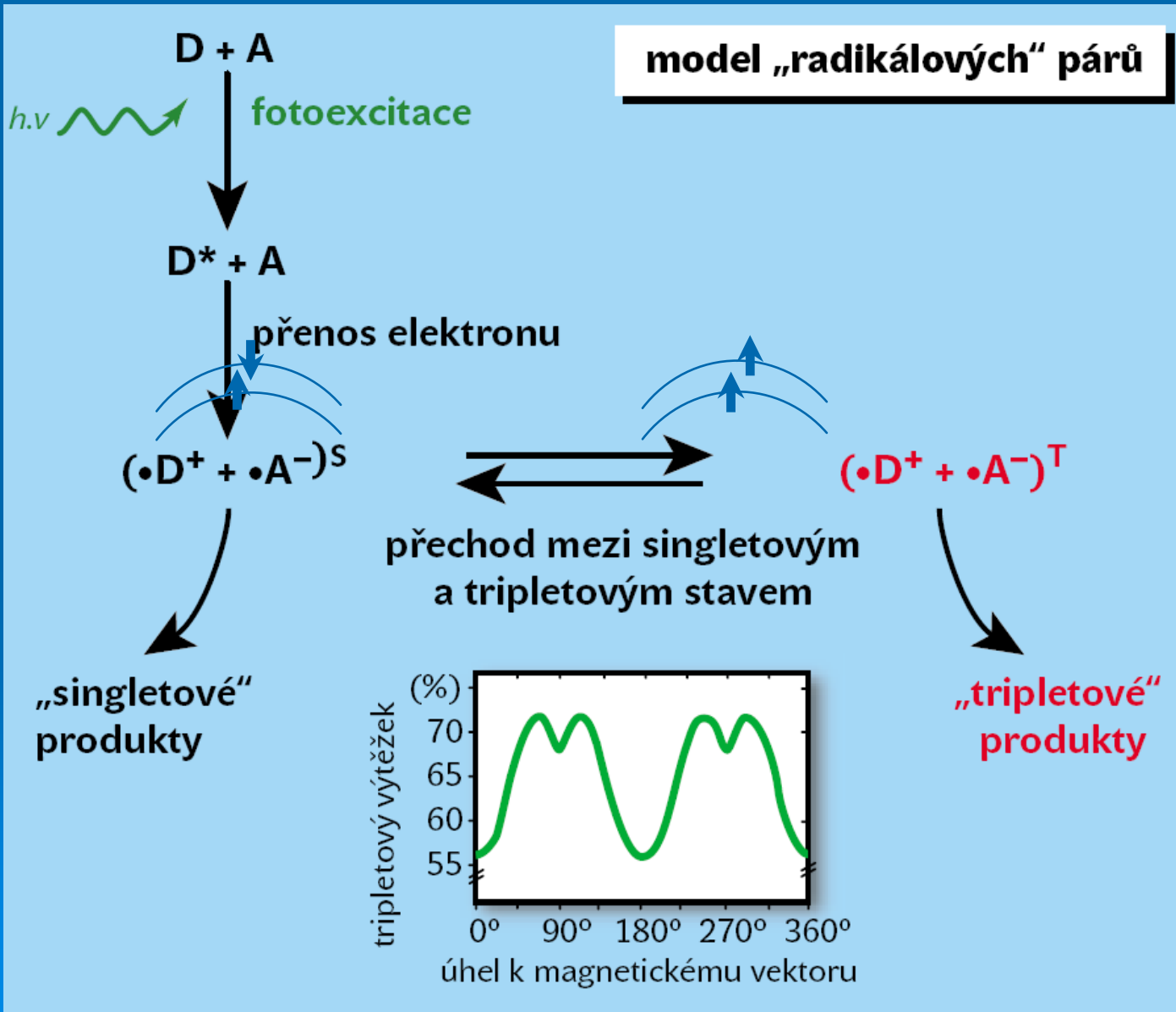

Fotochemický model založený na reakcích radikálových párů.

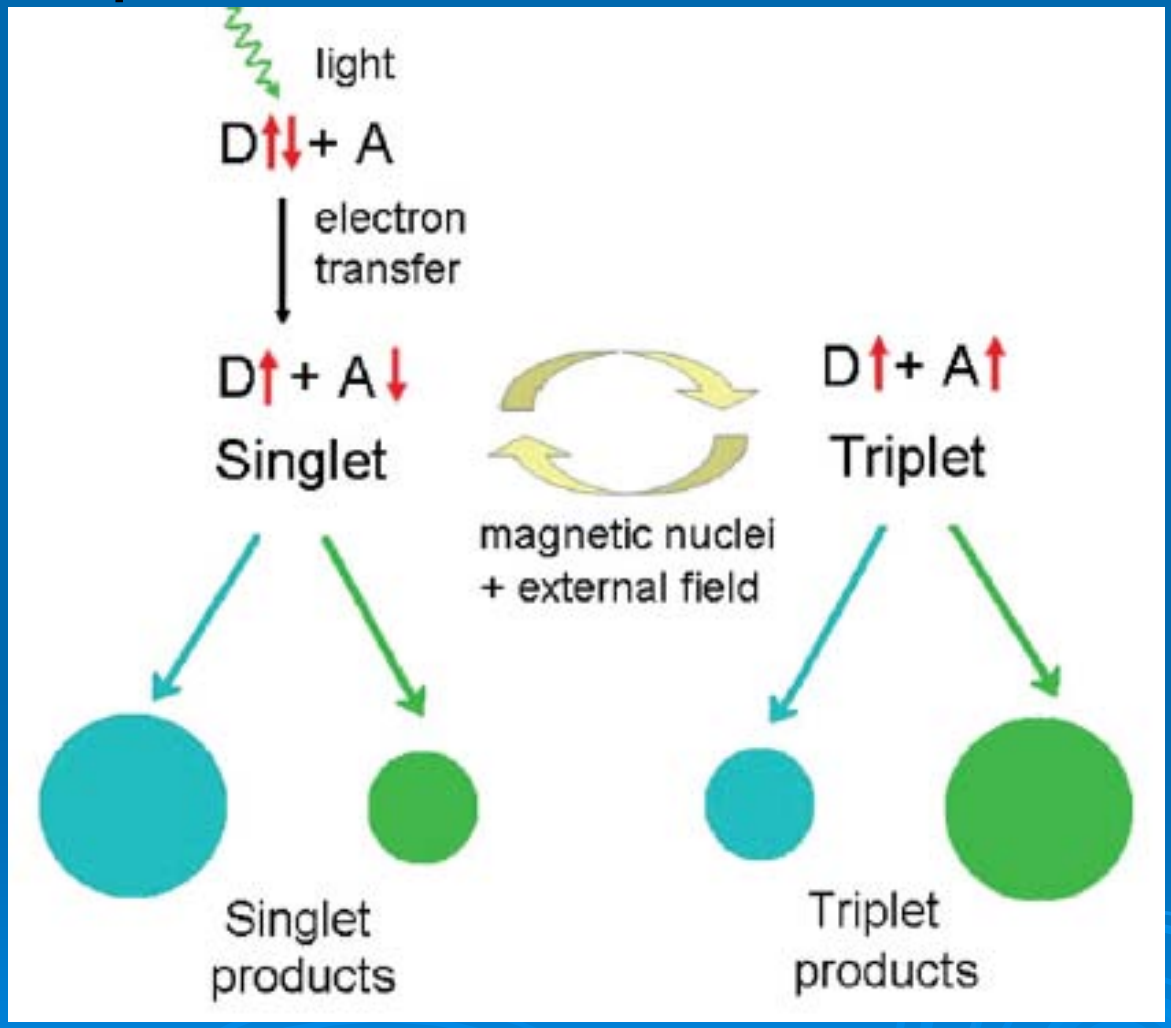

Ritz, T., Wiltschko, R., Hore, P. J., Rodgers, C. T., Stapput, K., Thalau, P., Timmel, C. R. and Wiltschko, W. (2009). Magnetic Compass of Birds Is Based on a Molecule with Optimal Directional Sensitivity. *Biophysical Journal* 96, 3451–3457.

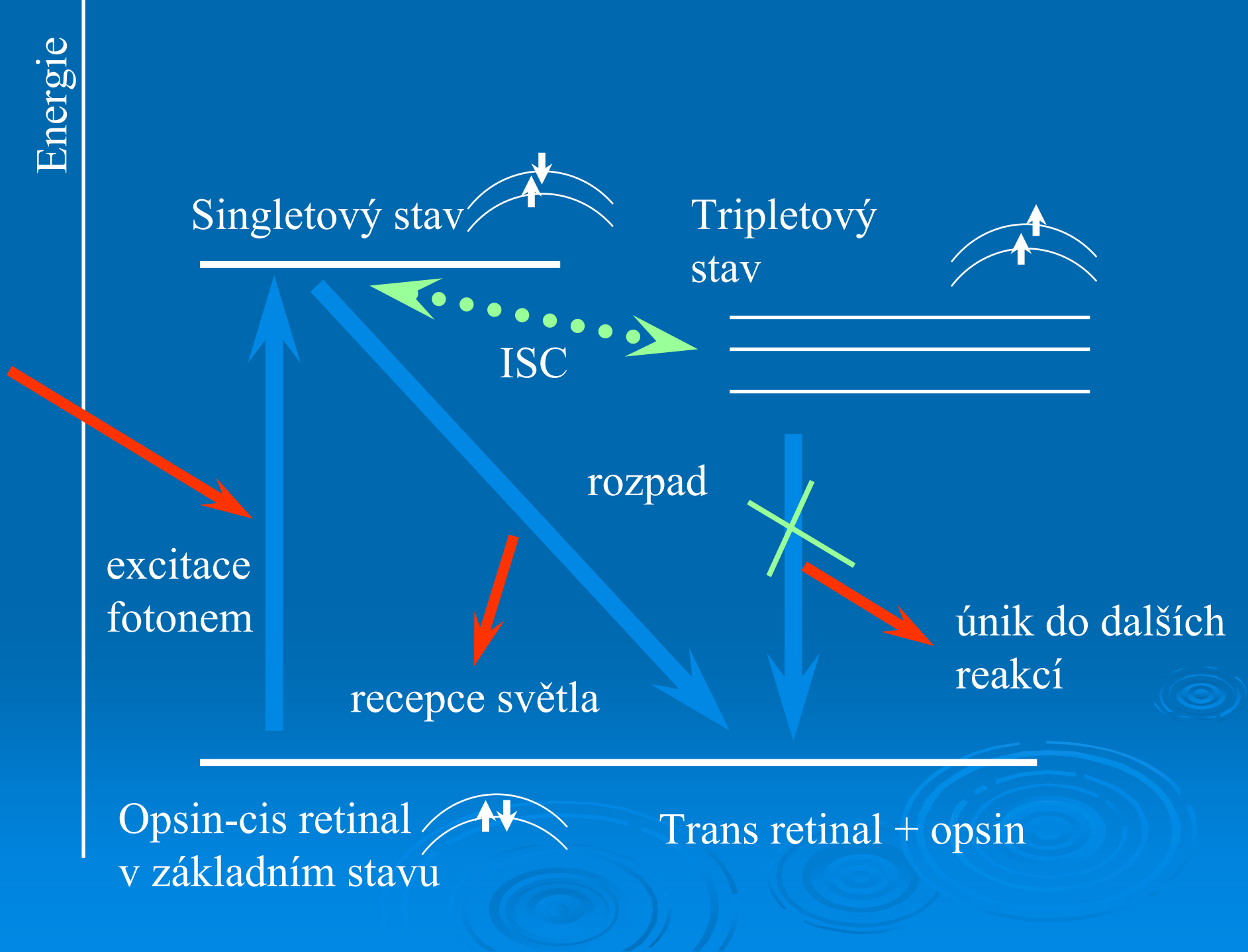
Energie
Singletový stav
Tripletový stav
ISC
rozpad
excitace fotonem
recepce světla
únik do dalších reakcí
Opsin-cis retinal v základním stavu
Trans retinal + opsin

Spontánní oscilace mezi dvěma stavy.

Posun v pravděpodobnosti výtěžku reakce.

Magnetická síla

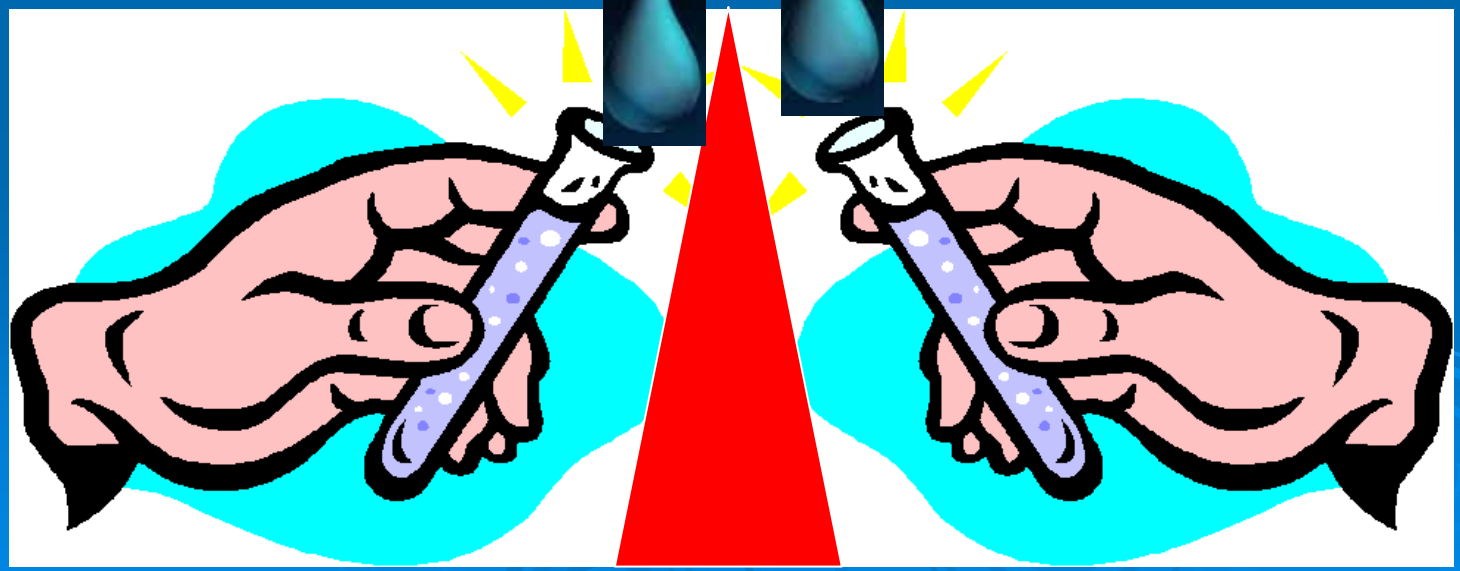

Kryptochromy:

- Nejpravděpodobnější kandidáti na magnetoreceptor zrakové dráhy.
- Signální proteiny zvířat i rostlin, homologní DNA fotolyázám.
- Součástí biologických hodin.

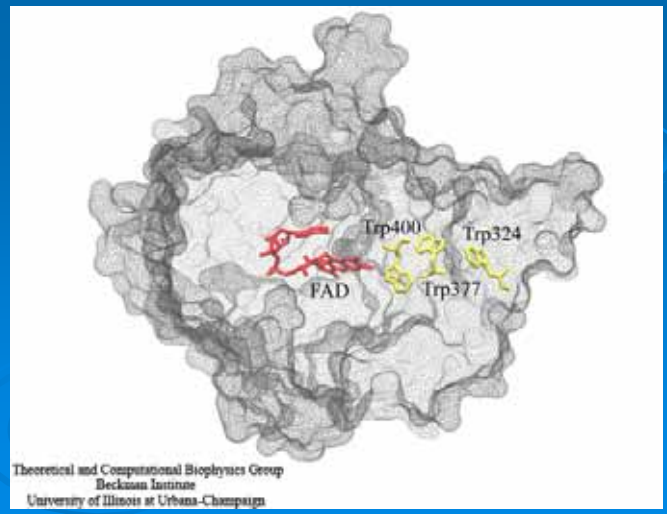

Kryptochromy:

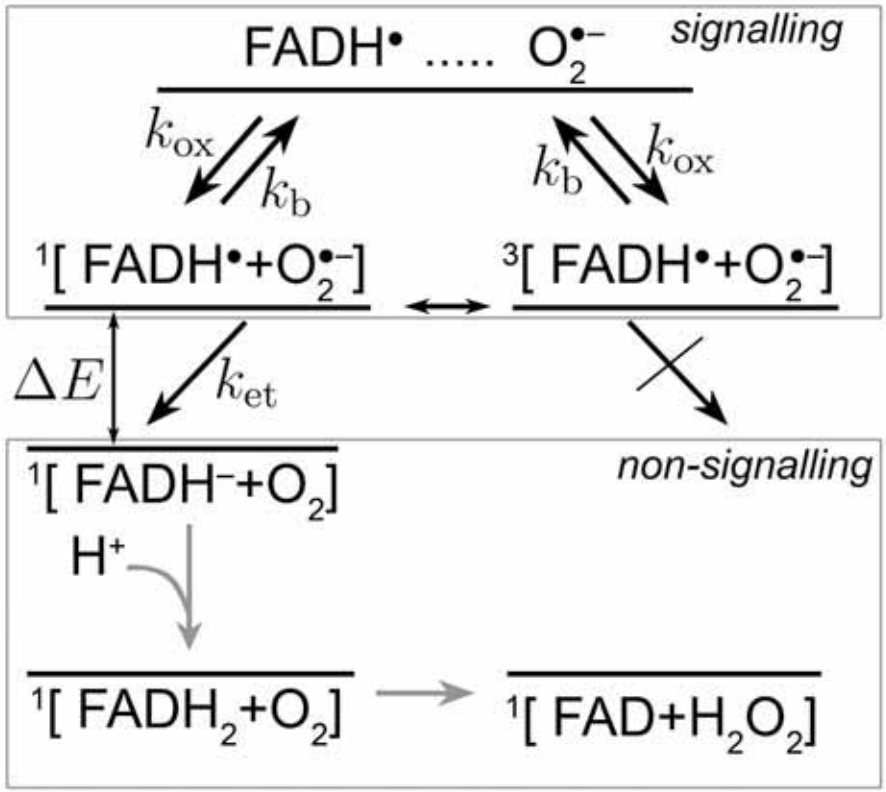

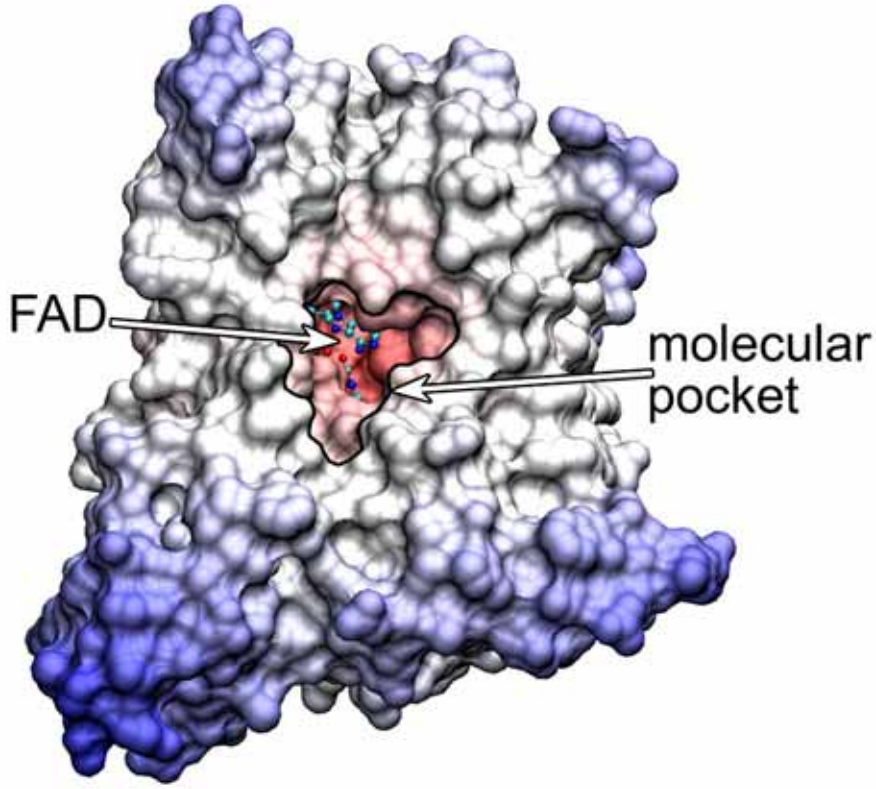

http://www.ks.uiuc.edu/Research/cryptochrome/

Superoxidový anion obsazuje molekulární kapsu kryptochromu a tvoří radikálový pár [FADH + $O_2^{\circ-}$], který se nachází v singletovém (25 %) nebo tripletovém (75 %) stavu.

Kryptochromy

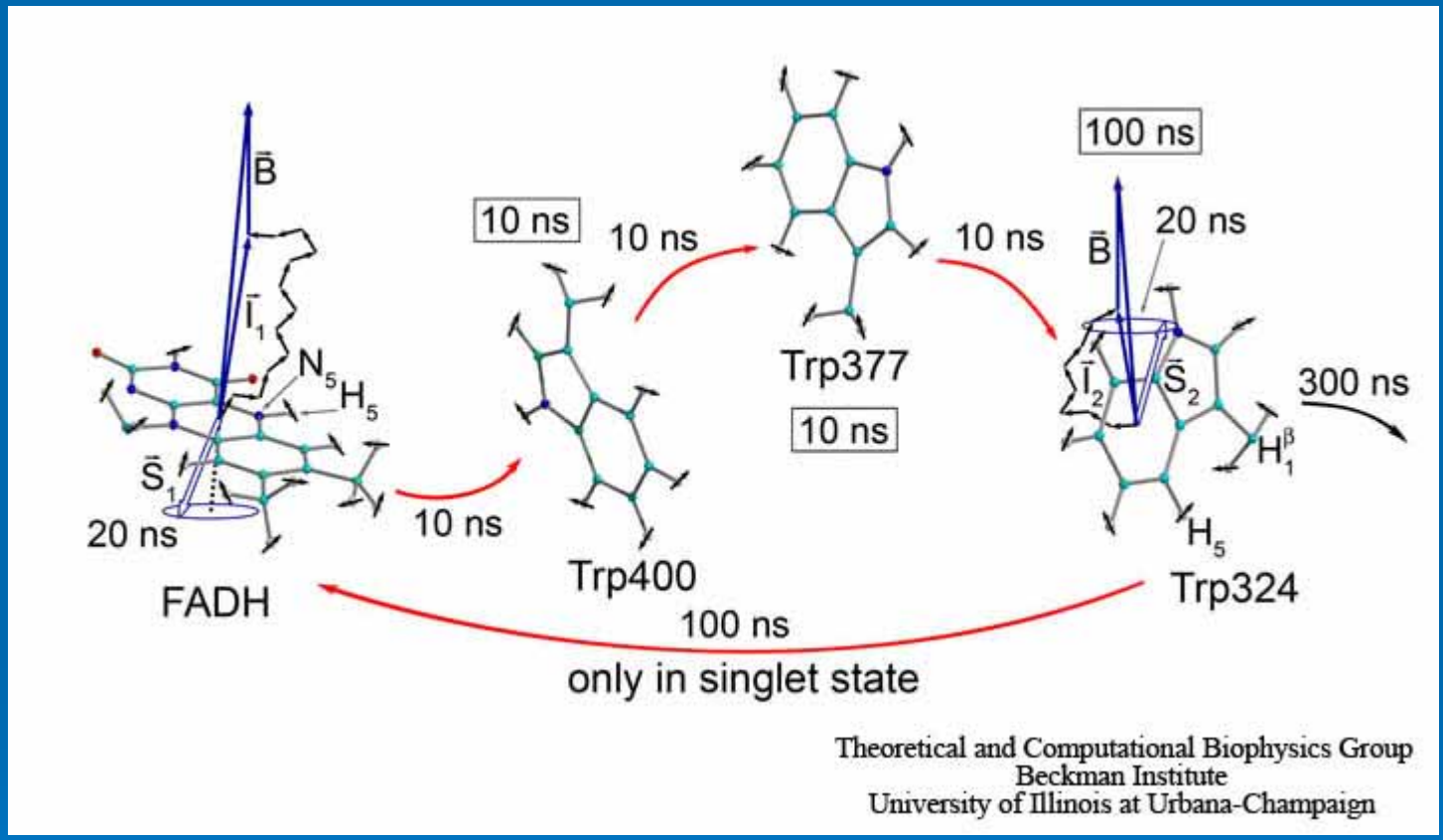

http://www.ks.uiuc.edu/Research/cryptochrome/

Kryptochrom je deaktivován, jestliže elektrony radikálového páru jsou v singletovém stavu. Magnetické pole tak ovlivní dobu po kterou je kryptochrom v aktivním – signálním stavu.

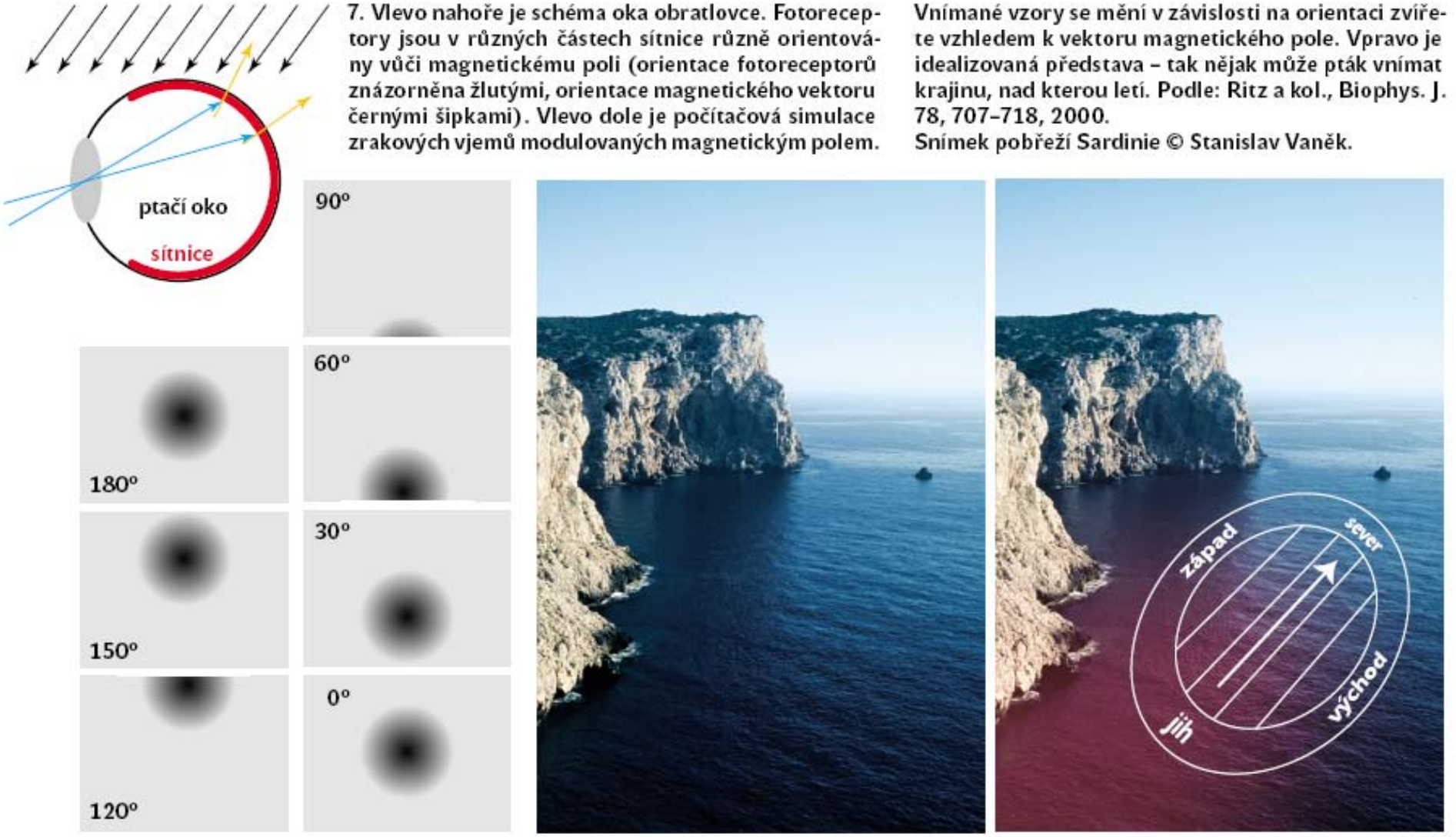

7. Vlevo nahoře je schéma oka obratlovce. Fotoreceptory jsou v různých částech sítnice různě orientovány vůči magnetickému poli (orientace fotoreceptorů znázorněna žlutými, orientace magnetického vektoru černými šipkami). Vlevo dole je počítačová simulace zrakových vjemů modulovaných magnetickým polem. Vnímané vzory se mění v závislosti na orientaci zvířete vzhledem k vektoru magnetického pole. Vpravo je idealizovaná představa – tak nějak může pták vnímat krajinu, nad kterou letí. Podle: Ritz a kol., Biophys. J. 78, 707–718, 2000.
Snímek pobřeží Sardinie © Stanislav Vaněk.

Reakce je směrově specifická a některé receptory budou ovlivněny více než ostatní.

Elektrorecepce

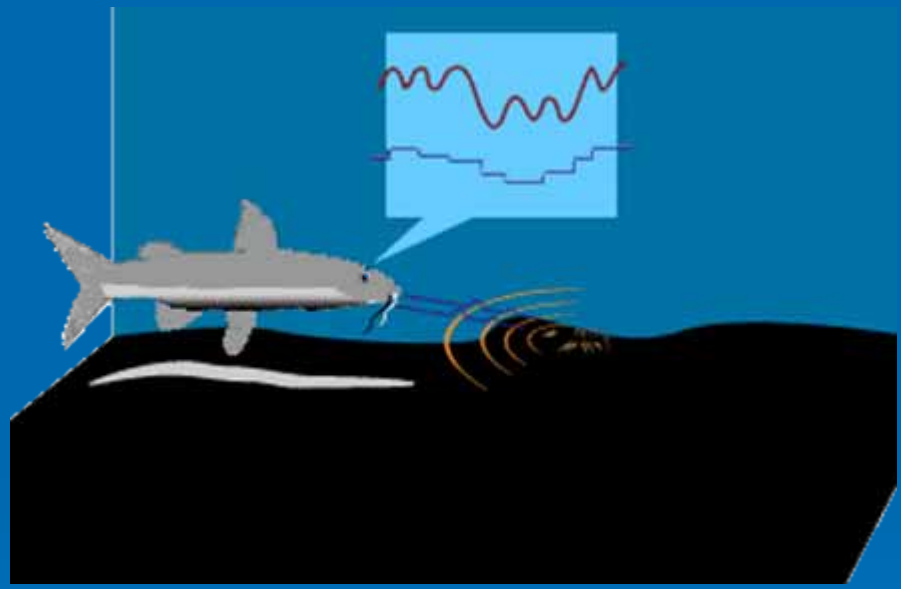

Lorenziniho ampule

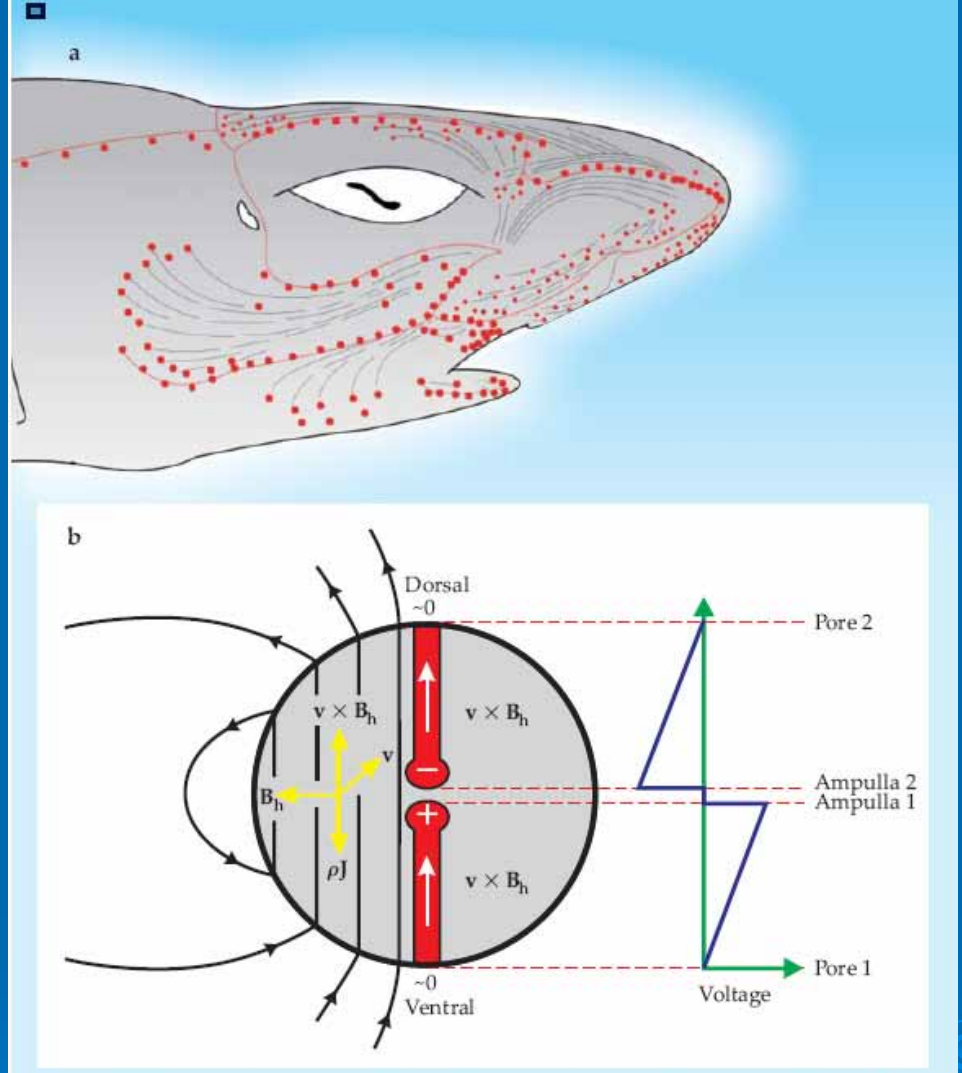

Figure 1. Inductive magnetoreception. (a) Side view of a shark's head, showing the ampullae of Lorenzini electroreceptors (red dots) and jelly-filled conductive canals (gray lines). The red lines are so-called lateral lines, used to detect vibrations in the surrounding water. (Image courtesy of Chris Huh.) (b) Schematic showing two ampullae with their canals. As the shark swims east and into the page with a velocity **v**, its movement across the horizontal component of Earth's field, $\mathbf{B}_h$, causes a vertical electromotive force of magnitude vB_h. Because the shark's body and especially its skin are highly resistive, the voltage drop due to the current density ρJ results in no potential difference between the dorsal and ventral surfaces of the animal. The high conductivity of the canals, however, results in a large voltage drop across the ampullae. The thick black lines illustrate the electric field surrounding and permeating the shark. (Adapted from A. Kalmijn, *IEEE Trans. Magn.* **17**, 1113, 1981.)

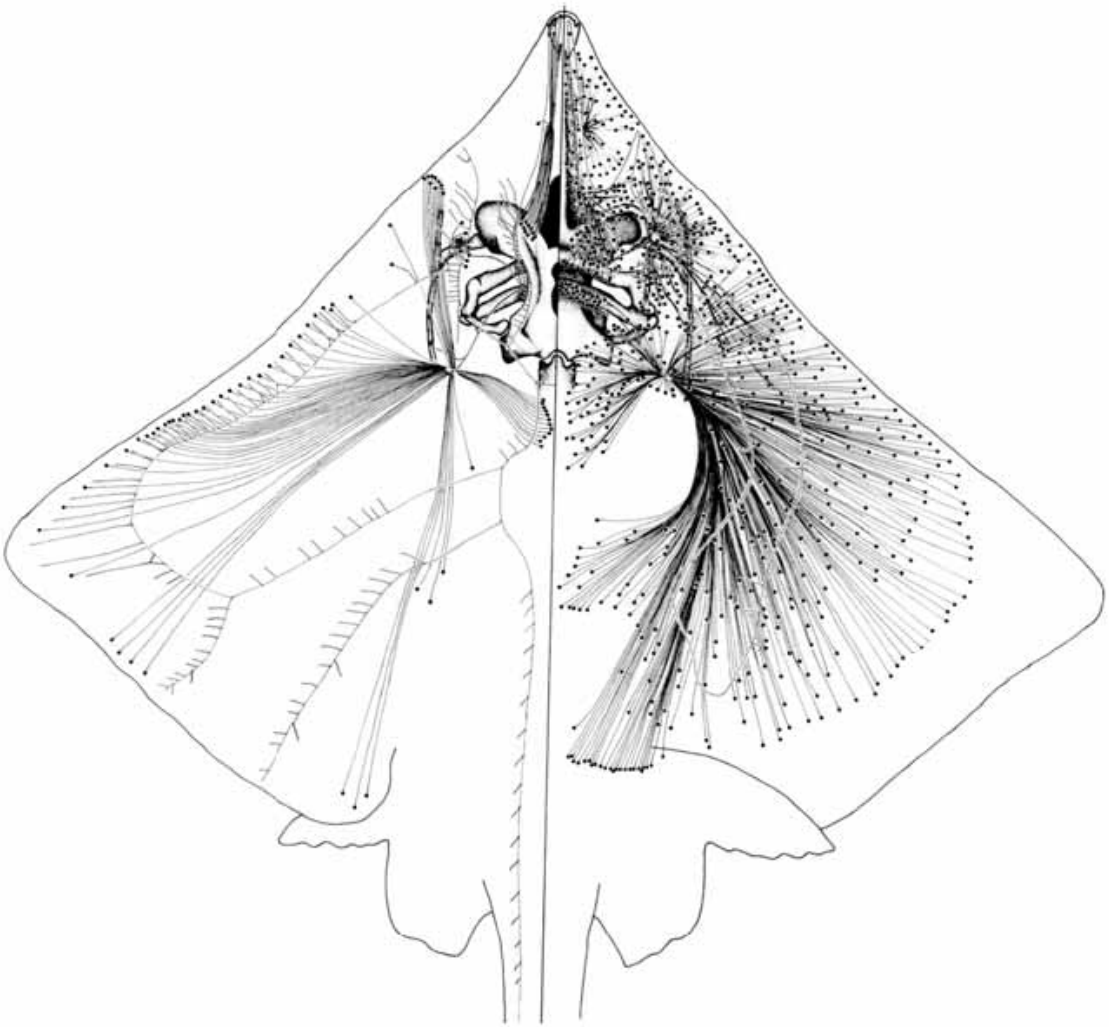

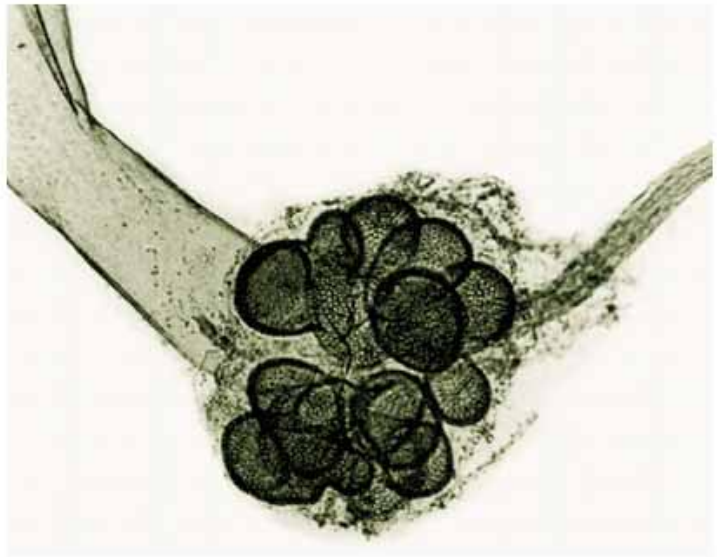

1. Rozmístění Lorenziniho ampul na těle rejnoka druhu *Raja laevis*. V levé polovině obrázku je znázorněna dorzální, v pravé polovině pak ventrální strana těla. Vpravo nahoře je detail izolované ampuly; dobře jsou viditelné receptorové buňky na dně ampuly a senzorický nerv. Podle: Raschi, J. Morphol. 189, 225–247, 1986.

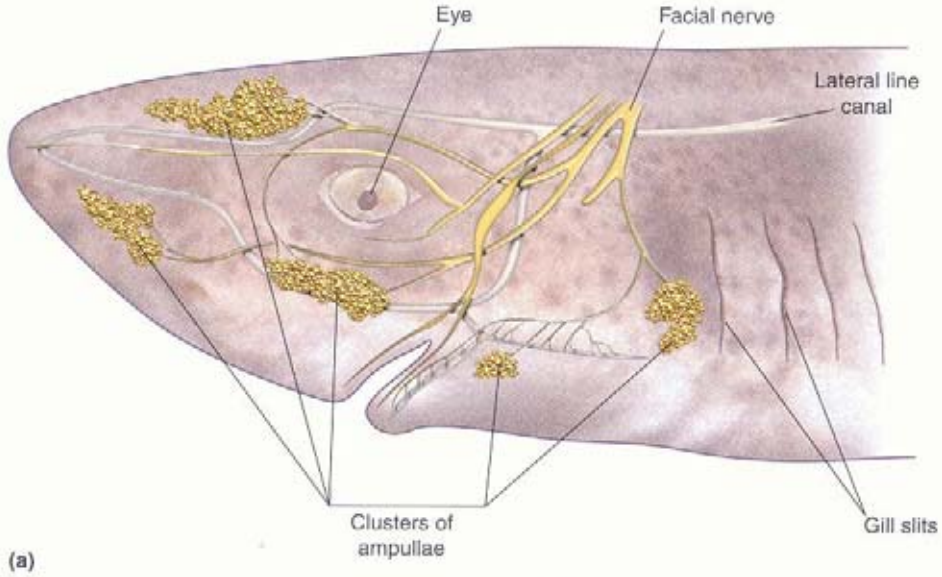

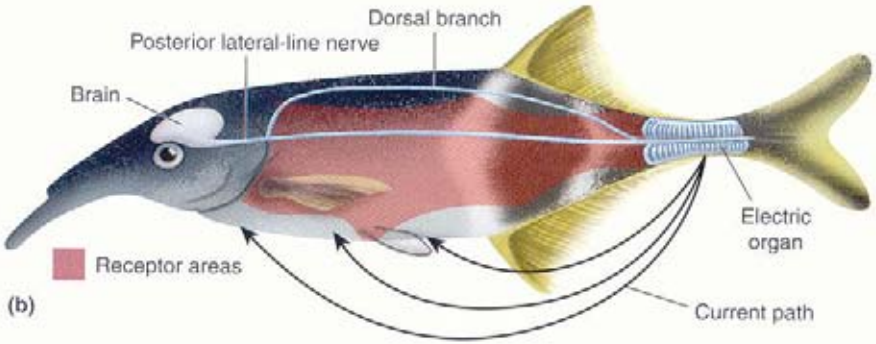

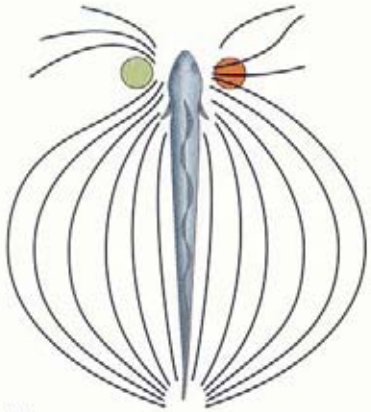

command center is
Gap junctions assur
maximizing signal i
pling of the medulla
tor that determines
of electrocytes capa

A few species, s
produce discharges
bodies, whereas in
range to millivolts t
or kill prey, whereas
for electrolocation a

Some animals

- Pasivní – detekce napětí vznikající svalovou a nervovou činností
- Aktivní – podobá se echolokaci

- Navigace
- Detekce kořisti } v kalných vodách
- Komunikace

Lorenziniho ampule – změna potenciálu otevírá Ca^{2+} kanály a stimuluje eflux mediátoru

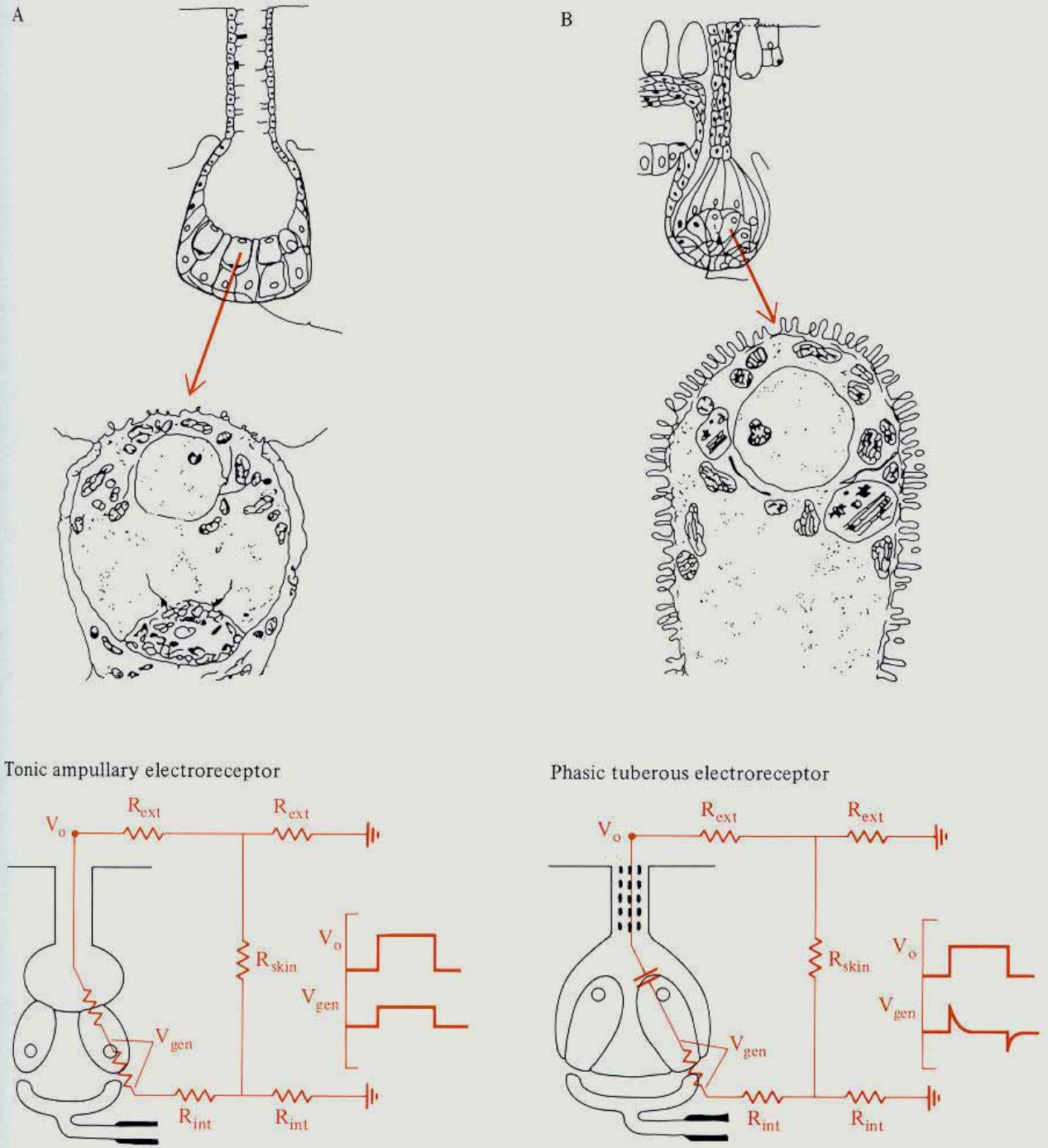
A
B
Tonic ampullary electroreceptor
Phasic tuberous electroreceptor
V_o
R_{ext}
R_{ext}
R_{skin}
V_o
V_{gen}
V_{gen}
R_{int}
R_{int}

Cítění přes TRP kanály
TRP – transient receptor potential

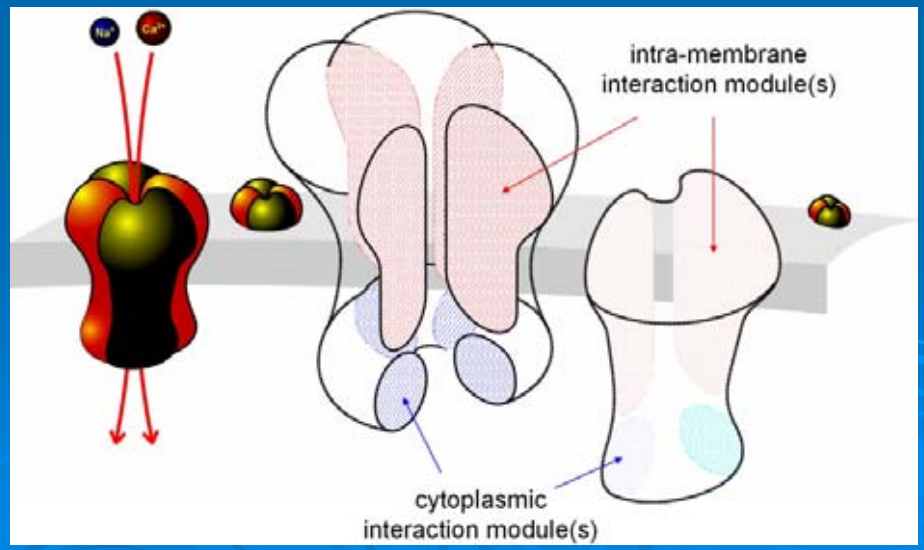

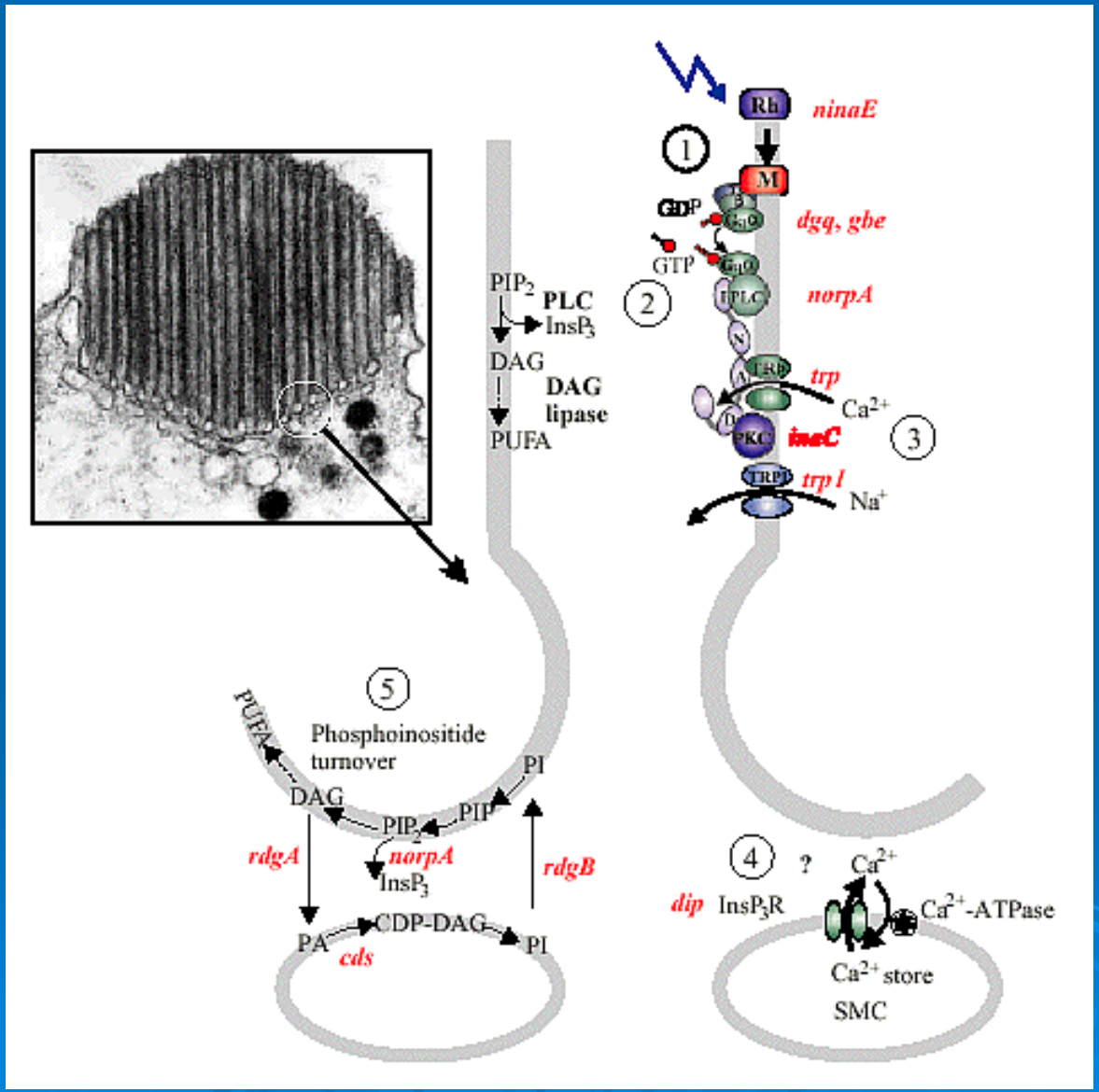
Rh
ninaE
1
M
GDP
GTP
dgq, gbe
norpA
2
PIP2
PLC
InsP3
DAG
DAG
lipase
PUFA
trp
Ca2+
PKC
inaC
3
TRPL
trpl
Na+
5
Phosphoinositide
turnover
PUFA
DAG
PI
PIP2
PIP
rdgA
norpA
InsP3
rdgB
PA
CDP-DAG
PI
cds
4
?
Ca2+
dip
InsP3R
Ca2+-ATPase
Ca2+ store
SMC

TRP kanály

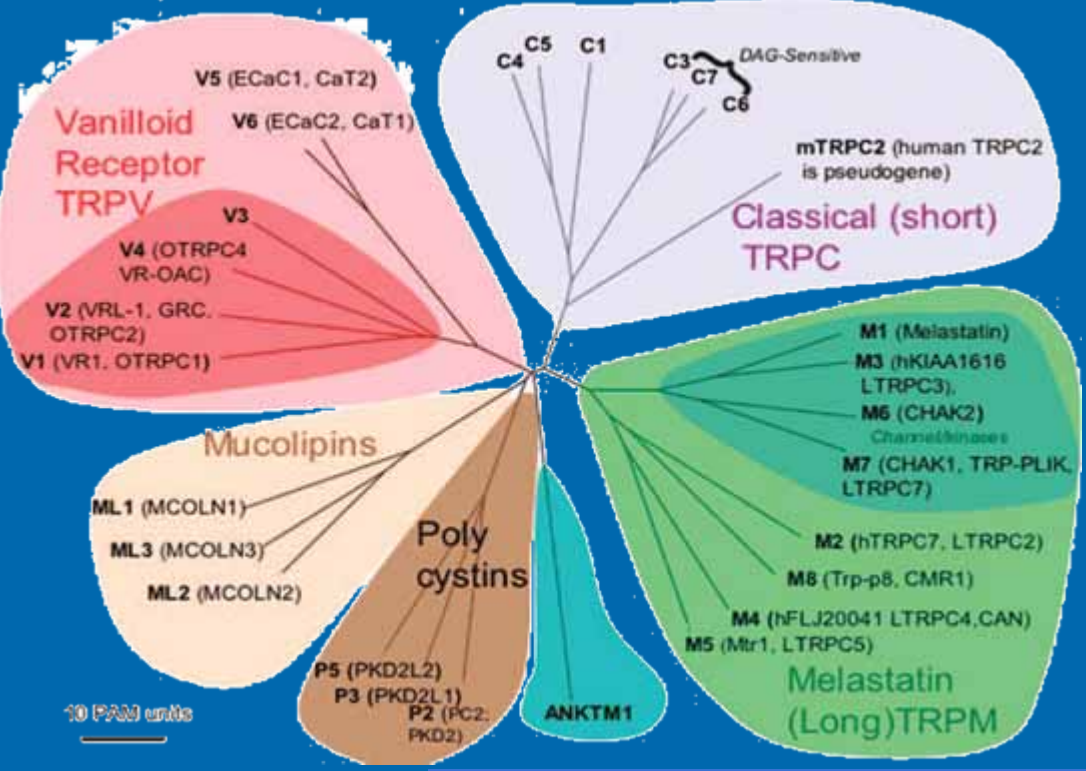
Vanilloid Receptor TRPV
V5 (ECaC1, CaT2)
V6 (ECaC2, CaT1)
V3
V4 (OTRPC4 VR-OAC)
V2 (VRL-1, GRC, OTRPC2)
V1 (VR1, OTRPC1)
C4
C5
C1
C3
C7
C6
DAG-Sensitive
mTRPC2 (human TRPC2 is pseudogene)
Classical (short) TRPC
M1 (Melastatin)
M3 (hKIAA1616 LTRPC3),
M6 (CHAK2)
M7 (CHAK1, TRP-PLIK, LTRPC7)
M2 (hTRPC7, LTRPC2)
M8 (Trp-p8, CMR1)
M4 (hFLJ20041 LTRPC4,CAN)
M5 (Mtr1, LTRPC5)
Melastatin (Long)TRPM
Mucolipins
ML1 (MCOLN1)
ML3 (MCOLN3)
ML2 (MCOLN2)
Poly cystins
P5 (PKD2L2)
P3 (PKD2L1)
P2 (PC2, PKD2)
ANKTM1
10 PAM units

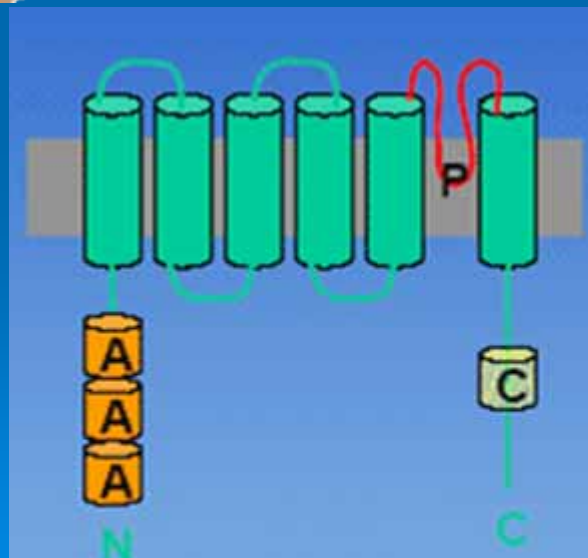
P
A
A
A
C
N
C

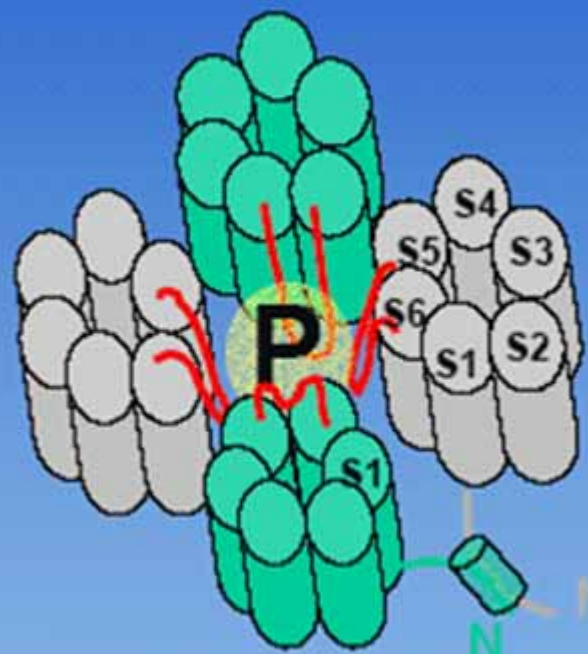
S4
S5
S3
S6
P
S1
S2
S1
N
N

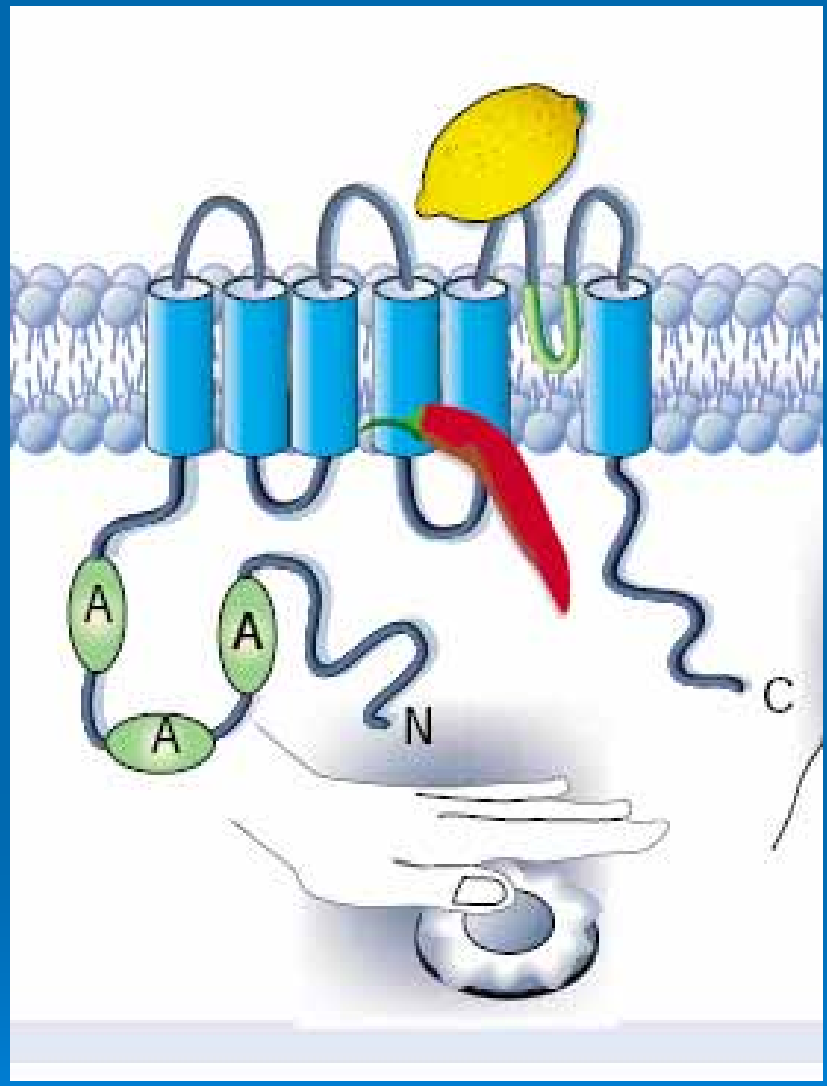
A
A
A
N
C

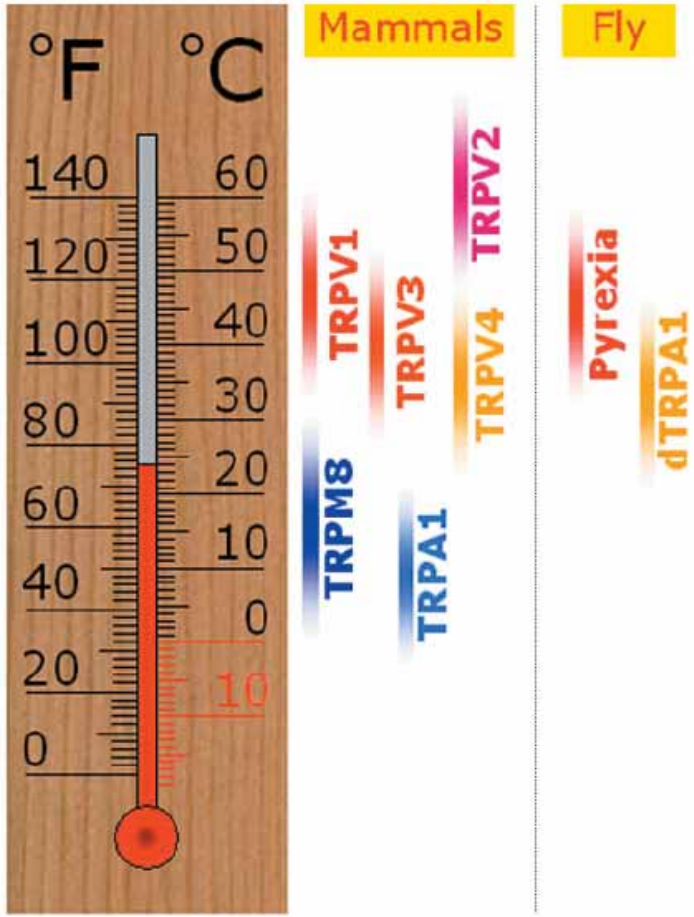

Figure 2 Activation range of human and *Drosophila* thermoTRPs. Indicative temperature range for activation of mammalian and *Drosophila* thermoTRPs in heterologous expression systems. Note that TRPM8 and TRPA1 are activatedupon cooling, whereas all other indicated channels are heat activated.

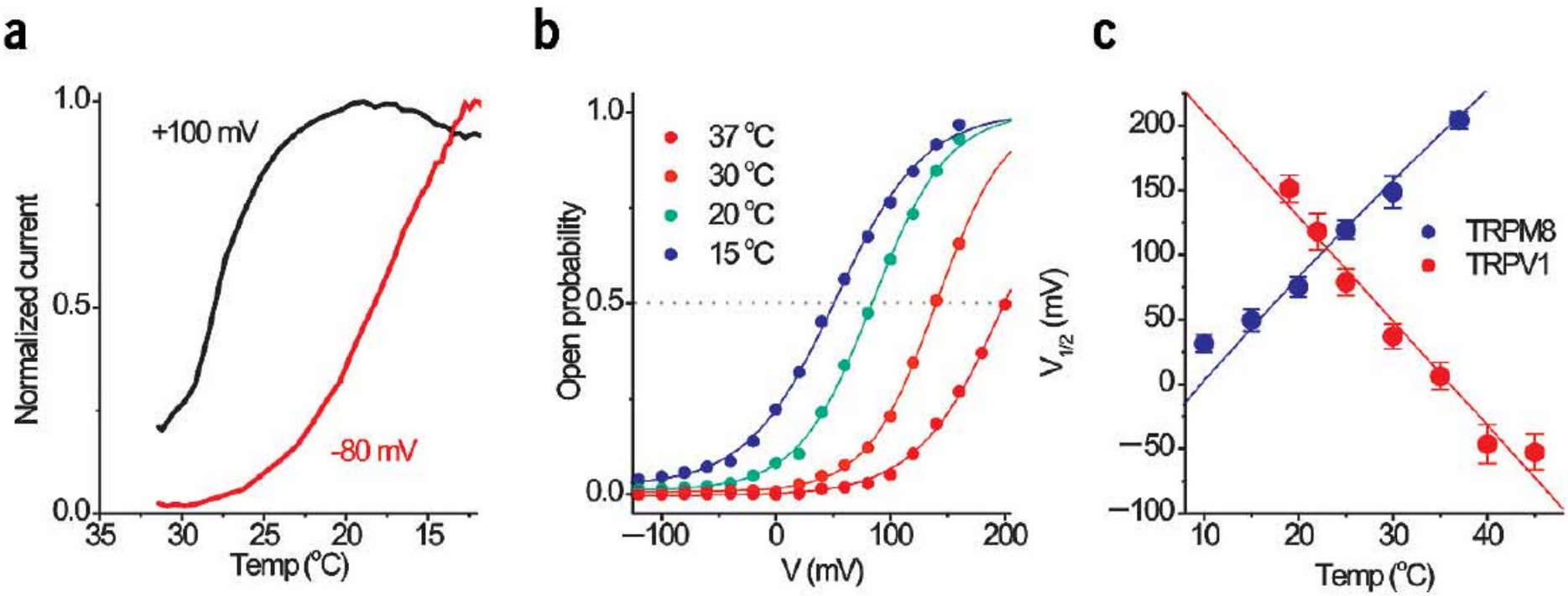

Figure 3 Temperature sensitivity is voltage dependent. (**a**) Normalized TRPM8 current in response to cooling at +100 and –80 mV. Note that at depolarized potentials, current activation occurs at higher temperatures than at more negative potentials. (**b**) Plot showing the open probability of TRPM8 in function of voltage at the indicated temperatures. (**c**) Plot of the midpoint of the activation curves ($V_{1/2}$) versus temperature for TRPV1 and TRPM8. Adapted from ref. 41.


(a)

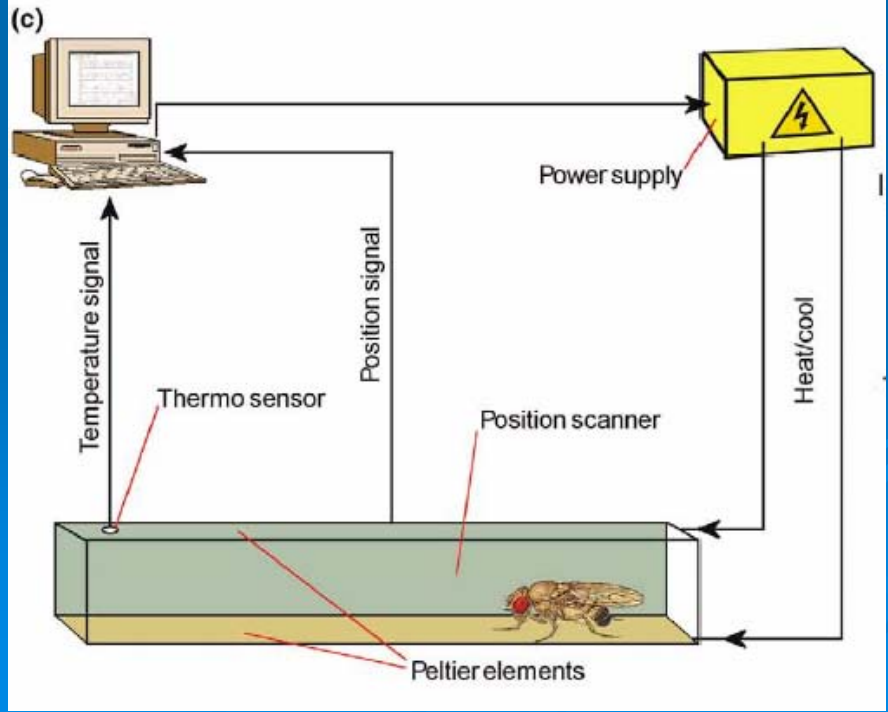
(c)
Power supply
Temperature signal
Position signal
Heat/cool
Thermo sensor
Position scanner
Peltier elements

Mechanosensitivita TRP
3 možné mechanismy

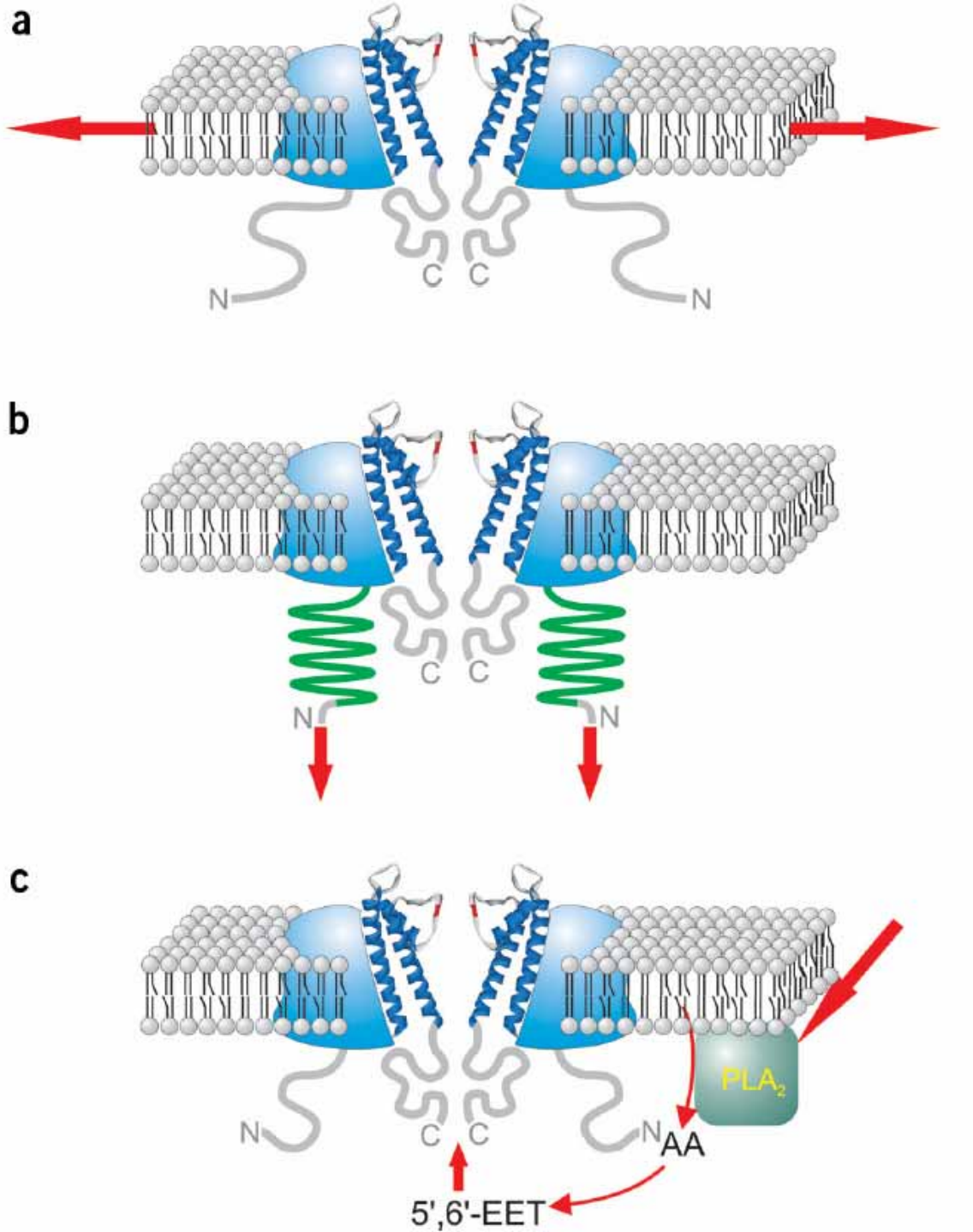

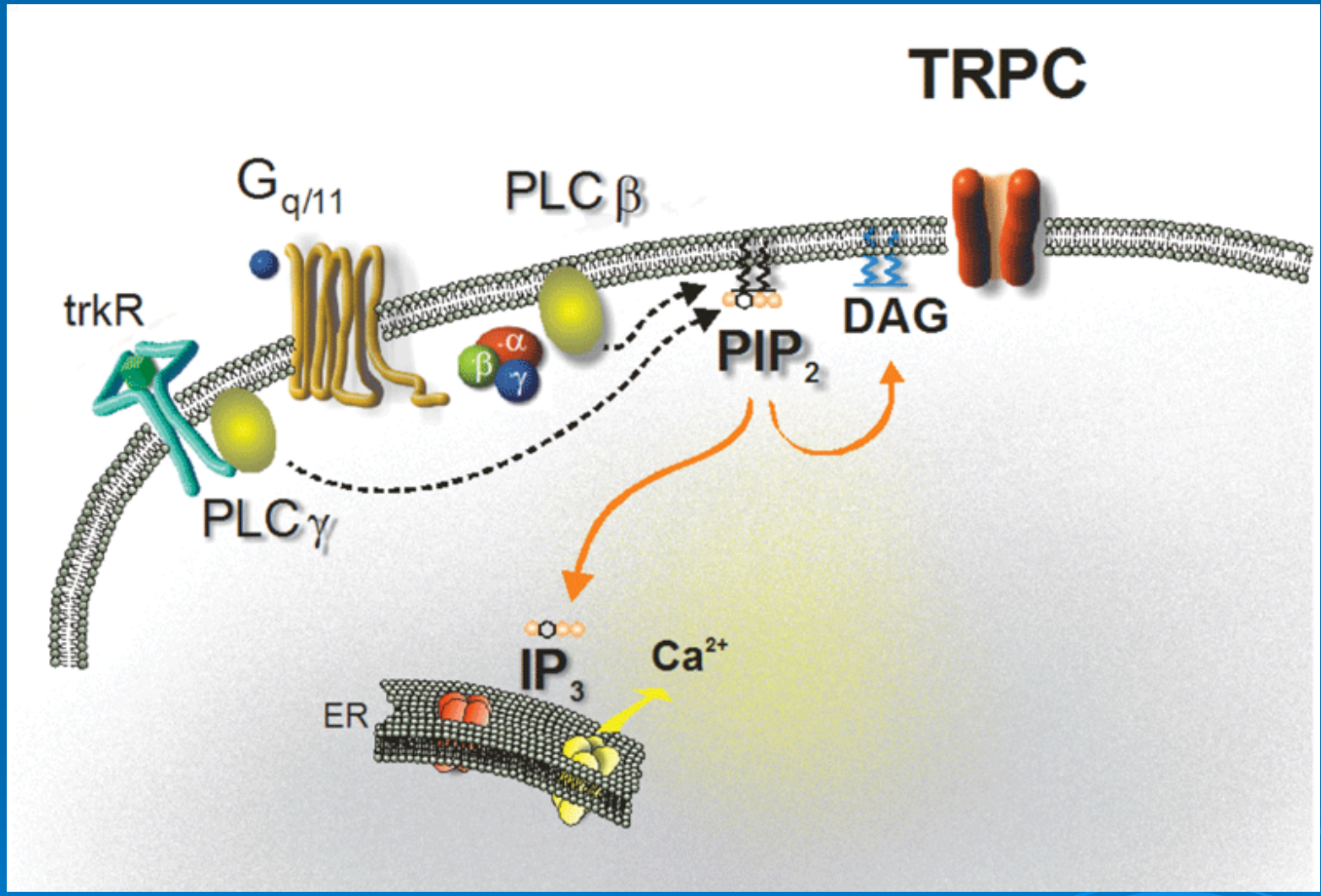

G protein typu Gq/11 aktivuje fosfolipázu Cβ (PLCβ). Fosfolipáza Cγ (PLCγ) je aktivována stimulací tyrozinkinázových receptorů (trkR). Aktivace fosfolipáz C vede k hydrolýze membránového fosfolipidu fosfatidylinozitol-4,5-bisfosfátu (PIP2) na rozpustný inozitol-1,4,5-trisfosfát (IP3) a membránově vázaný diacylglycerol (DAG). IP3 aktivuje receptory v endoplazmatickém retikulu (ER), což vede k výlevu vápníku do nitra buňky.

- Na příkladu TRP lze vidět, jak vše souvisí se vším a studiem smyslových schopností poznáváme obecná pravidla molekulární komunikace.